Supporting Information A (SI-A) to:

Identification of LC-HRMS Nontarget Signals in Groundwater After Source Related Prioritization

Karin Kiefer[1,2], Letian Du[1,2], Heinz Singer[1], Juliane Hollender[1,2]*

[1]Eawag, Swiss Federal Institute of Aquatic Science and Technology, 8600 Dübendorf, Switzerland
[2]Institute of Biogeochemistry and Pollutant Dynamics, ETH Zurich, 8092 Zurich, Switzerland

*Corresponding author: juliane.hollender@eawag.ch

Water Research, 2021

Table of Contents

SI-A1 Spike Solutions

For calibration standard preparation and spiking of samples, reference material was dissolved in ethanol, methanol, acetonitrile, ethanol/water mix, methanol/water mix, dimethyl sulfoxide, ethyl acetate, toluene, acetone, water, ethanol + 0.1 M HCl, or methanol + 0.1 M HCl at concentrations ranging from 100 to 1000 mgL^{-1}, depending on solubility and stability. Then, mix solutions were prepared in ethanol or acetonitrile at 10 mgL^{-1} which were combined for the final spike solutions (0.001, 0.01, 0.1 mgL^{-1}). The isotope labelled internal standard spike solution, containing 35 compounds, was prepared in ethanol at 0.1 mgL^{-1}.

SI-A2: LC-HRMS Settings

Table SI-A1: HPLC method

Autosampler: PAL RTC (CTC Analytics, Switzerland) **Pump: Dionex UltiMate3000 RS (Thermo Fisher Scientific, U.S.)** **Column: Atlantis T3 3 µm, 3.0 x 150 mm (Waters, Ireland)**	
Injection volume	140 µL
Flow rate	0.3 mL min^{-1}
Eluent A	Water + 0.1% formic acid
Eluent B	Methanol + 0.1% formic acid
Gradient	0 min: 100% eluent A, 0% eluent B 1.5 min: 100% eluent A, 0% eluent B 18.5 min: 5% eluent A, 95% eluent B 28.5 min: 5% eluent A, 95% eluent B 29 min: 100% eluent A, 0% eluent B 33 min: 100% eluent A, 0% eluent B

Table SI-A2: ESI-HRMS/MS settings

Mass spectrometer: Fusion Lumos (Thermo Fisher Scientific, U.S.)	
Spray voltage (kV)	3.5 / -2.5
Capillary temperature (°C)	300
Sheath gas (AU)	40
Auxiliary gas (AU)	10
S-lens RF level (AU)	60
Automatic gain control (AGC) target MS1	5×10^4
Maximum injection time MS1 (ms)	50
Scan range MS1 (m/z)	100 - 1000
Resolution MS1 (at m/z 200)	240,000
Internal calibration	Yes (EASY-IC™)
AcquireX enabled	TRUE
Cycle time	1 s
MS/MS activation type	Higher energy collisional dissociation (HCD)
Data-dependent trigger	Ions of mass list; if idle pick most intense
Min. precursor intensity to trigger MS/MS	10^4
Isolation window (m/z)	1
Resolution MS/MS (at m/z 200)	30,000
Automatic gain control (AGC) target MS/MS	1×10^4
Maximum injection time MS/MS (ms)	54
Dynamic exclusion time (s)	3
Normalized collision energy (NCE)	Stepped: 15, 30, 60

SI-A3: Quantification

Quantification was performed in two steps. First, extracted ion chromatograms (EICs) were plotted to check if the compound was detected in groundwater samples. The detected compounds were then identified and quantified using Trace Finder 4.1 (Thermo Fisher Scientific, U.S.).

To check for detections, the EIC of the compound (most intense ion: $[M+H]^+$, $[M+NH4]^+$, $[M+Na]^+$, $[M-H]^-$, $[M+FA-H]^-$ or in-source fragment according to in-house database) was extracted and plotted with a 5 ppm window and a 4 min retention time window for calibration standards, spiked samples, blank samples and groundwater samples using the R package MSnbase (Gatto and Lilley 2012). If the compound was not detected, the limit of quantification (LOQ) was defined as the smallest spike level in the spiked samples (1, 10, 100 or 250 ngL^{-1}), which resulted in a chromatographic peak, i.e. at least five consecutive data points.

Detected compounds were further identified by comparing the measured MS/MS fragments to the MS/MS fragments in the in-house library or mzVault. Quantification was based on the peak area ratio of analyte and isotope labelled internal standard (ILIS) using a linear calibration model (weighting 1/x). If a structurally identical ILIS was not available, an ILIS was selected eluting at similar retention time as the analyte and resulting in a relative recovery close to 100% in the spiked samples. Relative recoveries were calculated based on the concentration in the spiked and not spiked samples:

$$\text{Relative Recovery} = \frac{\left(c_{\text{spiked sample}} - c_{\text{not spiked sample}}\right)}{\text{Theoretical Spike Level}} \quad \text{(SI-1)}$$

ILIS selection was supported by an internal R script using the functions published on Zenodo (Schollée 2018). For a detailed description of the R script, see SI-A of Kiefer et al. (2019). Concentrations determined in Trace Finder 4.1 were corrected with the relative recovery, if a structurally identical ILIS was not available.

For compounds detected in groundwater, the LOQ in matrix (LOQ_{Matrix}) was estimated according to equation (SI-2) from the LOQ in ultrapure water ($LOQ_{Ultrapure}$) defined as the lowest calibration standard with at least five data points along the chromatographic peak (MS1 full scan mode).

$$LOQ_{Matrix} = \frac{LOQ_{Ultrapure}}{\text{Absolute Recovery}} \quad \text{(SI-2)}$$

If the sample concentration was in the range of the LOQ_{Matrix}, the so-defined LOQ_{Matrix} was lowered if the chromatographic peaks in the samples were defined by at least five data points. Furthermore, the LOQ_{Matrix} was set at least twice higher than the concentration in all blank samples.

Absolute recoveries were determined for each analyte by comparing the peak area in the matrix to the peak area in ultrapure water, as described in the following. If a structurally identical ILIS was available, the peak area of the ILIS in the matrix was divided by the peak area of the ILIS in ultrapure water (median of all enriched calibration standards):

$$\text{Absolute Recovery}_{\substack{\text{Identical} \\ \text{ILIS}}} = \text{Median} \frac{\text{Peak Area ILIS}_{\text{Matrix}}}{\text{Median (Peak Area ILIS}_{\text{Ultrapure}})} \quad \text{(SI-3)}$$

If a structurally identical ILIS was not available, the peak area of the analyte in the spiked sample (after subtracting the peak area in the not spiked sample) was compared to the peak area of the analyte in the calibration standard that corresponded to the spike level (10 and 100 ngL^{-1}):

$$\text{Absolute Recovery}_{\substack{\text{No Identical}\\\text{ILIS}}} = \frac{\text{Peak Area}_{\substack{\text{Spiked}\\\text{Sample}}} - \text{Peak Area}_{\substack{\text{Not Spiked}\\\text{Sample}}}}{\text{Peak Area}_{\substack{\text{Calibration}\\\text{Standard}}}} \quad \text{(SI-4)}$$

SI-A4: enviMass Settings

Data pre-processing for suspect and nontarget screening was performed using the enviMass workflow (v4.2633). Table SI-A3 and Table SI-A4 list the workflow options and settings.

Table SI-A3: Workflow options

Preprocessing	
Mass recalibration	Yes
Retention time alignment	Yes
Median intensity normalization	No
Blank / blind peak detection	Yes
Replicate filter	Yes
LOD interpolation	Yes
Targets	
Compound screening ILIS	Yes
Compound screening target	Yes
Intensity normalization using ILIS-profiles	Yes
Nontargets	
Peak shape correlation	Yes
File-wise componentization isotopologue	Yes
File-wise componentization adduct	Yes
File-wise componentization homologue series	No
Profile componentization	Yes
Watch list screening	No
Concentrations	
Calibration	No
Quantification	No
Recovery	No
Profiling	
Profile extraction	Yes
Profile filtering	Remove peaks from blinds: yes; remove peaks from spiked files: no
Profile blind detection	Yes
Trend detection	No
Comparisons	No

Table SI-A4: Workflow settings

Peak picking	
Filter RT range?	No
Filter mass range?	No
Parameter estimation	No
Maximum retention time gap in an EIC in s	300
Maximum m/z deviation of a centroid data in ppm	8.5
Minimum number of centroid data points per peak	3
…within a given a given RT window in s	3.8
Maximum RT gap length to be interpolated in s	10
Maximum RT width of a single peak ± from apex in s	120
Minimum log10(intensity) threshold	-10
Minimum Signal/Noise	3
Minimum Signal/Base	2
Maximum possible number of peaks within a single EIC	5
Peak area or peak intensoid?	Intensoid (max int.)
Instrument/resolution	OT_Fusion, QExactiveHF_240000@200
Tolerances	
+/- m/z tolerance	1 ppm
Maximum RT deviation between peaks of the same analyte in s	1.5
Intensity tolerance in %	30
Mass recalibration	
Reference compounds:	both
m/z tolerance	1 mmu
Maximum allowable m/z correction ...	1 mmu
RT tolerance in s	30
Alignment	
reference file to align all other files	pos: 201811_pos_189_QC_4_R1; neg: 201811_neg_213_QC_2_R2
m/z tolerance	1 ppm (pos), 1 ppm (neg)
Reference peaks/masses	All peaks (recommended)
Maximum permissible (or expected) RT shift correction in s	30
Maximum number of most intense reference peaks to include	1000
Maximum number of iteration for match window adaption	4
Only include replicable peaks (if applicable)?	Yes
Only plot but do not apply alignment results?	No

Table SI-A4 (continued)

Blind	
Factor by which the sample peak intensity must exceed the blank/blind peak intensity to not be subtracted	10
m/z tolerance in ppm	3
RT tolerances in s	60
Subtract with the blank/blind file(s) specified in the tag1 entry of each file (=comma-separated blind file IDs, otherwise set to FALSE)?	Yes
Replicates	
+/- m/z tolerance in ppm	2
RT tolerance window of peaks caused by the same analyte in s	30
Absolute log intensity tolerance X	10
Screening ILIS	
RT tolerance in s	60
Restriction to latest files	No
Cutoff score	0.8
Screen for MS/MS fragments	No
Screening targets	
RT tolerance in s	60
Restriction to latest files	No
Cutoff score	0.8
Screen for MS/MS fragments	No
Screening Adducts	
Positive adducts	M+H, M+NH4, M+Na, M+K
Negative Adducts	M-H
Quantification	Not done
Normalization	Yes (positive & negative)
Minimum of screened files covered by each ILIS profile in %	90
Screening threshold	0.8
Minimum number of ILIS profile peaks per file (= ensures coverage):	15
Use subsampling	Yes
Number of blank/blind profiles in subsample:	100
Number of sample profiles in subsample:	100
Profiles	
Peak mass deviation within profiles: +/- m/z tolerance in ppm	3
Peak deviation within profiles: RT tolerance in s	60
Omit files with table entry profiled=FALSE from profiling?	TRUE

Table SI-A4 (continued)

Trends	Not done
File wise Componentization Isotopologues	
Run atom bound estimation?	FALSE
File wise Componentization Adducts	
Positive Adducts	M+H, M+NH4, M+Na, M+K, M+DMSO+H, 2M+H
Negative Adducts	M-H, 2M-H, M+FA-H, M+Cl, M-2H
File wise Componentization Peak Shape Correlation	
Min. number of MS1 scans over which peak pairs co-elute to check for their peak shape correlation:	10
Min. Spearman correlation [0,1] coefficient:	0.9
Profile Componentization	
Restrict profile componentization to a set of latest files only?	FALSE
Filtering of outliers in profile component relations (recommended):	TRUE
Allow searching for additional adducts for peak shape correlated profiles?	FALSE
Restrict profile componentization to isotopologue and selected adduct relations only?	FALSE
Restrict profile componentization to top 100 most intense & trend profiles only?	FALSE

SI-A5: Estimation of Nontarget Concentrations

The concentration of nontargets was estimated from peak height intensities of target compounds in spiked samples. First, peak height intensities were determined using Trace Finder 4.1. Then, the 25th, 50th, and 75th percentiles of peak height intensities were calculated for each spiking level (1, 10, 100, 250 ngL^{-1}) and for positive and negative ionization mode separately. Target compounds which were detected at concentrations of >20% of the spiking level in one of the spiked samples were excluded. Then, linear calibration models (Figure SI-A1) were calculated to estimate nontarget concentrations assuming that nontargets (i) ionize on average less efficiently than targets (25th percentile), (ii) ionize on average as efficiently as targets (50th percentile), or (iii) ionize on average more efficiently than targets (75th percentile).

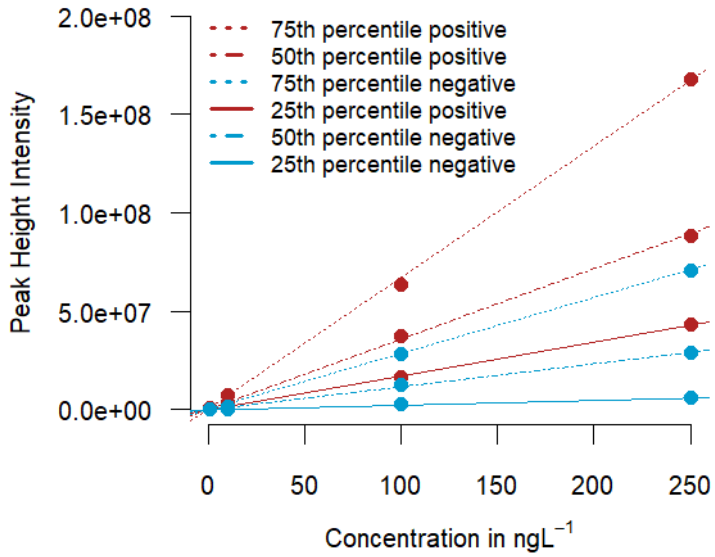

Figure SI-A1: Linear regression models between spiking levels (1, 10, 100, 250 ngL^{-1}) and 75th, 50th, and 25th percentiles of peak height intensities of target compounds in four groundwater samples. Regression was forced through the origin.

SI-A6: Structure Elucidation with MetFrag and SIRIUS4/CSI:FingerID

MetFrag (Ruttkies et al. 2016) and SIRIUS4/CSI:FingerID (Dührkop et al. 2015, Dührkop et al. 2019) were used (i) in the nontarget screening to support structure elucidation and (ii) in the suspect screening to test if the experimental MS/MS spectrum fits to the suspect structure.

First, MS1 and MS/MS spectra were extracted for each nontarget/suspect profile for the monoisotopic ion from the mzXML files using the RMassBank package (Stravs et al. 2013). The most intense MS1 and MS/MS scans at given retention time (±30 s) were written to txt files after removing peaks with intensity <1% relative to the base peak to reduce noise signals. The enviMass workflow (version 4.2633) exports the m/z of the most intense feature within a component. However, the most intense feature is not necessarily the monoisotopic ion (e.g. brominated or multiple chlorinated compounds). Therefore, the isotope pattern of profiles with mass defect <0 (Br, Cl have a negative mass defect) were checked manually and the m/z of the monoisotopic ion was selected for MS1 and MS/MS spectra

extraction. For further processing with MetFrag and SIRIUS4/CSI:FingerID, the spectra from the mzXML file, where the nontarget/suspect was detected at highest intensity, was used and it was assumed that the m/z represents the $[M+H]^+$ or $[M-H]^-$.

MetFrag CL 2.4.5 was run in batch mode using the R functions MetFragConfig and runMetFrag adapted from the R package ReSOLUTION (Schymanski 2020). For each profile, MetFrag retrieved candidates matching the m/z within 2 ppm from a local csv file. For details on the compound lists used in suspect and nontarget screening, respectively, refer to the manuscript and Table SI-A5. Salts and stereoisomers were removed using the unconnected compound and InChIKey filters implemented in MetFrag. The candidates were fragmented in silico using a bond dissociation approach. In silico fragments were compared to experimental fragments with a relative mass deviation of 7 ppm (mass accuracy in MS/MS scan mode was lower than in MS1 scan mode). The maximum tree depth was 2. Finally, candidates were ranked using different scoring terms (Table SI-A6).

MS1 and MS/MS spectra were converted to ms and msp format, and then imported in batch mode to SIRIUS4/CSI:FingerID or the NIST Mass Spectral Search Program (version 2.3). SIRIUS4/CSI:FingerID was operated with the same local compound lists as used with MetFrag. Molecular formula prediction was limited to formulae available in the compound lists as otherwise for many nontarget/suspect profiles unrealistic formulae were suggested.

Table SI-A5: Number of compounds originating from various lists used for structure elucidation in nontarget and suspect screening. Stereoisomers were removed by filtering for the first block of the InChIKey. The column "Additional Compounds" refers to the number of compounds, which are not included in lists above; e.g. NORMAN SusDat comprises 65,596 compounds (without stereoisomers), but 51,887 are part of CompTox.

Compound List in Nontarget Screening	**No. of Compounds**	**Additional Compounds**
CompTox (Schymanski 2019)	773,232	773,232
NORMAN SusDat (Norman Network et al. 2020)	65,596	13,709
PubChemLite tier1 (Bolton and Schymanski 2020)	363,911	200,698
Extended PMT (H.-P. Arp and S.E. Hale, personal communication)	2,124	215
STOFF-IDENT (Letzel et al. 2017)	11,071	95
SwissPest19 (Kiefer et al. 2020)	1,472	521
Further pesticide transformation products (T. Poiger, personal communication)	618	71
Compound List in Suspect Screening	**No. of Compounds**	**Additional Compounds****
Extended PMT (H.-P. Arp and S.E. Hale, personal communication)*	607	548
UBAPMT (Arp and Hale 2020)	215	38
Schulze et al. (2019)	64	21
KEMI Market List (Fischer 2017)*	796	555

*Original lists contain more compounds. Lists were filtered for compounds that are more likely to occur in groundwater (see details in manuscript). **Only compounds with heteroatoms and exact mass >100.

Table SI-A6: MetFrag scoring terms and their weightings used for nontarget and suspect screening.

Scores in Nontarget Screening	**Weighting**
FragmenterScore	1
AutomatedPeakFingerPrintAnnotationScore (Ruttkies et al. 2019)	1
AutomatedLossFingerPrintAnnotationScore (Ruttkies et al. 2019)	1
RetentionTimeScore →retention time prediction based on target compounds	1
OfflineMetFusionScore (Gerlich and Neumann 2013)	1
OfflineIndividualMoNAScore → similarity with candidate in MassBank of North America (MoNA; built into MetFrag)	1
PatentCountScore → patent count from PubChem	0.25
CompTox DATA_SOURCES	0.25
KEMI_ExposureScore_Water_0to1	0.25
PMT_Emission_likely → emission likely? Yes or no (according to H.-P. Arp, personal communication)	0.25
Scores in Suspect Screening	**Weighting**
FragmenterScore	1
RetentionTimeScore →retention time prediction based on target compounds	1
SuspectListScore → higher ranking if structure on suspect list	1
PatentCountScore → patent count from PubChem	1

SI-A7: Suspect/Nontarget Confirmation and Quantification

Ten samples and one pooled sample comprising all prioritized suspects and nontargets (sample aliquots which were not thawed previously), five spiked samples (100, 250, 1000 ngL^{-1}), two blanks, and four calibration standards were enriched and measured as described in SI-A2 with the following slight modifications. AcquireX was not used. The mass list comprised only the m/z of the prioritized suspects and nontargets. The dynamic exclusion time was reduced to 1 s to increase the number of MS/MS scans along a chromatographic peak.

Suspects and nontargets were confirmed based on matching MS/MS spectra and retention time in standard and sample with the following method. Using the R package MSnbase (Gatto and Lilley 2012), the EICs of the most intense adduct in standard, sample and spiked sample were extracted (mass window 5 ppm) and plotted to check the retention time. Then, the five most intense fragments in the standard were determined, and the EICs of these fragments (in standard and samples) were plotted. Head to tail plots were created with the R package MSMSsim (https://github.com/dutchjes/MSMSsim). The resulting plots are compiled in SI-A12.

Concentrations were determined in the 60 samples by applying the calibration model determined later with the same LC-HRMS system. The calibration standards used for this calibration model were prepared with the same ILILS spike solution as was used for the first analysis. The quality of quantification was evaluated based on relative recoveries in spiked samples (ideally 80-120% in all spiked samples) and consistency of concentrations determined in samples, which were measured twice (i.e. first analysis and together with calibration standards). For some compounds, quantification was not satisfactory so that either no concentrations or concentration ranges were reported.

SI-A8: Sample Classification based on Target Screening

The classification based on the target screening was consistent with the pre-classification based on long-term monitoring data for 53 out of 60 monitoring sites. For three sites pre-classified as urban impacted, the concentration sum of urban targets was (slightly) below the cut-off of 100 ngL^{-1} (i.e. 42, 53 and 99 ngL^{-1}). Two of these sites were classified as having high agricultural influence, one exhibited only low urban and agricultural influence. Four sites were pre-classified as having low anthropogenic impact but showed 140 to 640 ngL^{-1} of agricultural targets (concentration sum of urban targets <28 ngL^{-1}) resulting in a classification as sites with high agricultural influence.

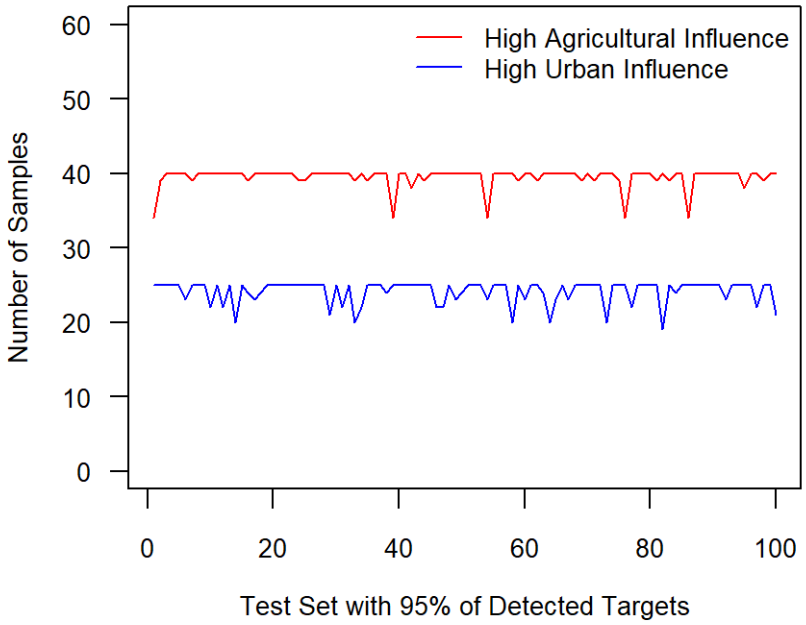

Figure SI-A2: The 60 groundwater monitoring sites were classified using 100 randomly selected subsets of target compounds. Each subset comprised 95% of detected targets. The number of samples classified as having high agricultural or urban influence ranged from 34 to 40 and 19 to 25, respectively.

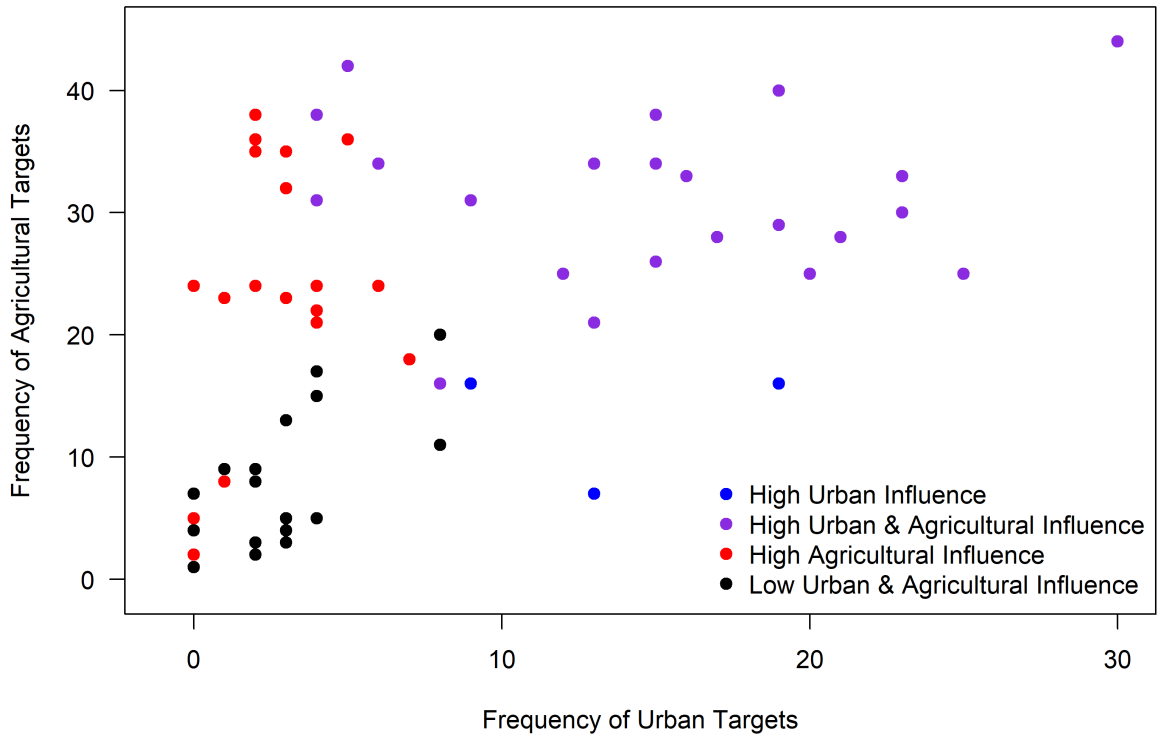

Figure SI-A3: Detection frequency of agricultural targets versus detection frequency of urban targets at each monitoring site. The monitoring sites are coloured according to their classification based on concentration sums.

Table SI-A7: Target compounds with detections ≥100 ngL^{-1}. The $logD_{OW\ pH7}$ (water-n-octanol distribution coefficient considering the speciation at pH 7) was predicted with JChem for Office, version 19.22.0.548, ChemAxon Ltd. LOQ (limit of quantification). c_{max} (maximum concentration) in the 60 groundwater samples.

Target Compound	**Classification**	**$LogD_{ow\ pH7}$**	**LOQ in ngL^{-1}**	**Detec-tions**	**c_{max} in ngL^{-1}**
Sum 4- &5-methyl-benzotriazole	Corrosion inhibitor	1.8	0.1	33	100
Benzotriazole	Corrosion inhibitor	1.3	0.2	40	220
Melamine	Industrial chemical	-2.5	5	14	690
Diatrizoate	Pharmaceutical	-0.6	1	17	240
N-N-Didesvenlafaxin	Pharmaceutical TP	-0.4	1.5	3	410
Acesulfame	Sweetener	-1.5	0.1	52	150
Sucralose	Sweetener	-0.5	100	2	230
N-N-Dimethylsulfamide	Pesticide/biocide TP	-1.5	1	30	470
Atrazine	Pesticide	2.2	0.1	52	160
Bentazone	Pesticide	-0.2	0.2	14	210
Cycluron	Pesticide	2	1	1	140
Mecoprop	Pesticide	-0.3	1	1	240
Atrazine-desethyl	Pesticide TP	1.5	0.1	51	100
Chloridazon-desphenyl	Pesticide TP	-0.7	1	33	1600
Chloridazon-methyl-desphenyl	Pesticide TP	-0.6	0.5	37	610
Chlorothalonil TP R417888	Pesticide TP	-0.7	0.5	50	940
Chlorothalonil TP R419492	Pesticide TP	-4.5	5	36	740
Chlorothalonil TP R471811	Pesticide TP	-1.7	3	60	2200
Chlorothalonil TP SYN507900	Pesticide TP	0.4	1	13	130
Metazachlor-OXA	Pesticide TP	-1	5	5	120
Metolachlor-ESA	Pesticide TP	-0.3	0.5	41	920
Metolachlor TP CGA 368208 (=Acetochlor sulfonic acid)	Pesticide TP	-0.5	2	22	280
Nicosulfuron TP UCSN	Pesticide TP	-2.3	1	38	140
Terbuthylazine TP CSCD648241	Pesticide TP	-2.5	0.2	44	120

SI-A9: Characterization of Compounds

Natural organic matter (NOM): Naturally occurring compounds should be located in the centre of Figure 2 (see manuscript), either because the NOM molecules occur at each site or are randomly distributed. Therefore, we investigated the compounds located in the centre of Figure 2 with >40 detections and retention time >4 min in more detail. 40% of these compounds (profiles) were composed of several profiles (>2) grouped in the post-processing, i.e. these profiles were grouped together due to a similar m/z and retention time (<2 ppm, <30 s; section 2.5.1 in manuscript). These 106 compounds were detected in positive ionization mode and eluted after 10 min (except for one compound). In the whole dataset, only 328 compounds were composed of >2 profiles exported from enviMass and eluting after 10 min (319 compounds in positive mode, 9 compounds in negative mode). The EICs were manually checked and showed mostly a broadly-eluting peak (>5 min, Figure SI-A4), which was found either in all samples or only in some samples (but not in blank samples). Such broad peaks cannot be correctly detected in peak picking algorithms so that several profiles are formed. Furthermore, these compounds had on average a more positive mass defect and higher m/z than the compounds from the remaining dataset (Figure SI-A5). 24 profiles with a broadly-eluting peak were annotated using MetFrag and SIRIUS4/CSI:FingerID (SI-B2). The molecular formulae of the candidates comprised in most cases only C, H, O, and partially N, S, and Si atoms. Therefore, we speculate that these profiles represent NOM.

Cl-containing compounds: To get further evidence for an anthropogenic origin, the MS1 spectra of each compound were checked for characteristic isotope patterns such as Cl. Accordingly, at least 50 of the 488 compounds indicated the presence of one or more Cl atoms (SI-B2). However, 11 of the putatively mono-chlorinated compounds likely represented Cl adducts ($[M+Cl]^-$), which is supported by a co-eluting peak of the m/z of the corresponding $[M-H]^-$. Analogously, a nontarget compound classified as potential urban contaminant was finally elucidated as the $[M+Cl]^-$ of the target compound sucralose. The $[M+Cl]^-$ was ten times more intense than the $[M-H]^-$.

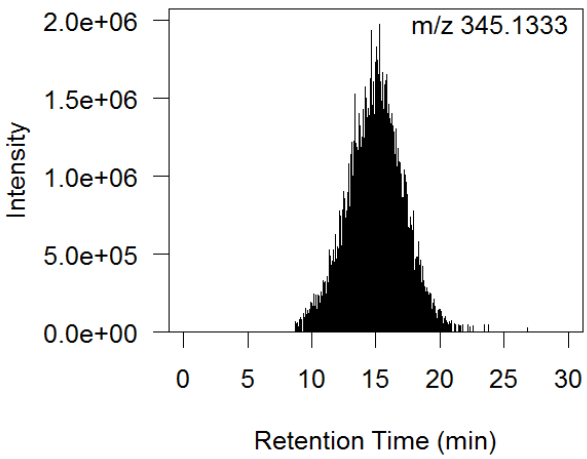

Figure SI-A4: Extracted ion chromatograms of a grouped profile composed of four profiles exported from enviMass (positive ionization, m/z 345.1333). A broad peak was detected in all samples except for blank samples (enriched ultrapure water).

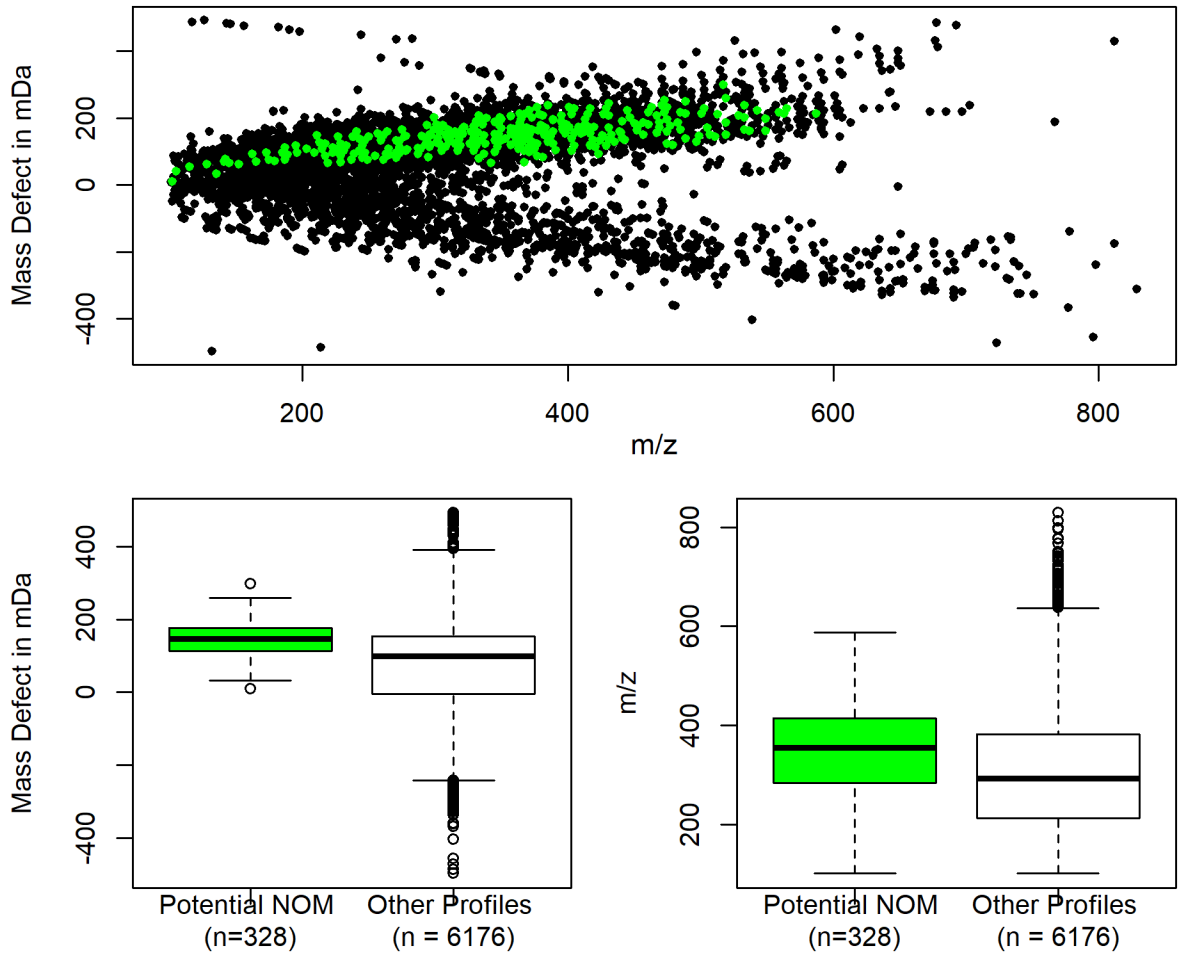

Figure SI-A5: Mass defect and m/z range of the 328 profiles representing potential natural organic matter (NOM, green) and of the remaining 6176 profiles (black). The potential NOM profiles were extracted from the dataset by filtering for grouped profiles (composed of >2 profiles) with retention time >10 min.

SI-A10: Evaluation of AcquireX

To investigate if AcquireX increased the MS/MS coverage, we compared the MS/MS coverage for the 488 nontargets (maximum intensity >5 × 10^6) and 695 suspects (maximum intensity >10^6) in the first replicate injections (mass list contained only precursor m/z of targets), with the MS/MS coverage in the second replicate injections (mass list contained precursor m/z of targets and features detected by AcquireX), and third replicate injections (precursor m/z which were triggered in second injection were shifted from mass list to exclusion list).

Assuming that without the use of AcquireX, MS/MS coverage would be in all three replicates similar, because always the most intense precursors are triggered, AcquireX increased the MS/MS coverage of nontargets by 39%, i.e. 28% more MS/MS were triggered in the second replicate injections than in the first injections and 11% additional MS/MS were triggered in the third injections compared to the first injections. In case of the suspects, AcquireX increased the MS/MS coverage by 73%, i.e. 56% more MS/MS were triggered in the second replicate injections than in the first injections and 17% additional MS/MS were triggered in the third injections compared to the first injections. Probably, AcquireX showed a smaller influence on the nontargets than on the suspects, because the nontargets were on average more intense and therefore also triggered without AcquireX (median of maximum intensity of nontargets vs. suspects: 1.2 × 10^7 vs. 1.7 × 10^6). Moreover, AcquireX improved the MS/MS coverage especially in positive ionization mode, possibly, because less compounds ionize in negative mode so that also without AcquireX a high MS/MS coverage is achieved.

SI-A11: Characterization of Groundwater Monitoring Sites

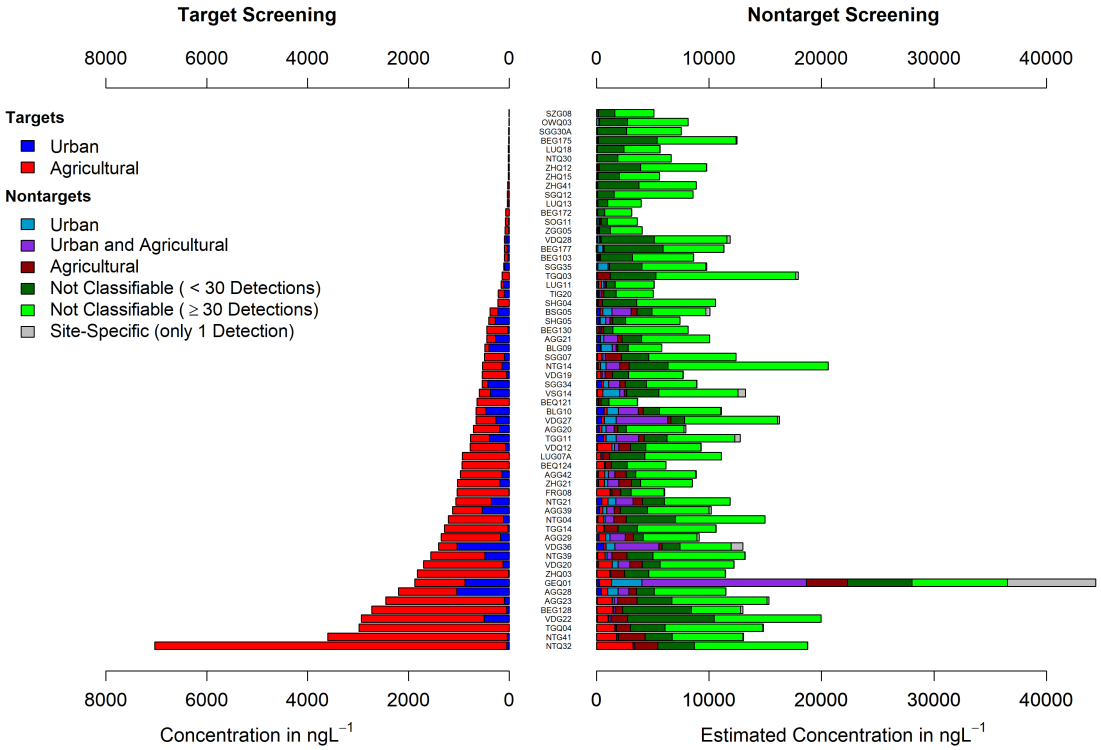

Figure SI-A6: Total concentrations determined in the target screening (left) and estimated concentrations determined in the nontarget screening. In contrast to Figure 3 (manuscript), all compounds (profiles) are included.

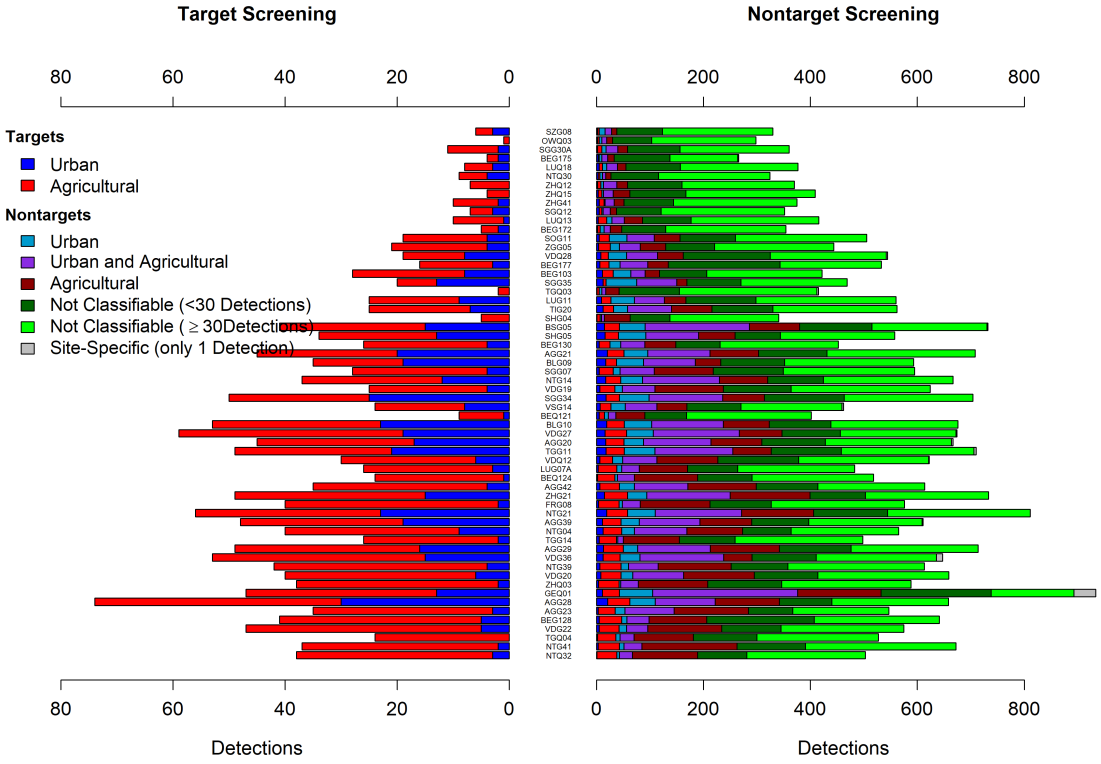

Figure SI-A7: Number of detections in the target screening (left) and number of detected compounds (profiles) in the nontarget screening (right). Potential false positives (see manuscript) are not shown.

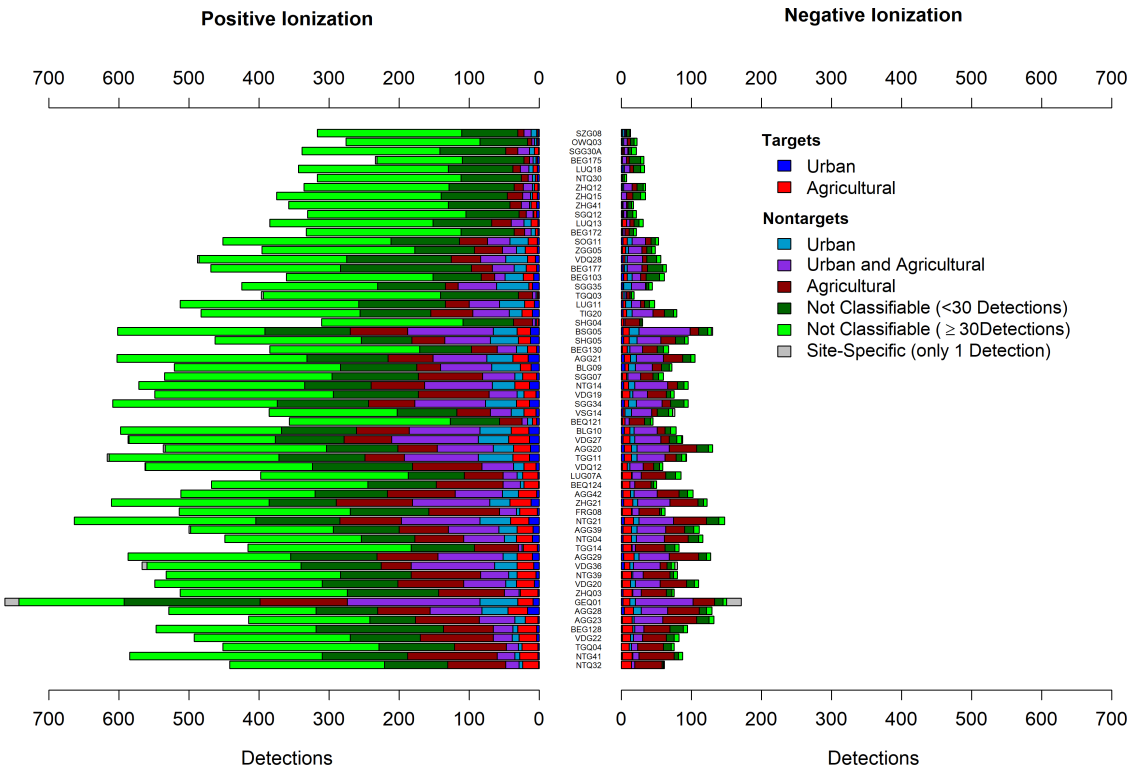

Figure SI-A8: Number of detections in the nontarget screening in positive ionization mode (left) and negative ionization mode (right). Potential false positives (see manuscript) are not shown.

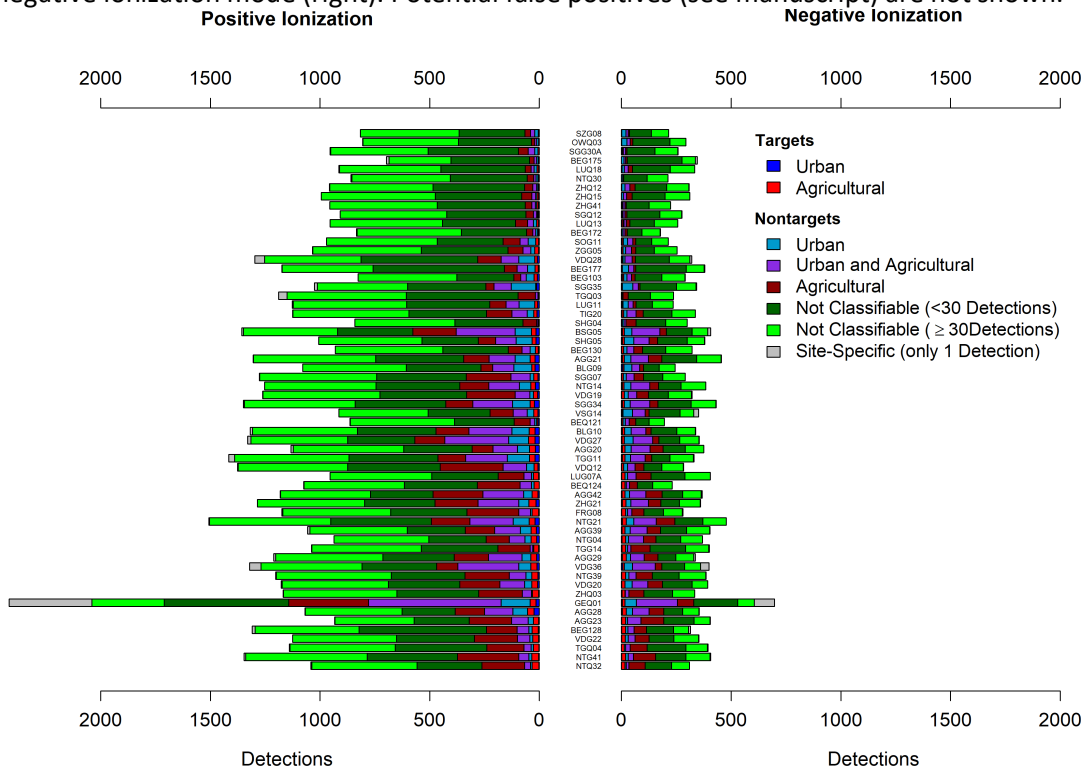

Figure SI-A9: Number of detections in the nontarget screening in positive ionization mode (left) and negative ionization mode (right). All compounds (profiles) are shown.

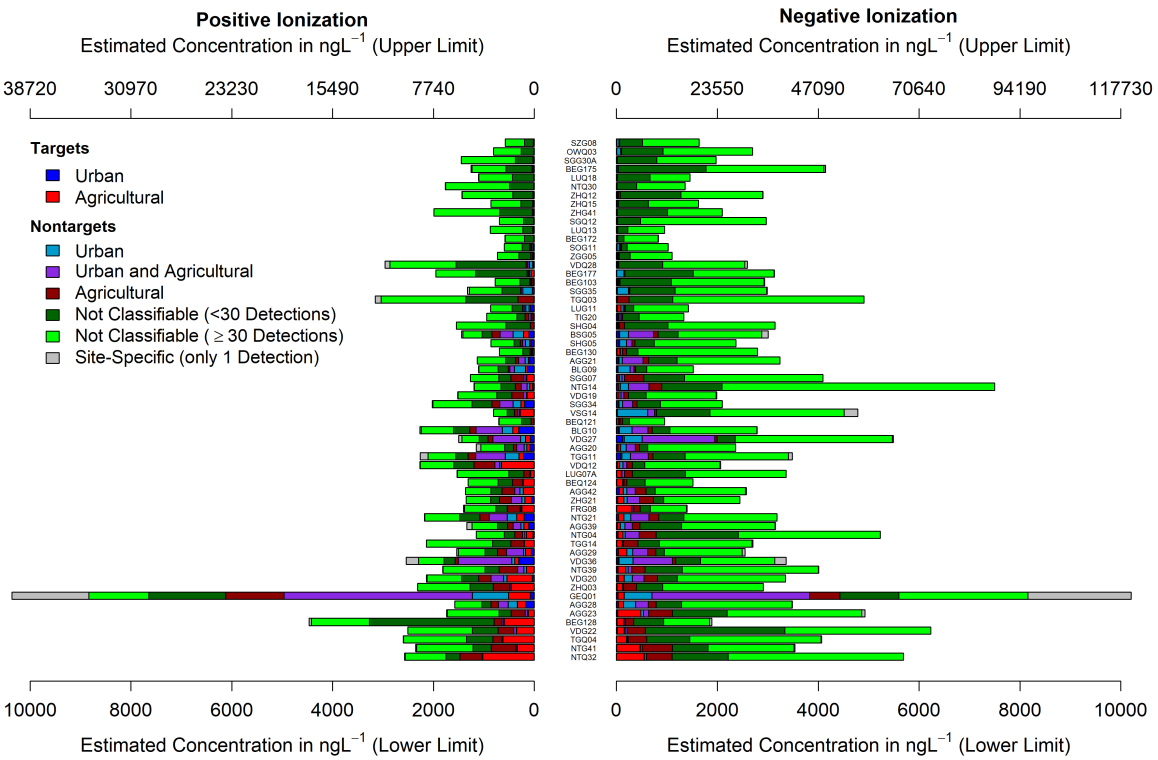

Figure SI-A10: Upper (top x-axis) and lower (bottom x-axis) estimated concentrations of all compounds (profiles) detected in positive and negative ionization mode.

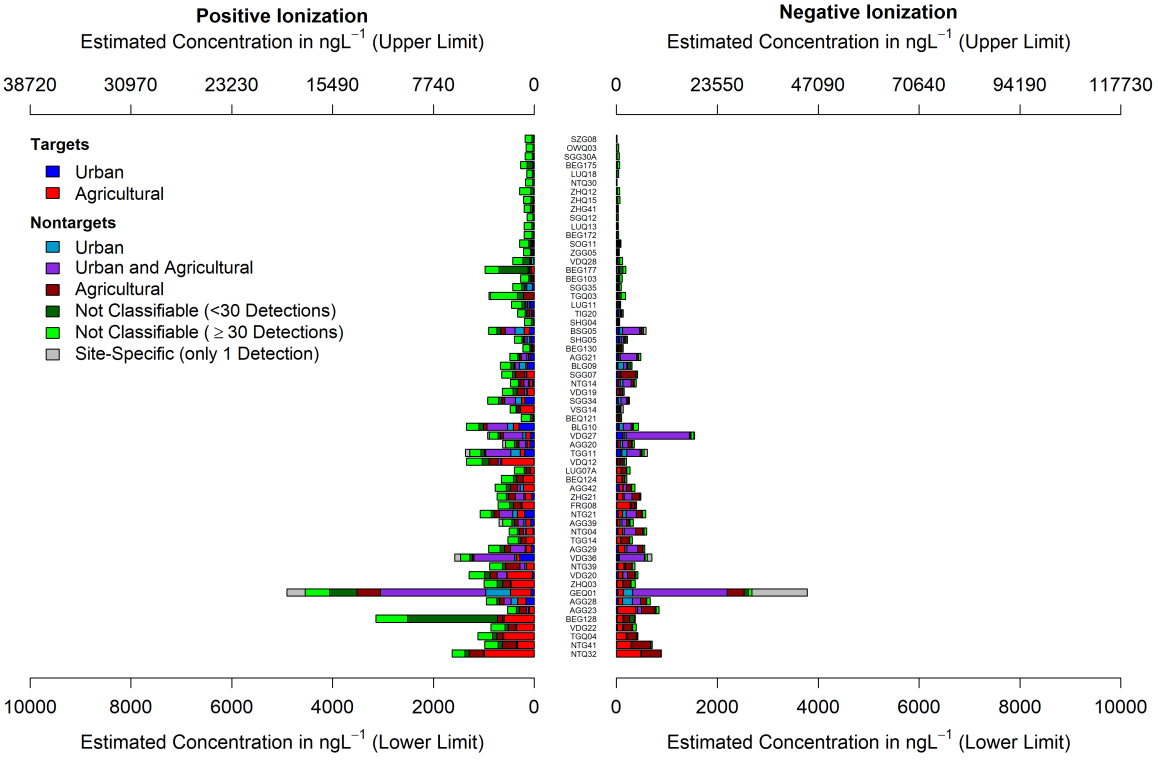

Figure SI-A11: Upper (top x-axis) and lower (bottom x-axis) estimated concentrations of compounds (profiles) detected in positive and negative ionization mode. Potential false positives (see manuscript) are not shown.

SI-A12: Confirmation of Suspects and Nontargets

The following figures illustrate the EICs of the precursor ion and of the five most intense MS/MS fragments in standards, samples, and spiked samples for suspects and nontargets identified unequivocally (Level 1). By comparing the EICs of the MS/MS ions and precursor ions, background ions (i.e. no true fragments of the precursor) can be identified (see e.g. 2-Acrylamido-2-methyl-1-propanesulfonic acid). Fragmentation was performed at three different NCEs (15, 30, 60), i.e. mix MS/MS spectra are shown. Using head to tail plots, MS/MS spectra of standard and sample are compared. In case of Level 2a candidates, MS/MS spectra are provided and fragments reported in literature (Kormos et al. 2009, Reemtsma et al. 2013, Schulz et al. 2008) or mzCloud (www.mzcloud.org) were marked. In case of Level 3 candidates, MS/MS spectra were annotated with structure proposals.

2,5-Dichlorobenzenesulfonic Acid
GEQ01, Level 1
[M-H]- 224.91854
(STD 100 ng/L)

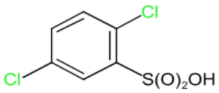

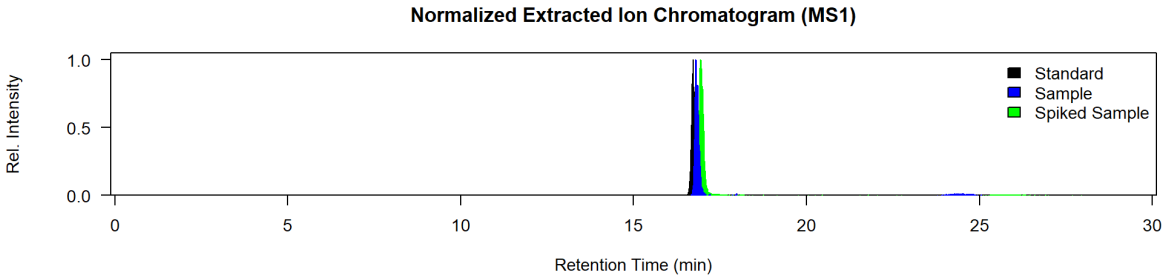

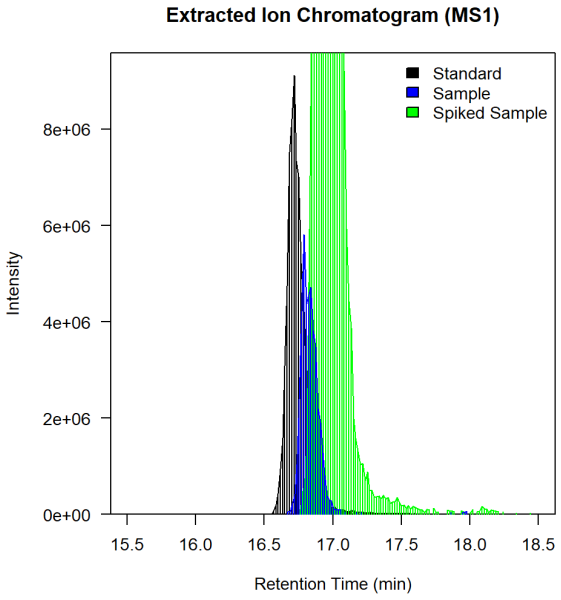

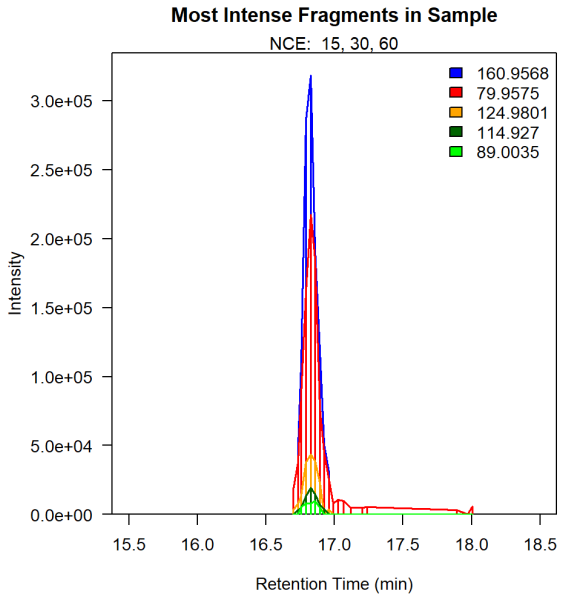

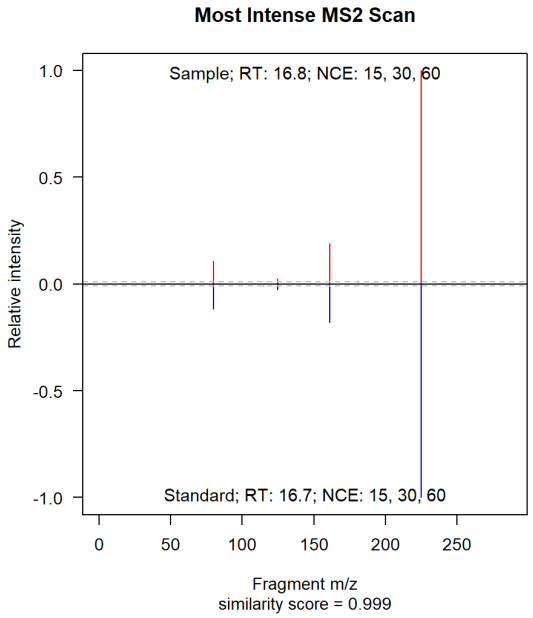

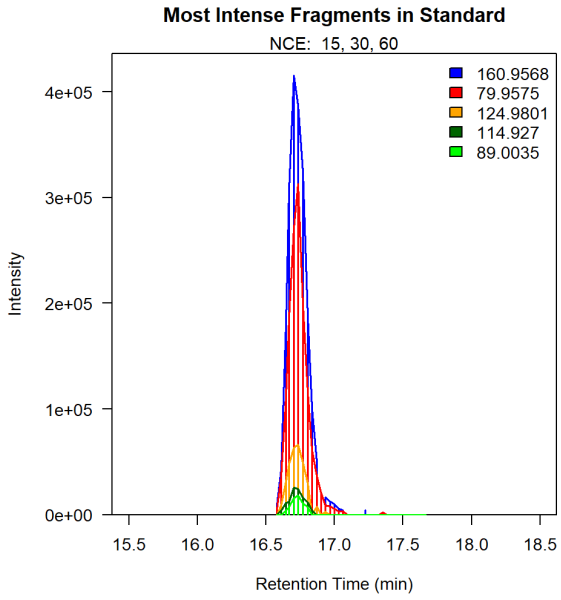

Phenylphosphonic Acid
VDG36, Level 1
[M+H]+ 159.02056
(STD 100 ng/L)

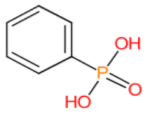

Normalized Extracted Ion Chromatogram (MS1)

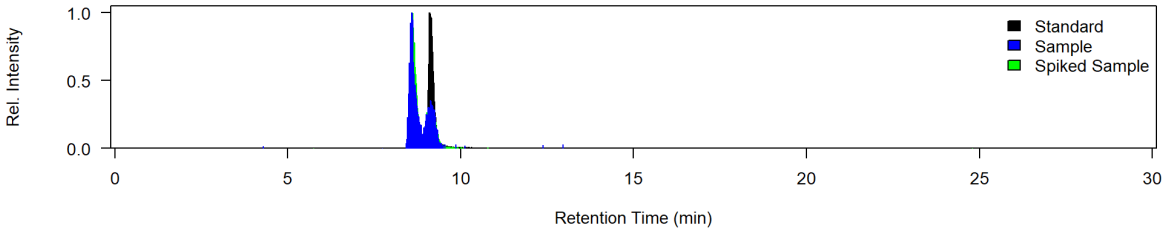

Extracted Ion Chromatogram (MS1)

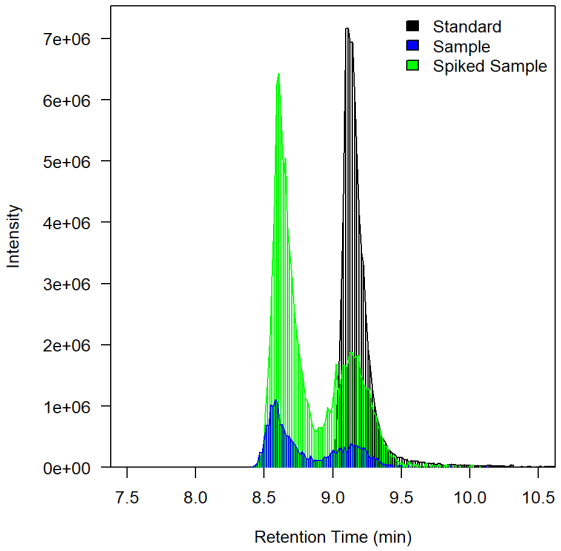

Most Intense Fragments in Sample

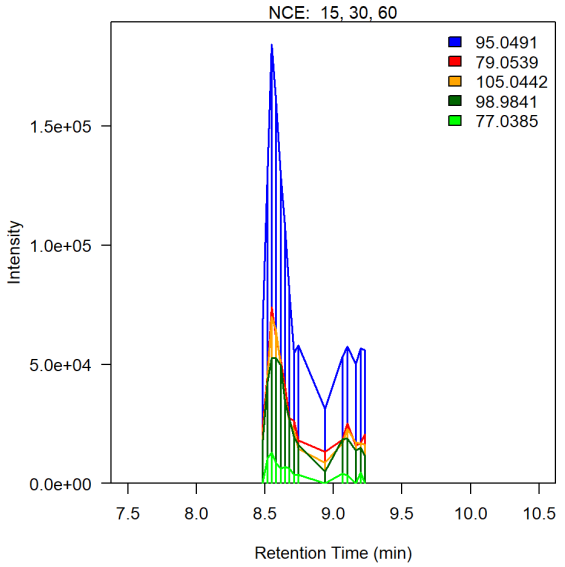

Most Intense MS2 Scan

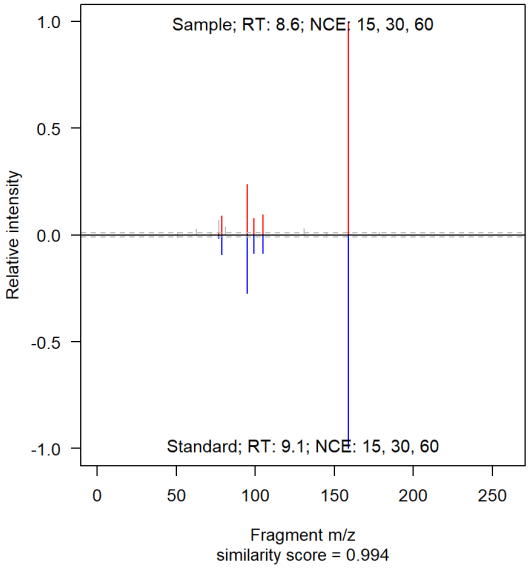

Most Intense Fragments in Standard

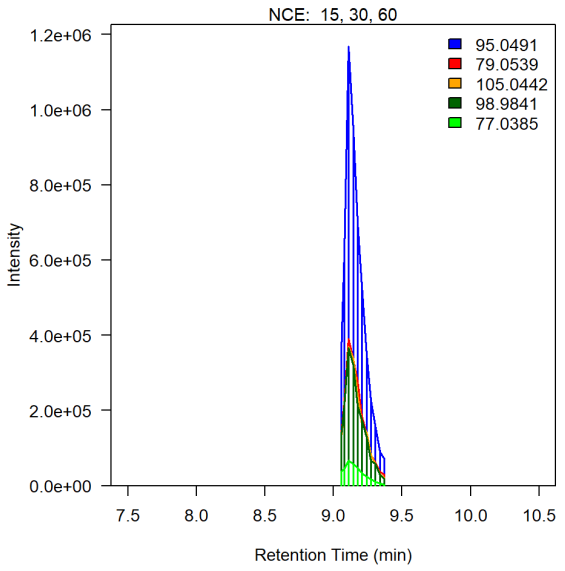

Triisopropanolamine borate
BLG10, Level 1
[M+H]+ 199.14888
(STD 100 ng/L)

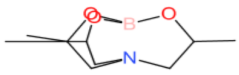

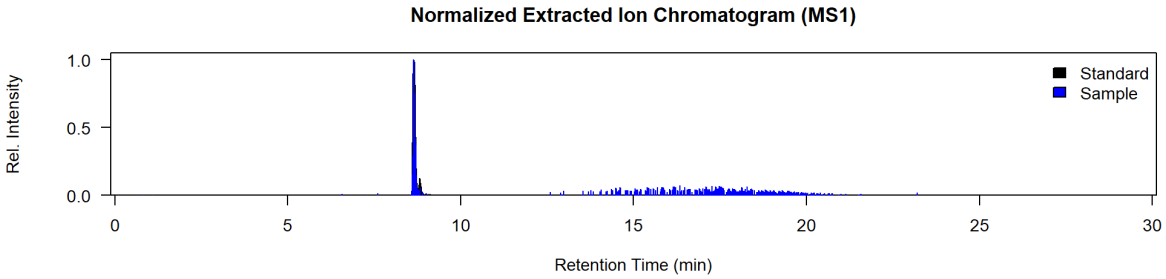

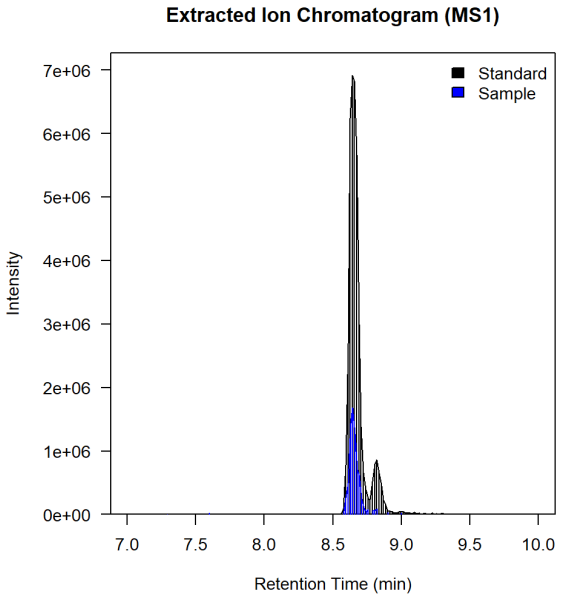

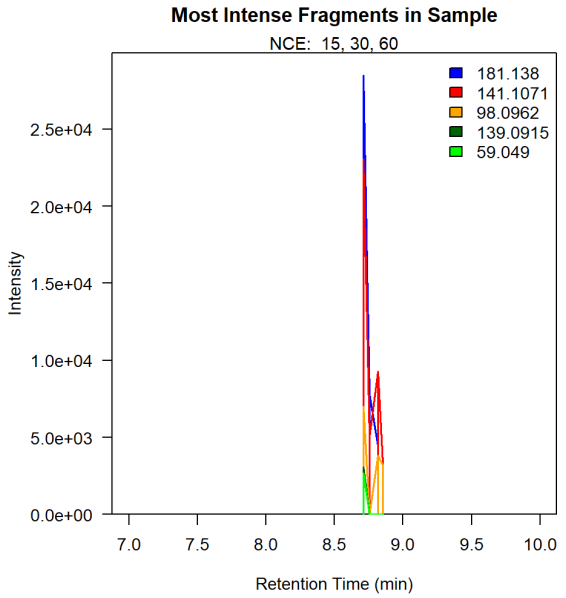

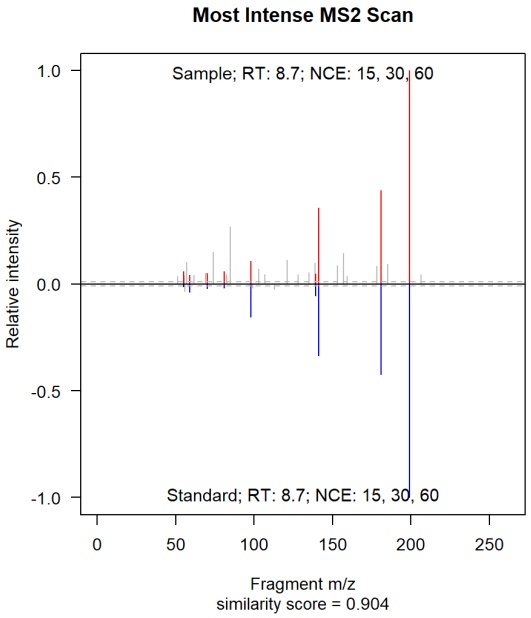

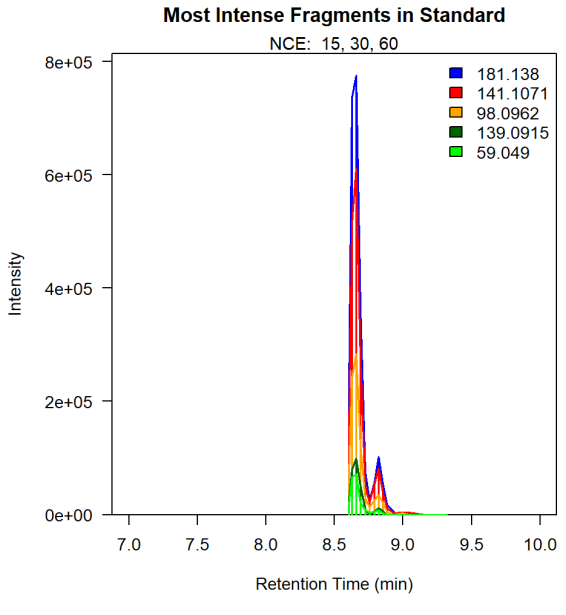

2-Methyl-5-Nitrobenzenesulfonic Acid
BSG05, Level 1
[M-H]- 215.99722
(STD 100 ng/L)

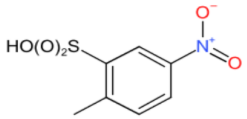

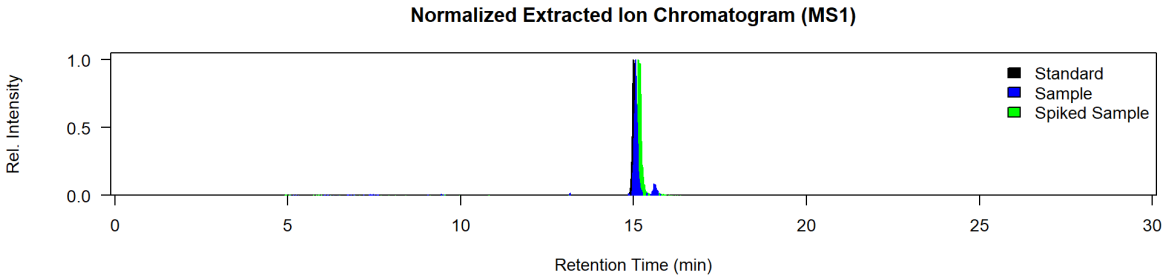

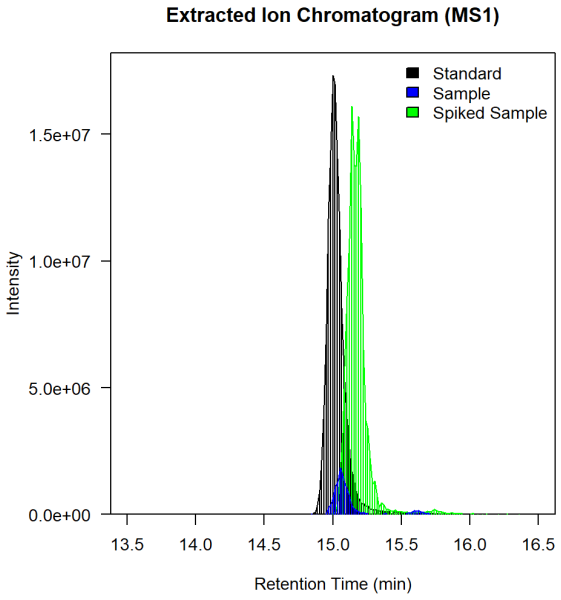

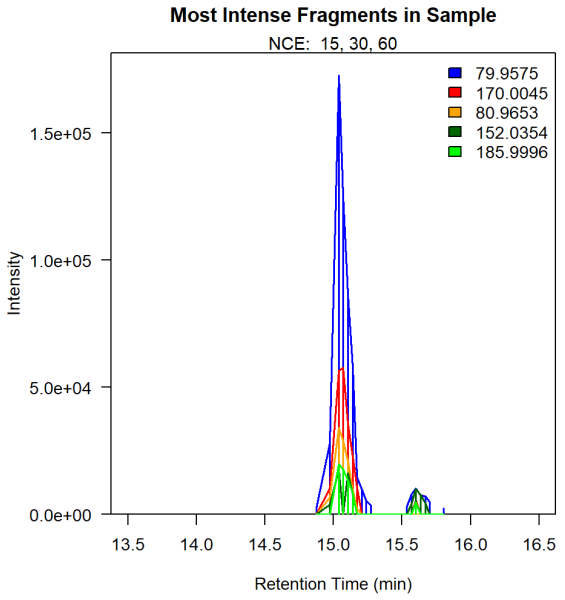

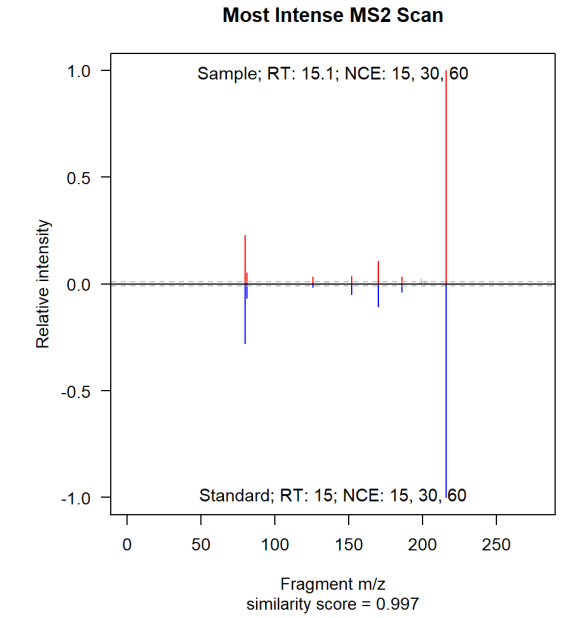

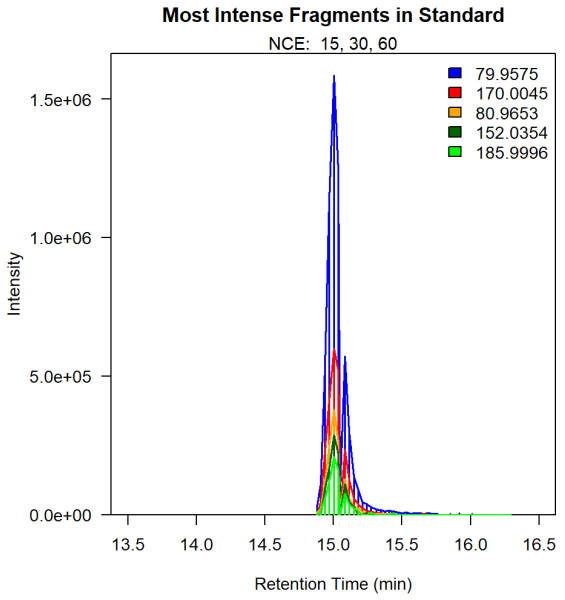

O-Des[2-aminoethyl]-O-carboxymethyldehydroamlodipine
BLG10, Level 1
[M+H]+ 422.10011
(STD 10 ng/L)

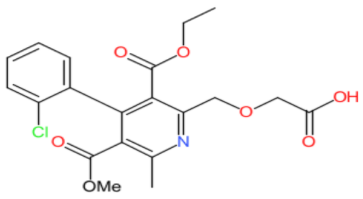

Normalized Extracted Ion Chromatogram (MS1)

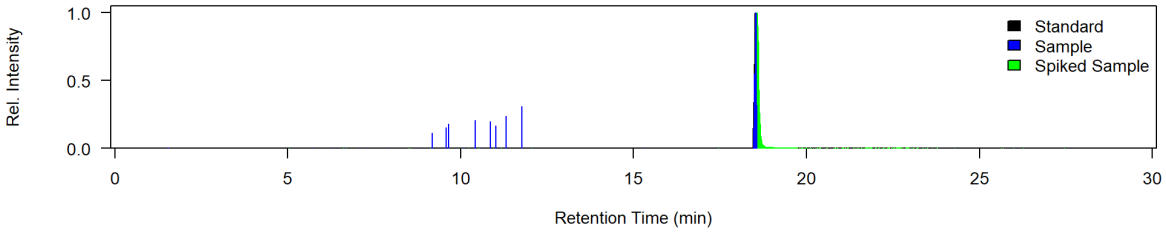

Extracted Ion Chromatogram (MS1)

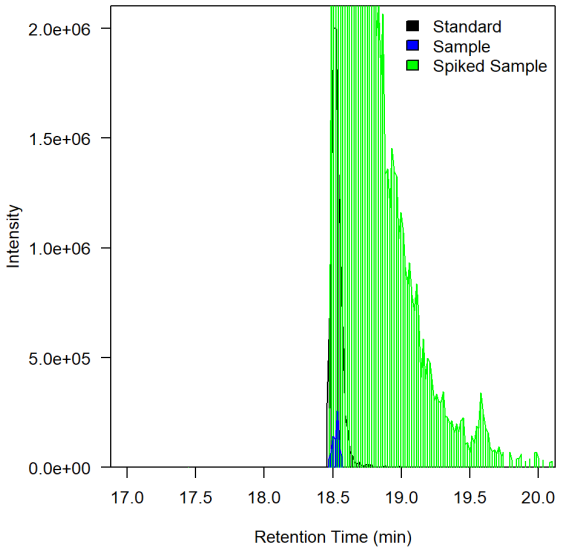

Most Intense Fragments in Sample

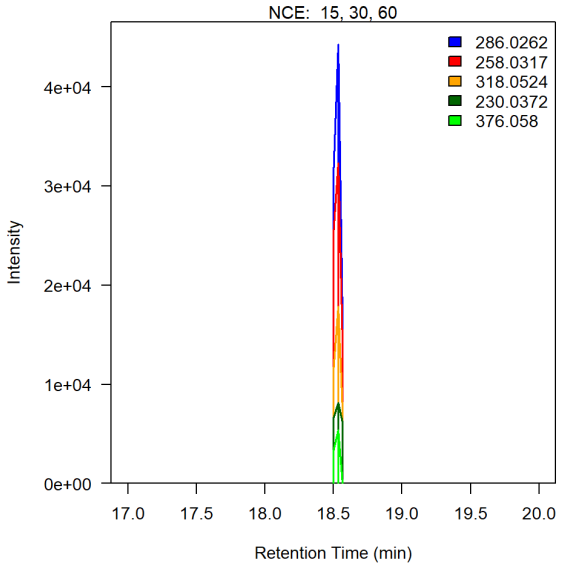

Most Intense MS2 Scan

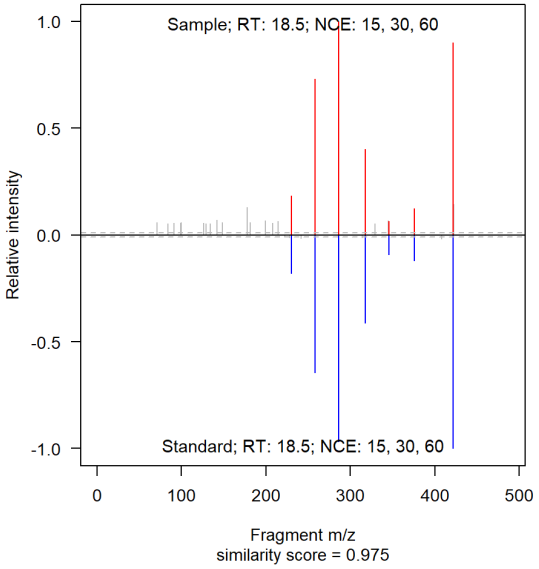

Most Intense Fragments in Standard

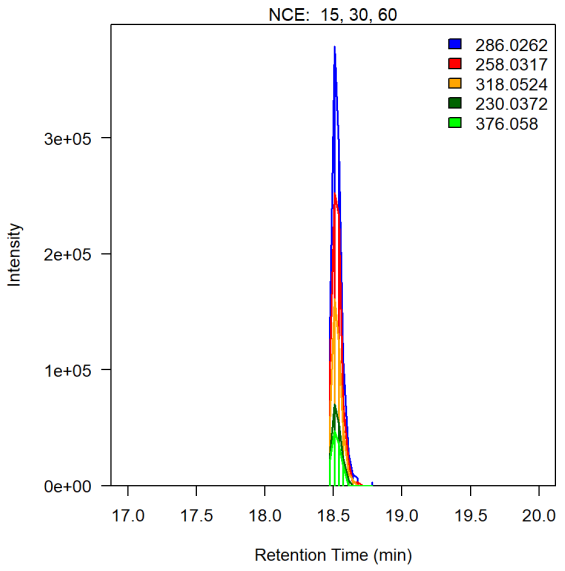

Xipamide
AGG39, Level 1
[M-H]- 353.03683
(STD 100 ng/L)

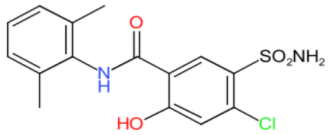

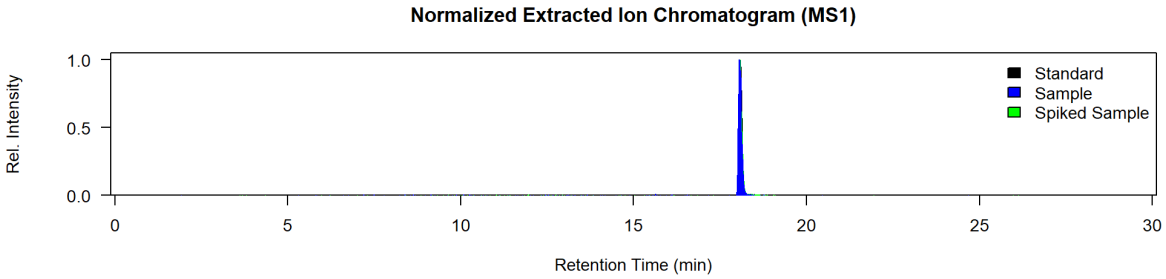

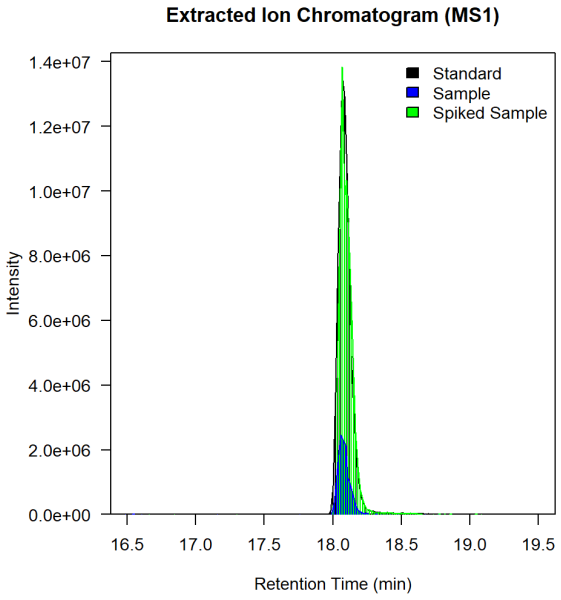

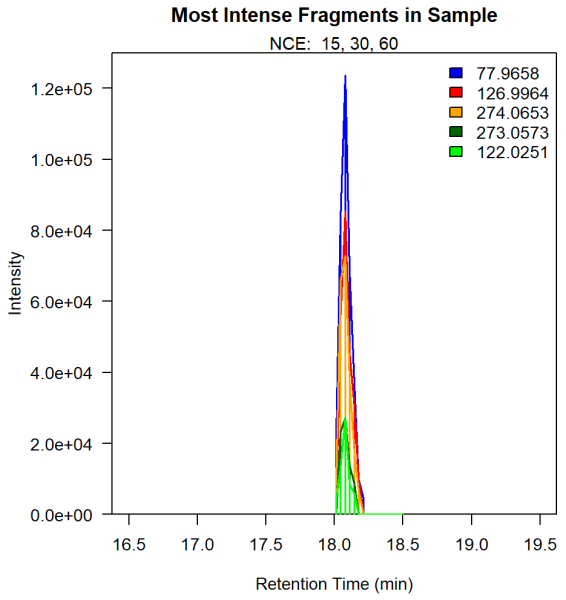

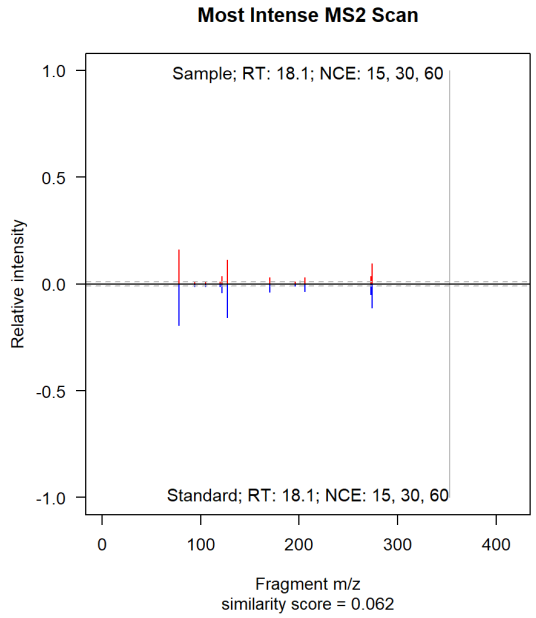

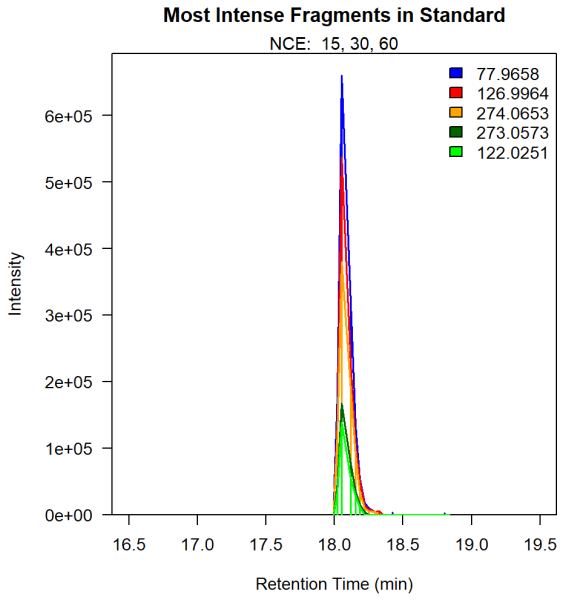

Metolachlor TP SYN542490
NTG41, Level 3
[M-H]- 342.10168

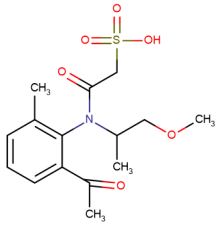

Extracted Ion Chromatogram (MS1)

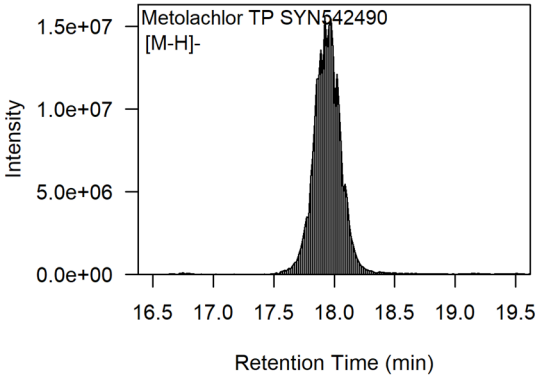

Most Intense Fragments in Sample

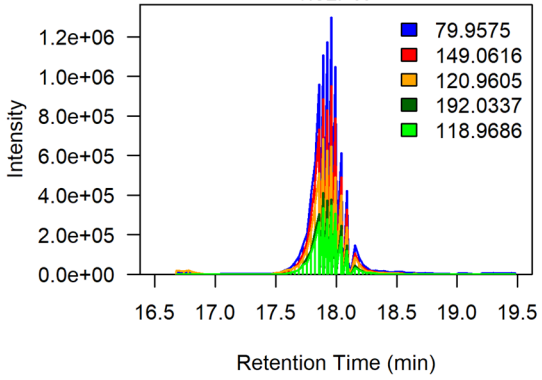

MS/MS Spectrum
Level 3

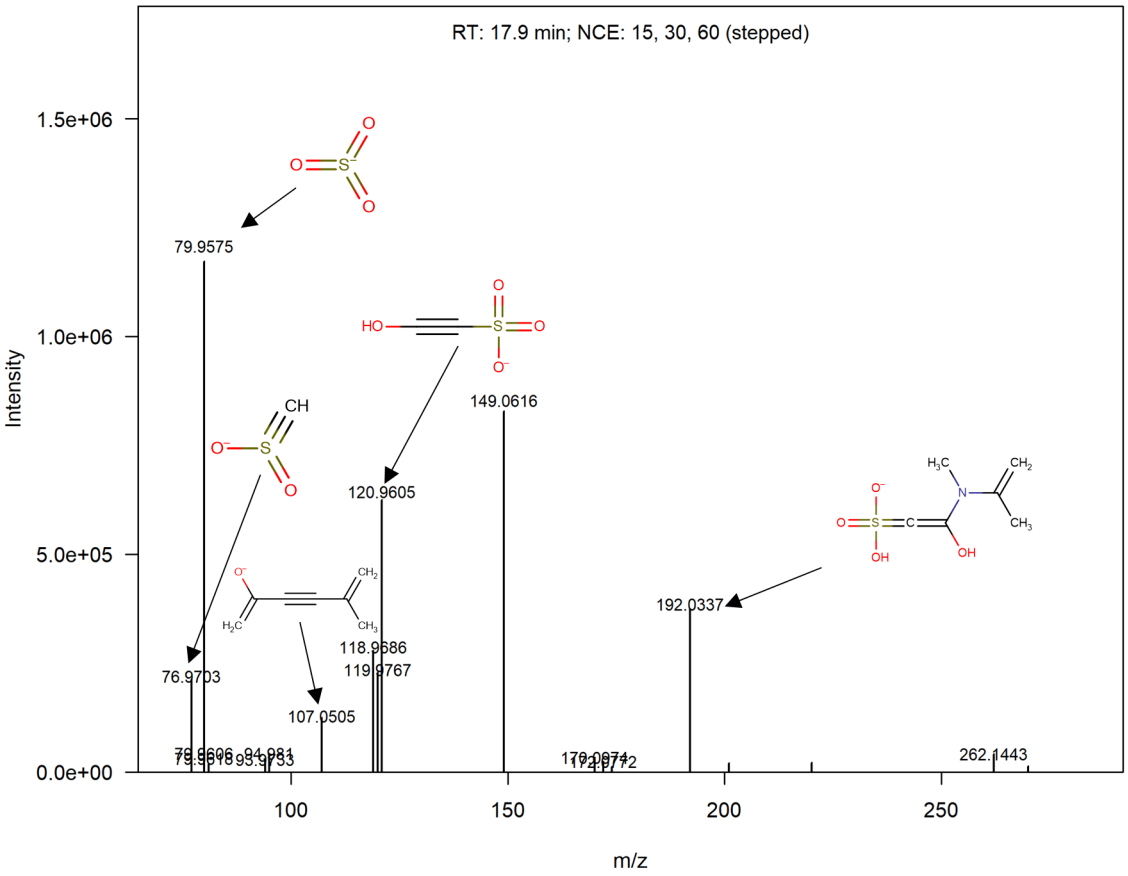

Metolachlor TP SYN547969 & SYN542488
NTG41, Level 3
[M-H]- 308.11396

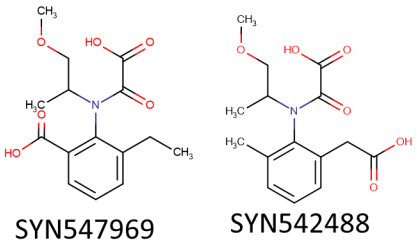

Extracted Ion Chromatogram (MS1)

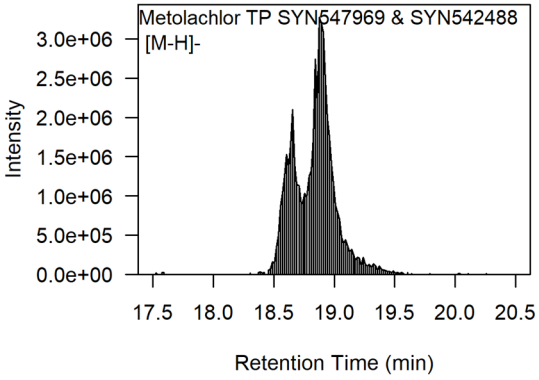

Most Intense Fragments in Sample

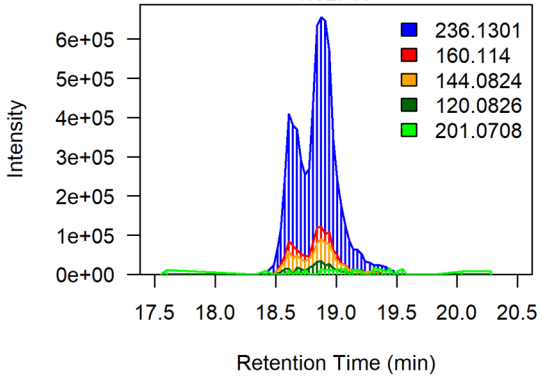

MS/MS Spectrum
Level 3

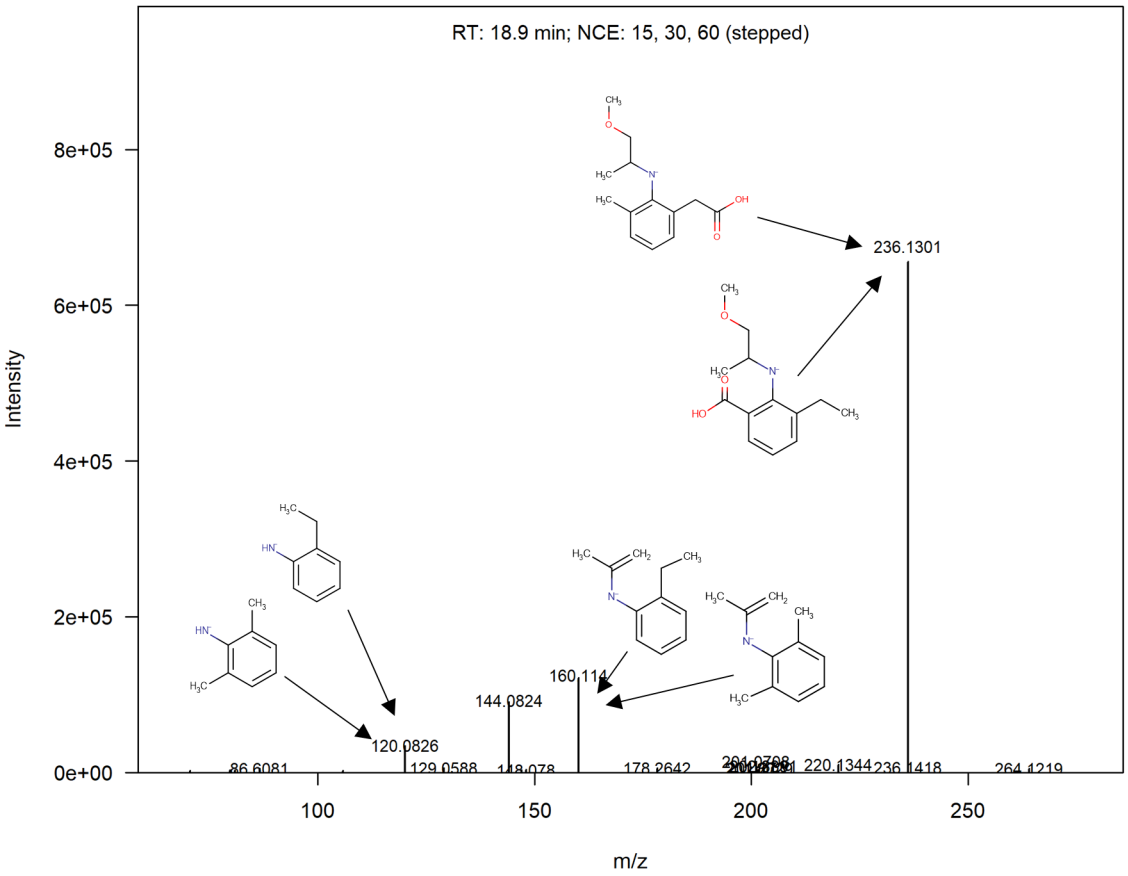

Metolachlor TP SYN547977
NTG41, Level 3
[M+H]+ 298.12045

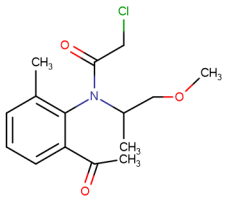

Extracted Ion Chromatogram (MS1)

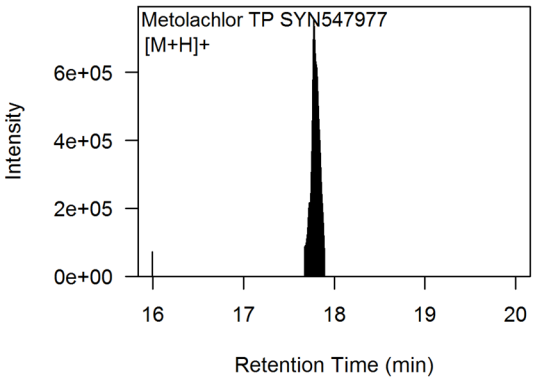

Most Intense Fragments in Sample

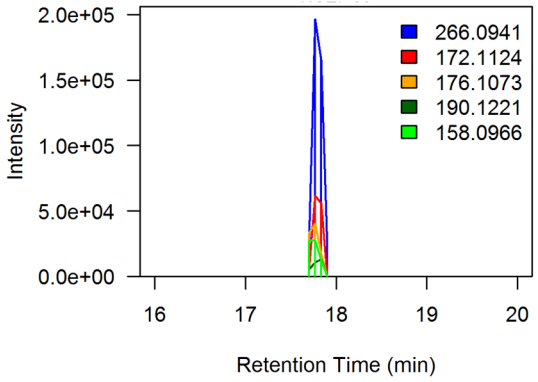

MS/MS Spectrum
Level 3

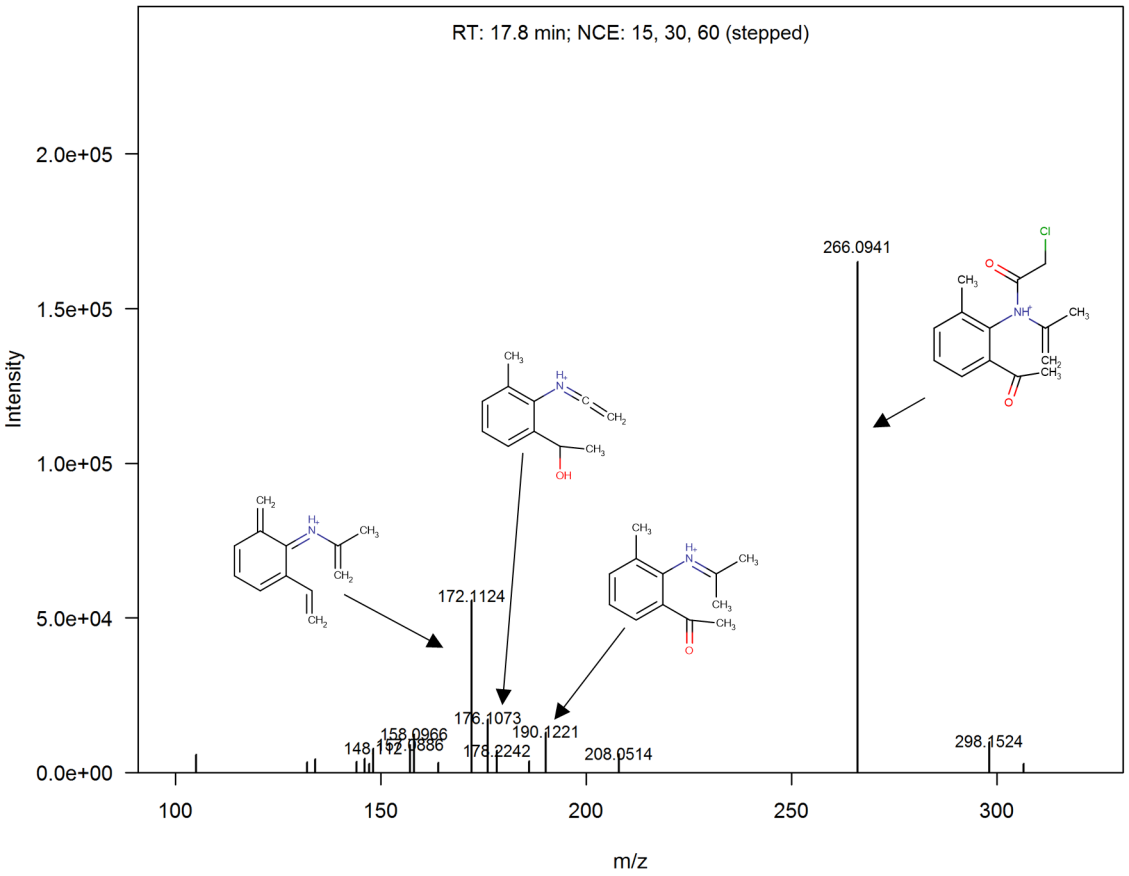

Metolachlor TP SYN542489
NTG41, Level 3
[M-H]- 294.1347

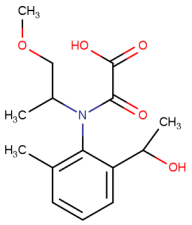

Extracted Ion Chromatogram (MS1)

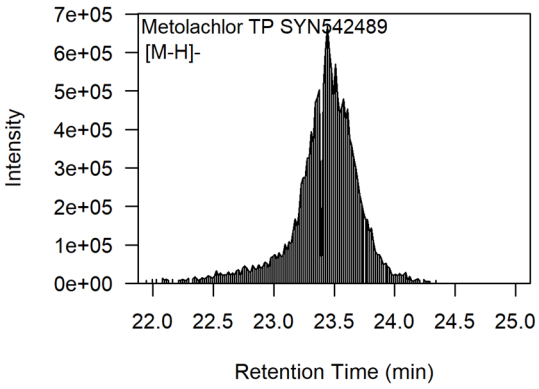

Most Intense Fragments in Sample

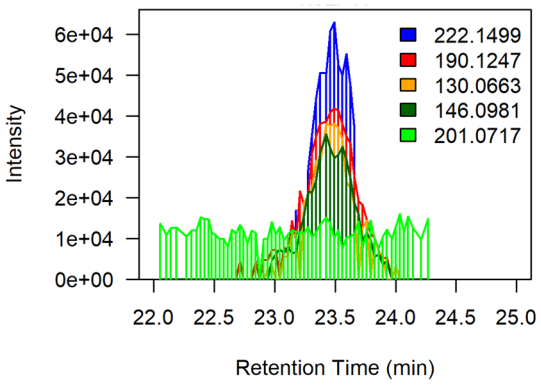

MS/MS Spectrum
Level 3

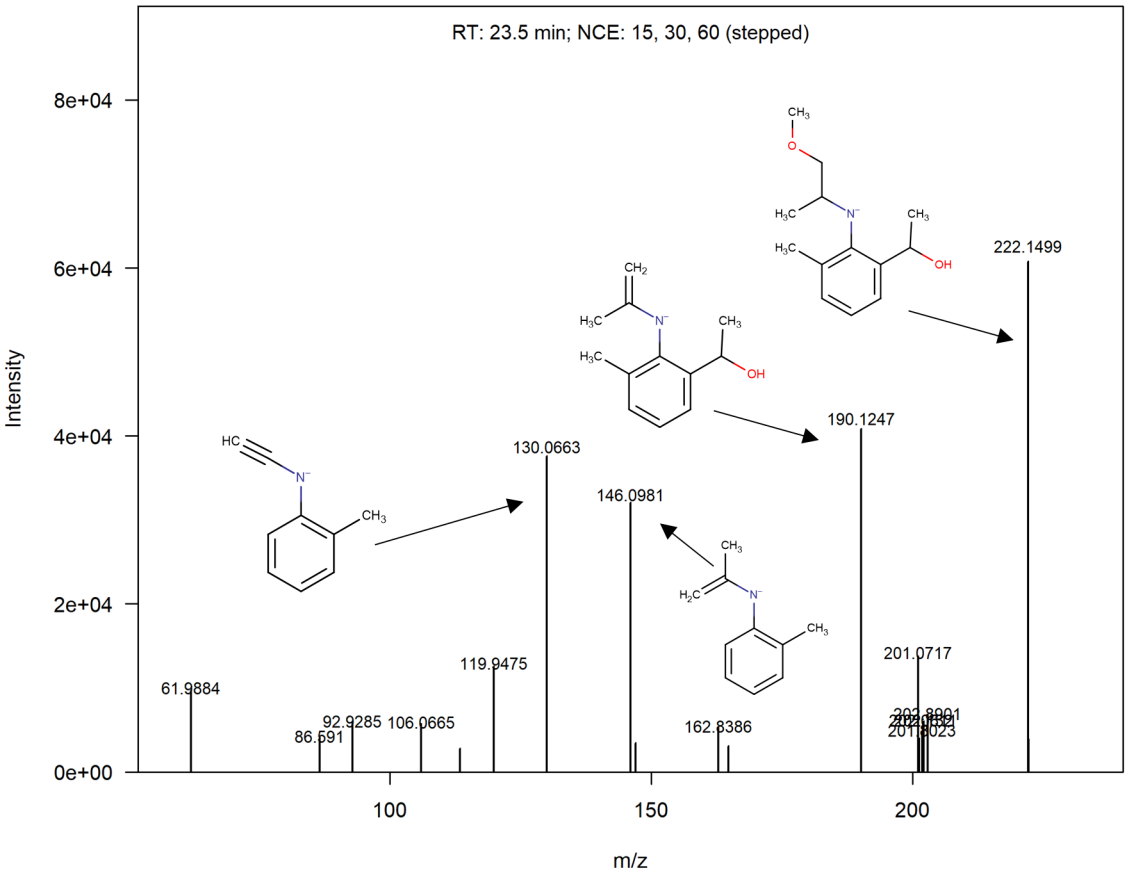

Metolachlor TP SYN542607
NTG41, Level 3
[M-H]- 344.11733

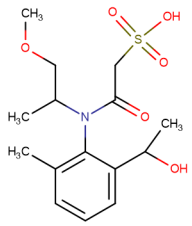

Extracted Ion Chromatogram (MS1)

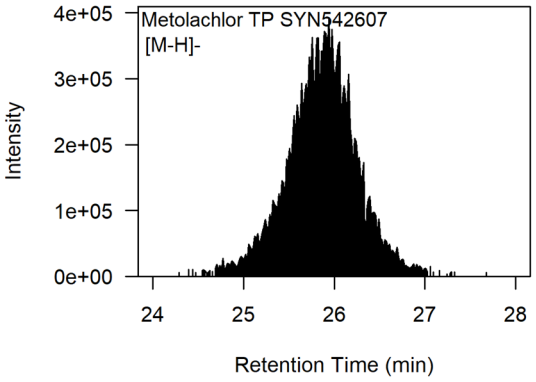

Most Intense Fragments in Sample

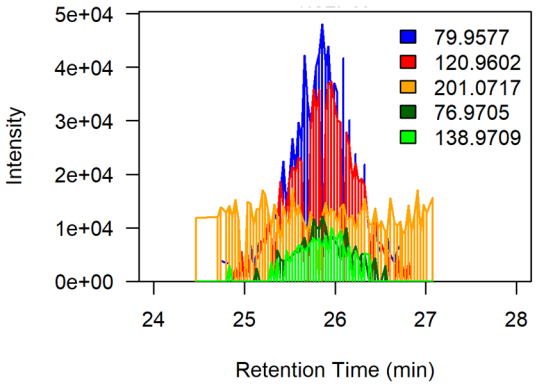

MS/MS Spectrum
Level 3

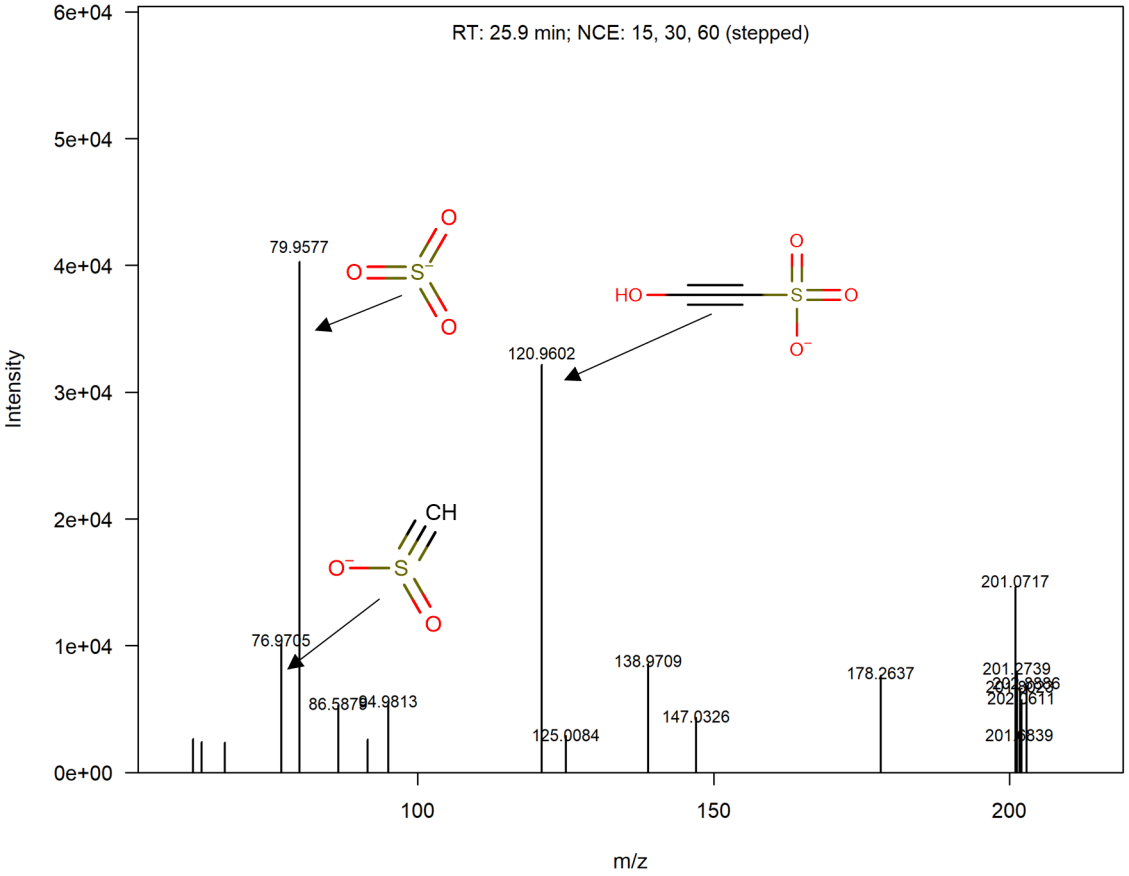

Metolachlor TP SYN542491
NTG41, Level 3
[M-H]- 294.09831

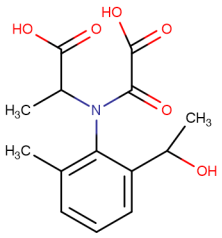

Extracted Ion Chromatogram (MS1)

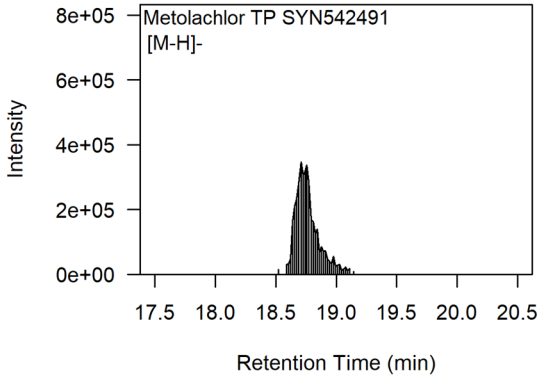

Most Intense Fragments in Sample

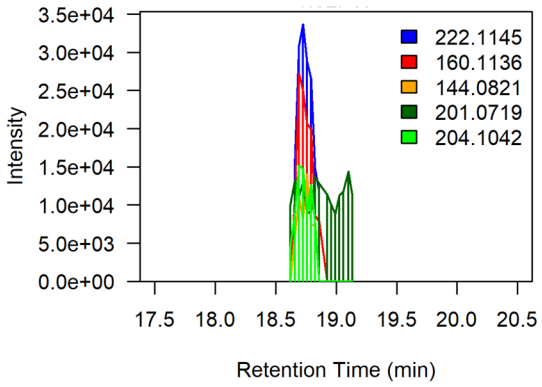

MS/MS Spectrum
Level 3

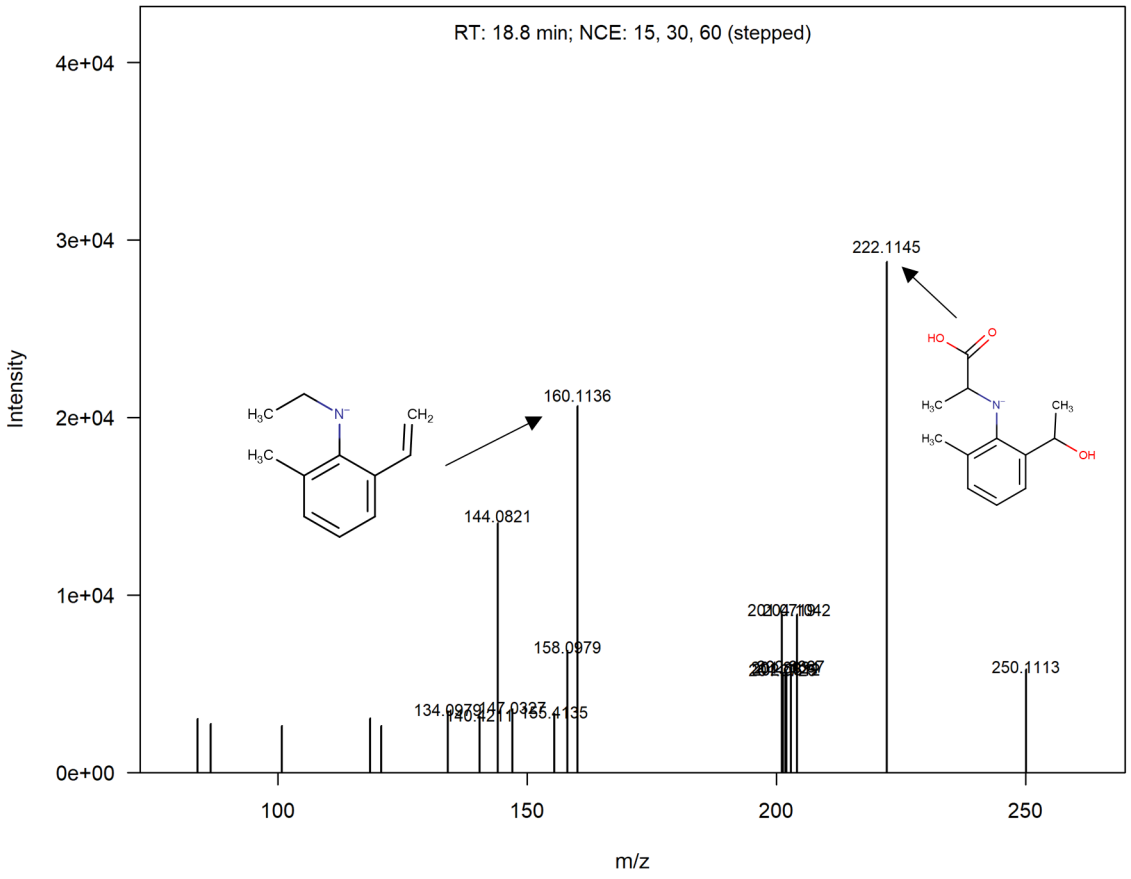

Pyroxsulam TP PSA
VDG27, Level 3
[M-H]- 255.98968

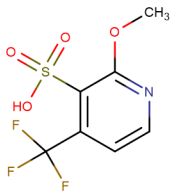

Extracted Ion Chromatogram (MS1)

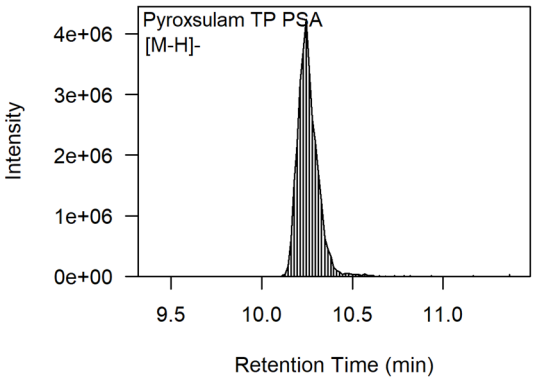

Most Intense Fragments in Sample

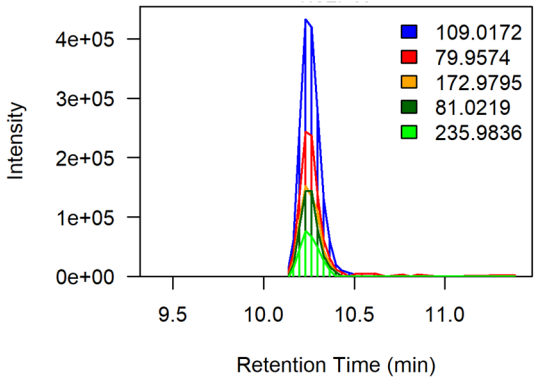

MS/MS Spectrum
Level 3

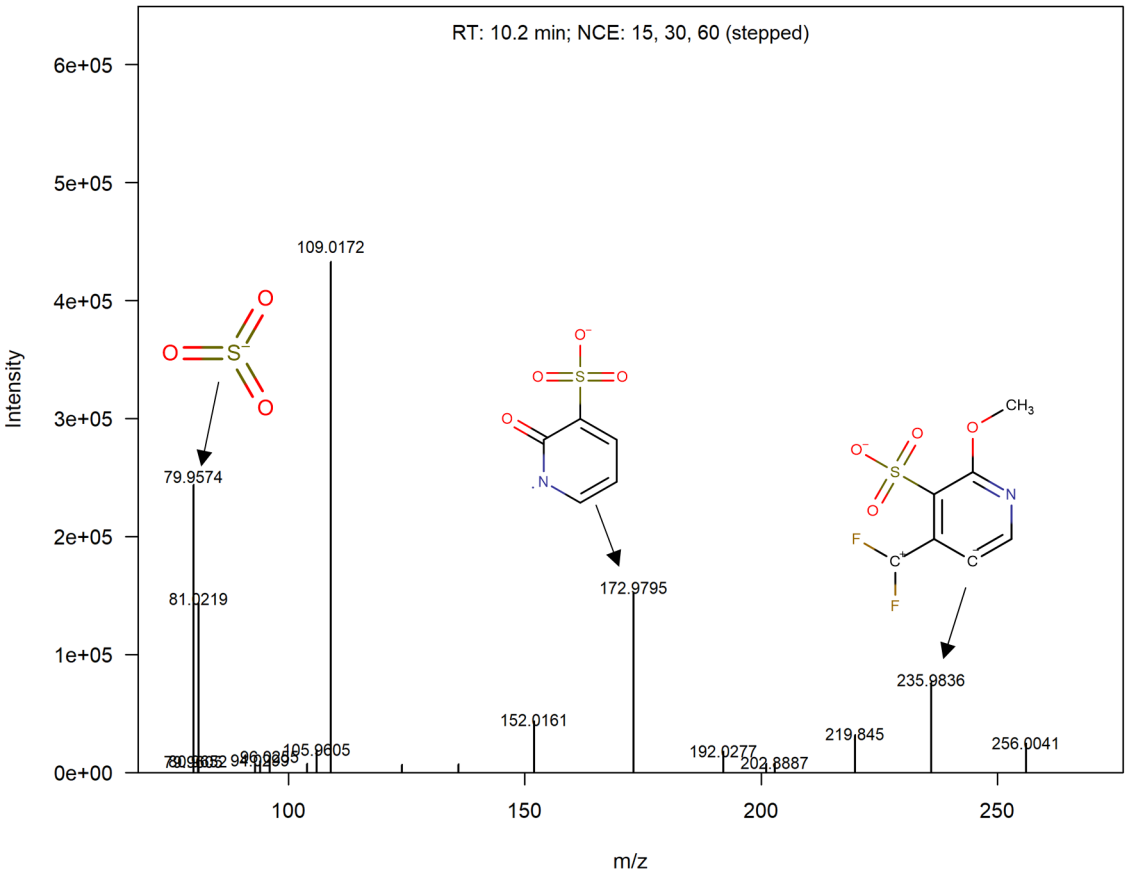

Trifluoroacetic acid
VDQ28, Level 1
[M-H]- 112.98559
(STD 1000 ng/L)

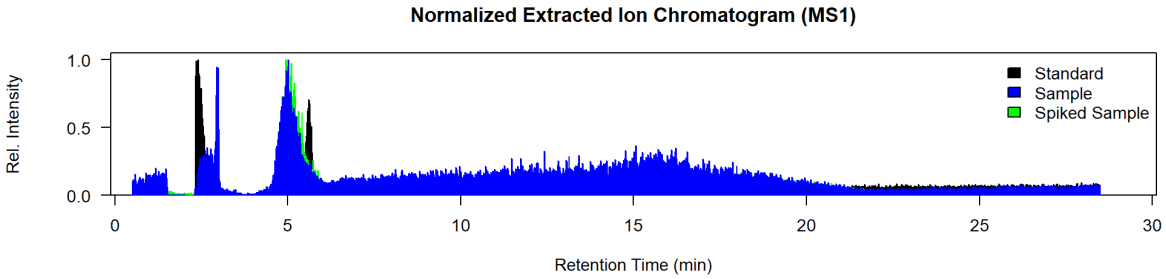

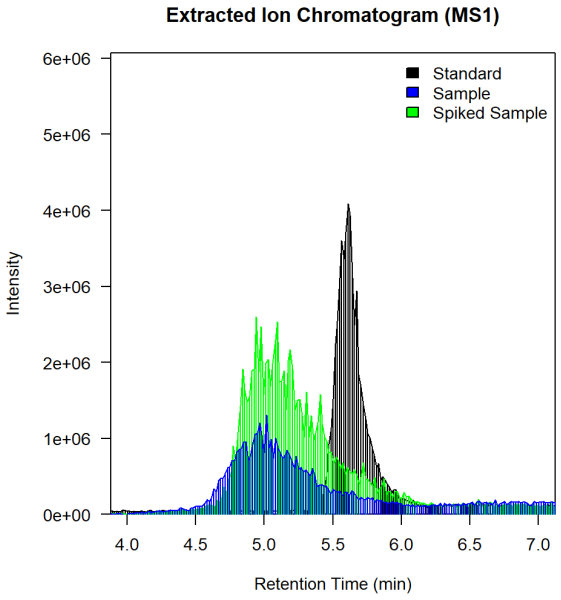

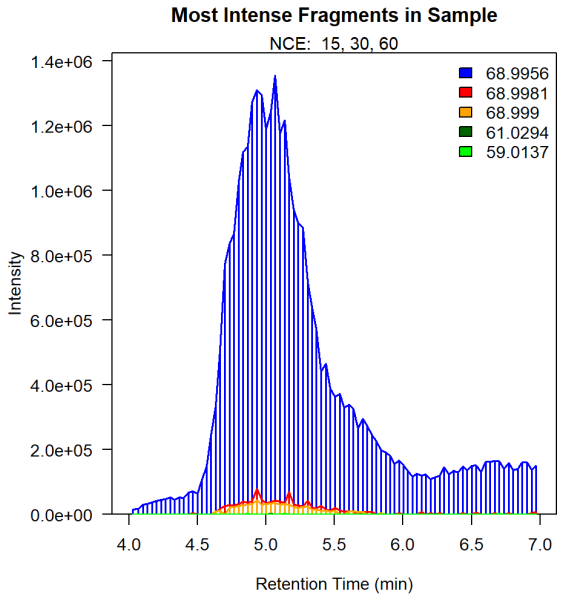

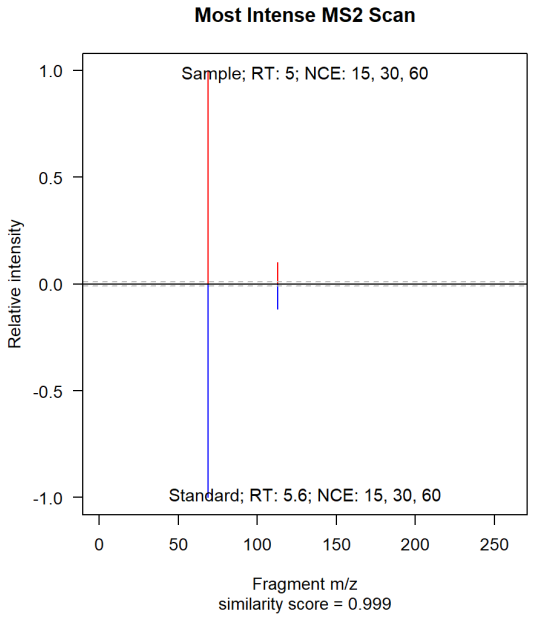

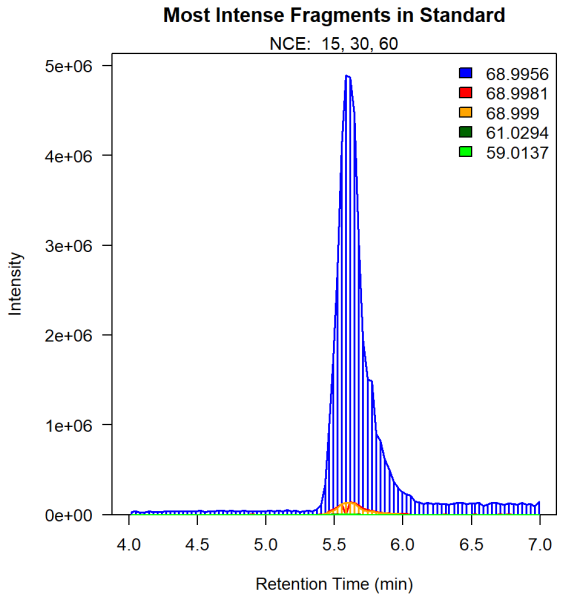

Trifluoromethanesulphonic acid
Pooled Sample, Level 1
[M-H]- 148.95257
(STD 100 ng/L)

Normalized Extracted Ion Chromatogram (MS1)

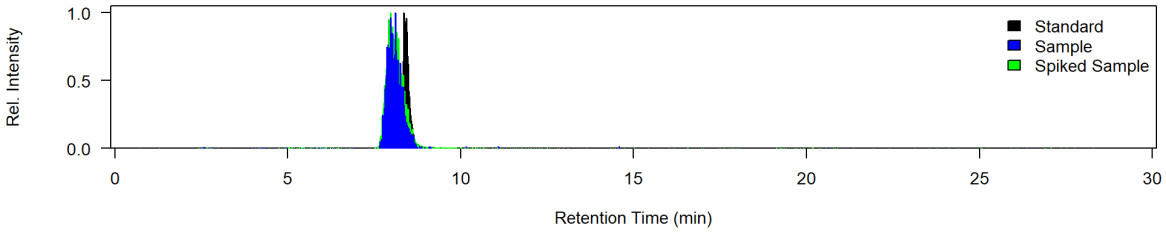

Extracted Ion Chromatogram (MS1)

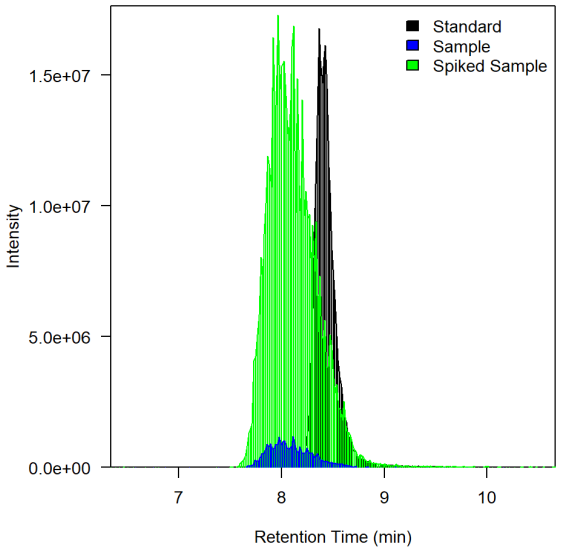

Most Intense Fragments in Sample

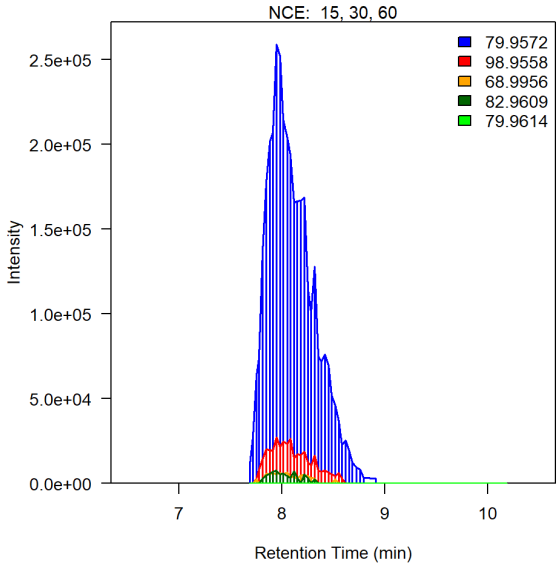

Most Intense MS2 Scan

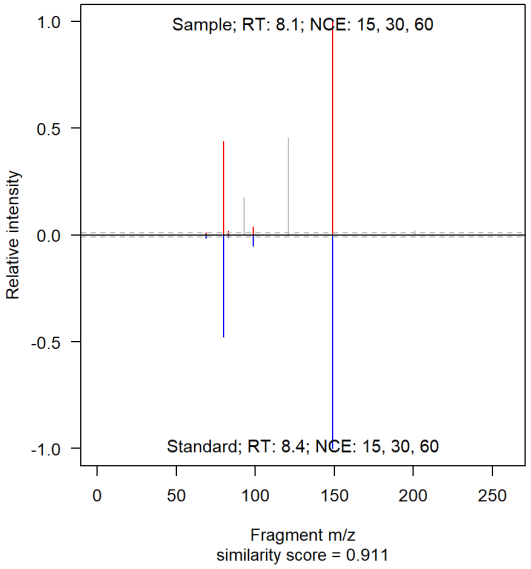

Most Intense Fragments in Standard

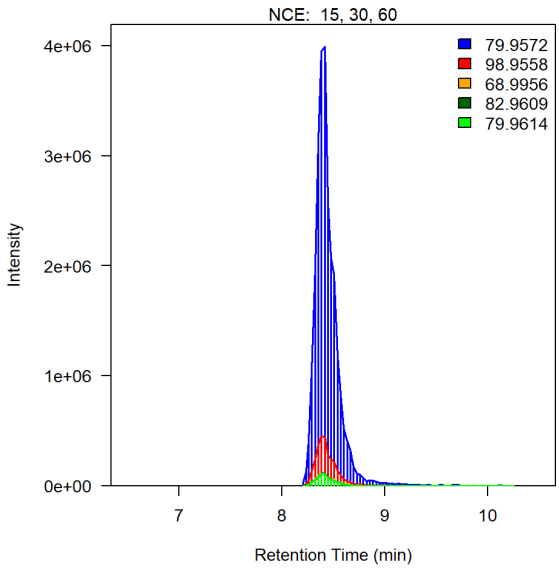

Atrazine-desethyl-desisopropyl
BSG05, Level 1
[M+H]+ 146.0228
(STD 100 ng/L)

Normalized Extracted Ion Chromatogram (MS1)

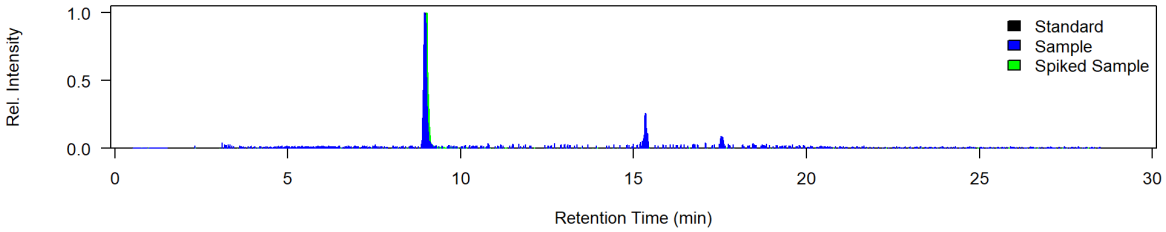

Extracted Ion Chromatogram (MS1)

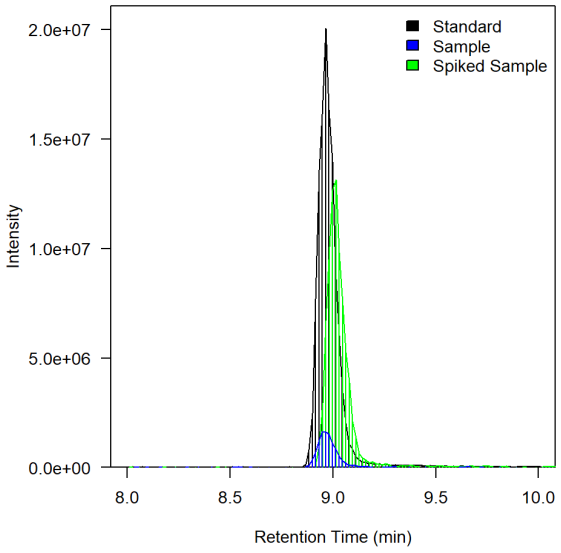

Most Intense Fragments in Sample

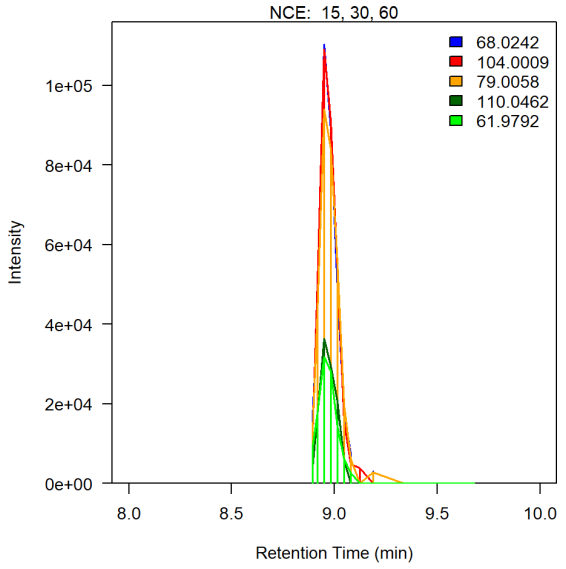

Most Intense MS2 Scan

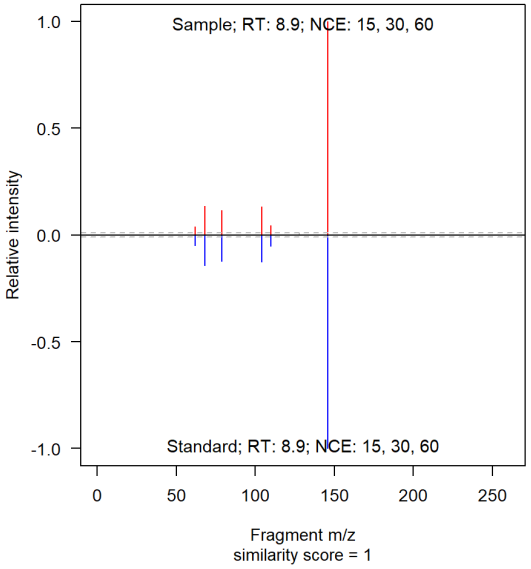

Most Intense Fragments in Standard

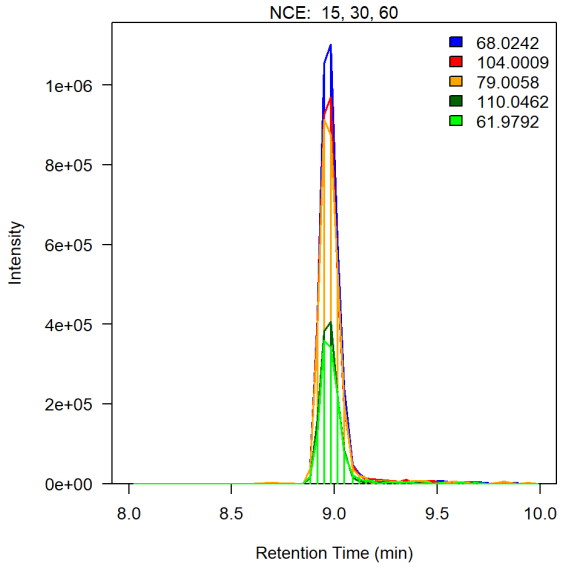

Perfluoropropanesulfonic Acid
BSG05, Level 1
[M-H]- 248.94619
(STD 100 ng/L)

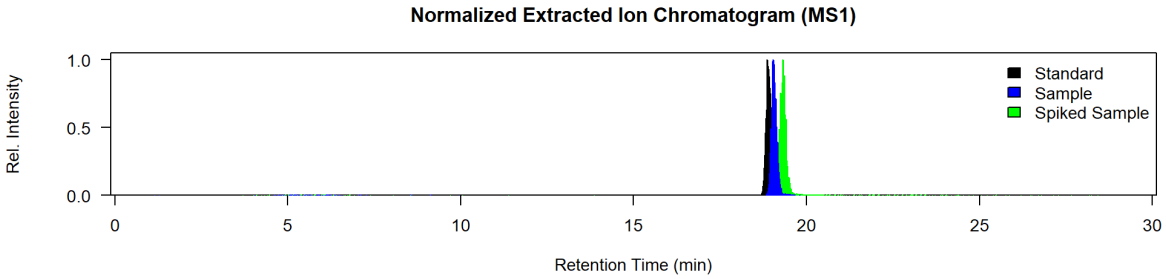

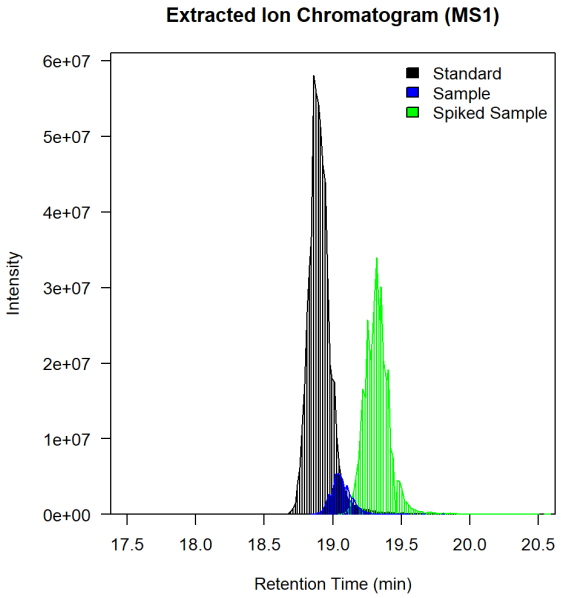

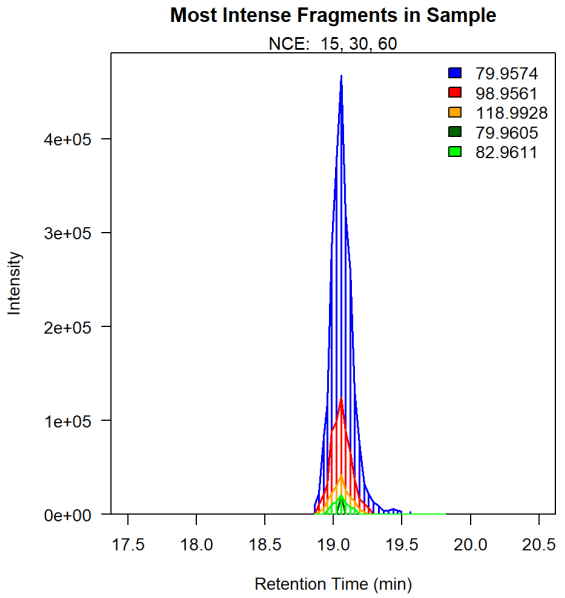

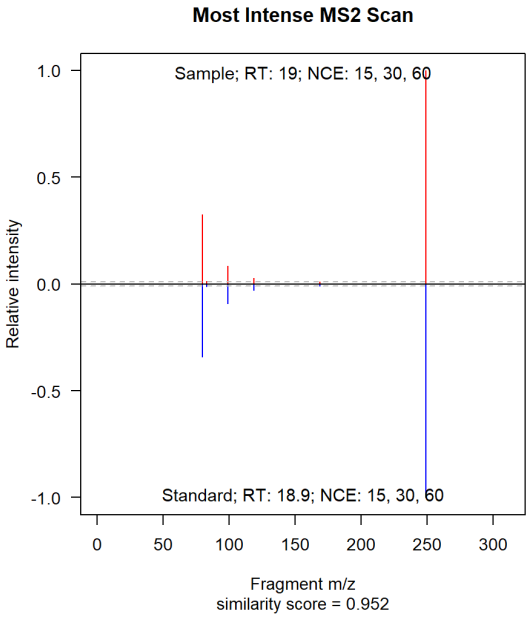

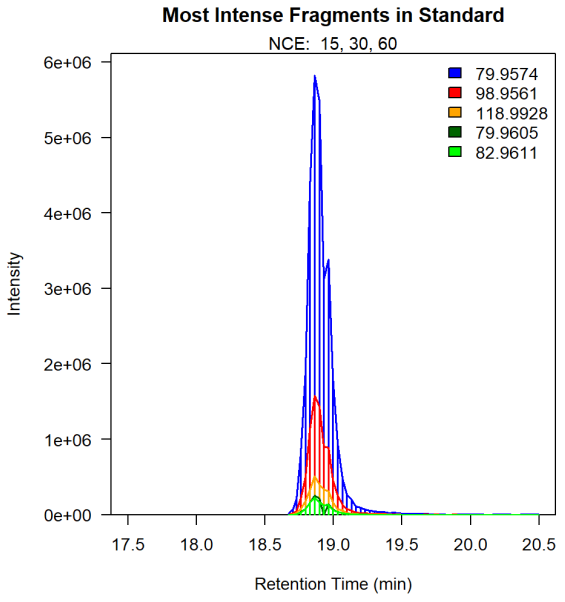

Oxypurinol
AGG28, Level 1
[M+H]+ 153.0407
(STD 1000 ng/L)

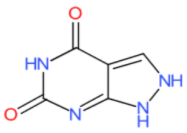

Normalized Extracted Ion Chromatogram (MS1)

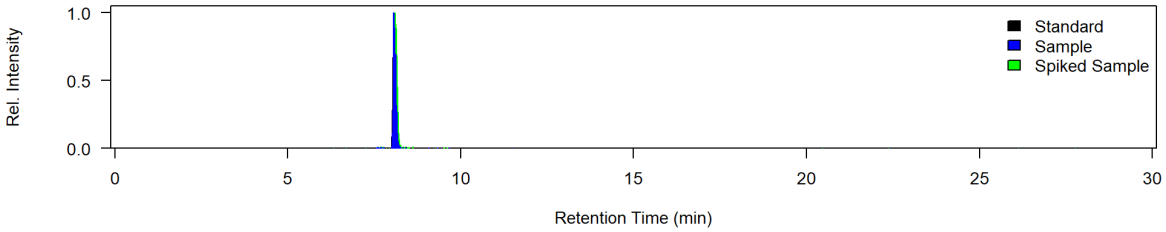

Extracted Ion Chromatogram (MS1)

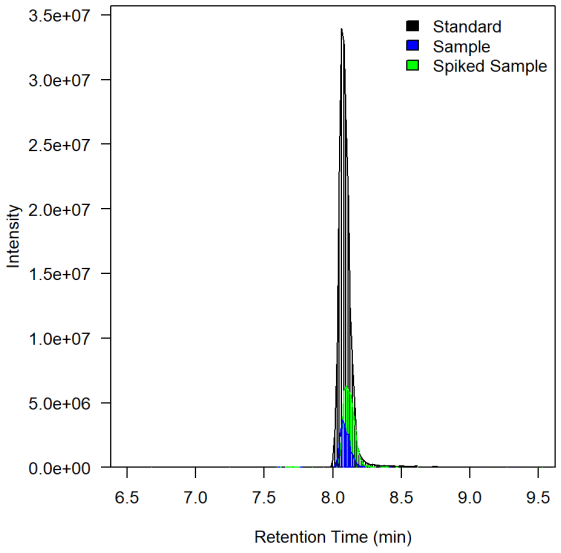

Most Intense Fragments in Sample

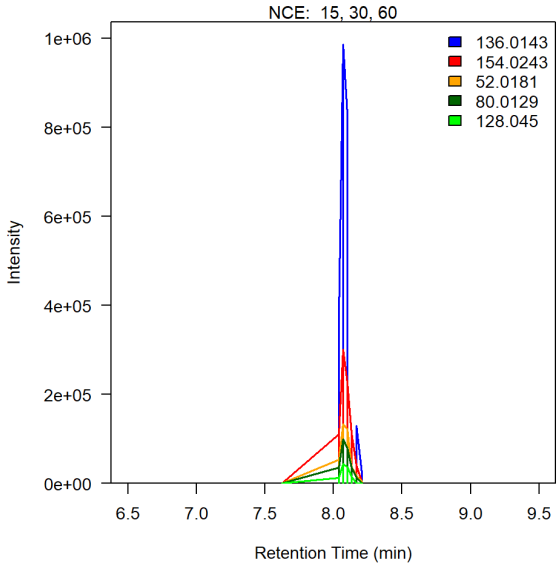

Most Intense MS2 Scan

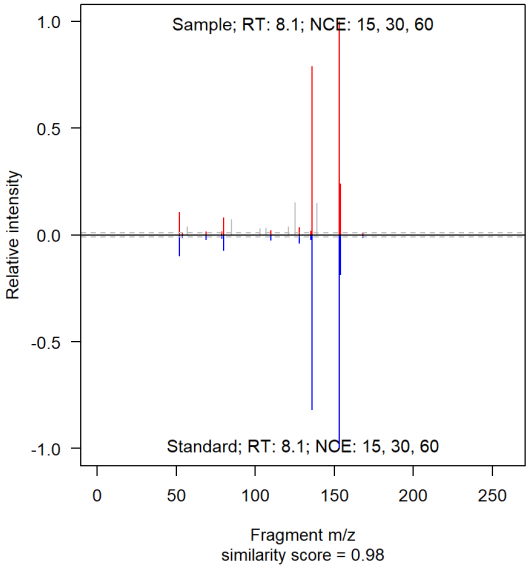

Most Intense Fragments in Standard

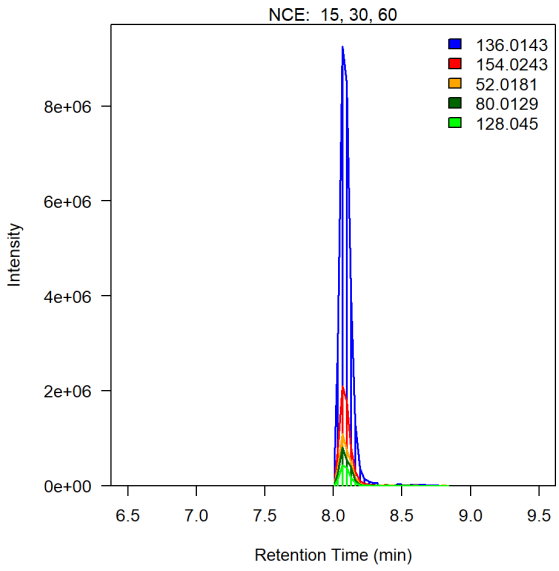

Oxypurinol
AGG28, Level 1
[M-H]- 151.02615
(STD 1000 ng/L)

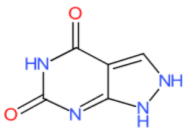

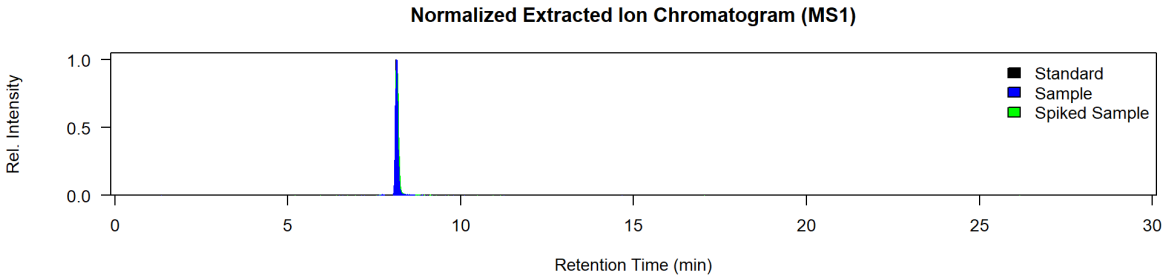

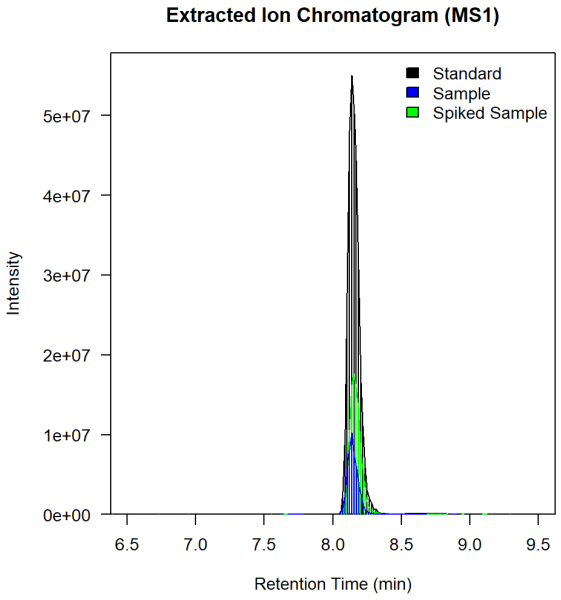

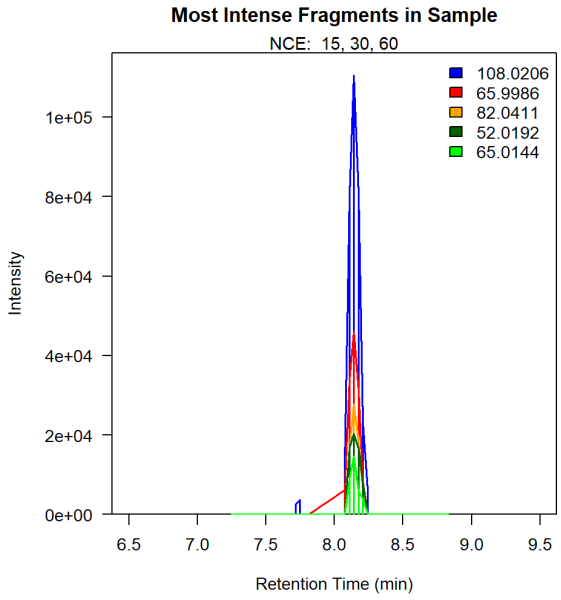

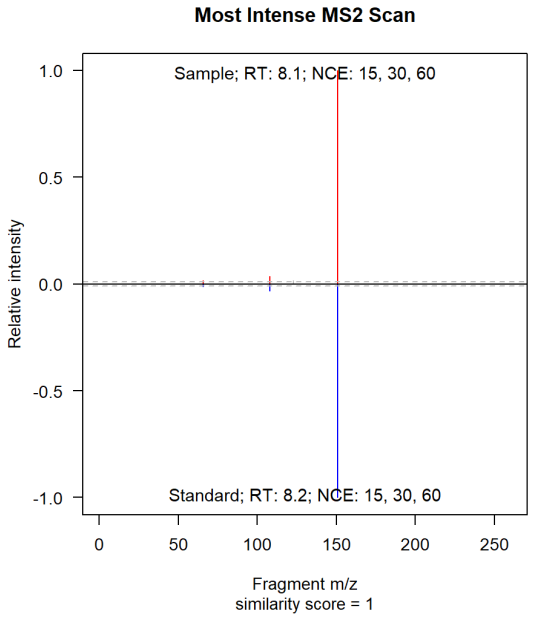

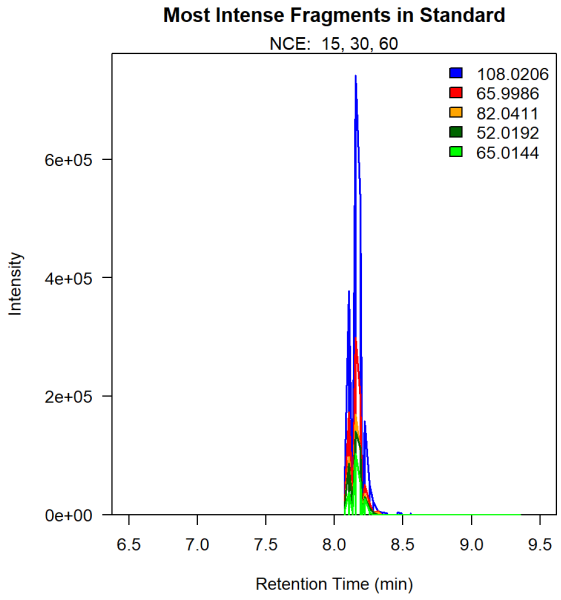

Methyldiphenylphosphine oxide
BLG10, Level 1
[M+H]+ 217.07768
(STD 0.1 mg/L, no enrichment)

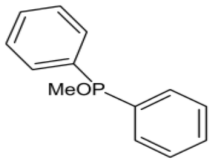

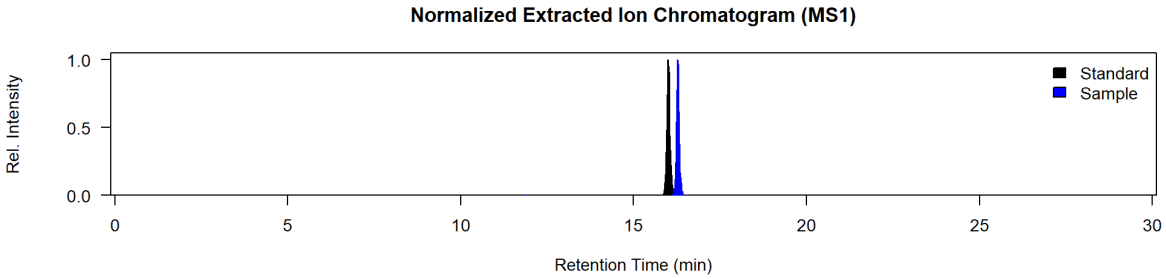

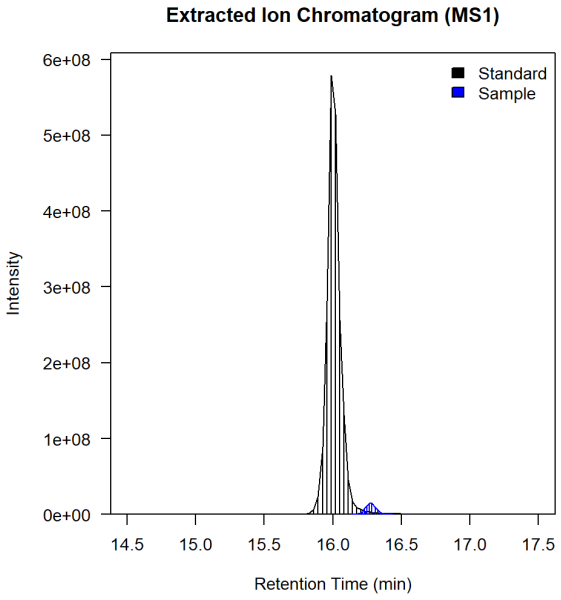

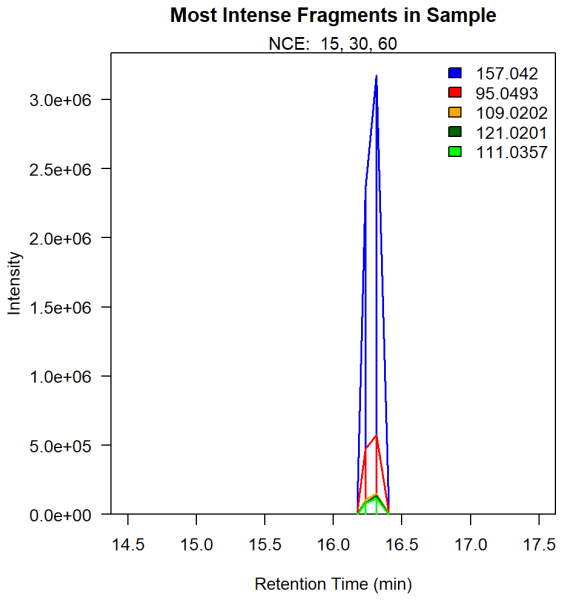

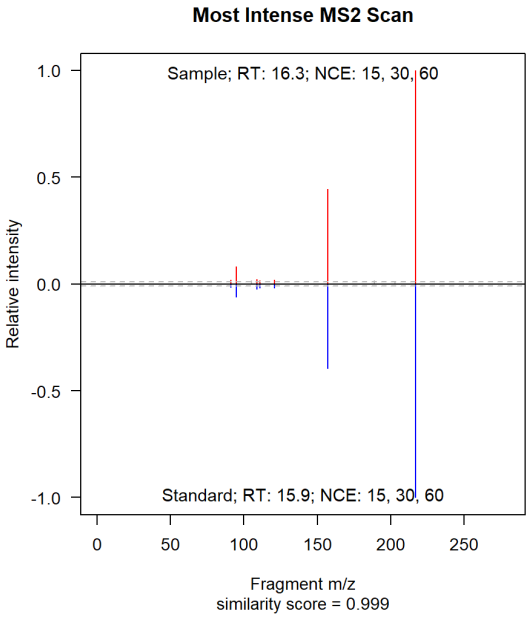

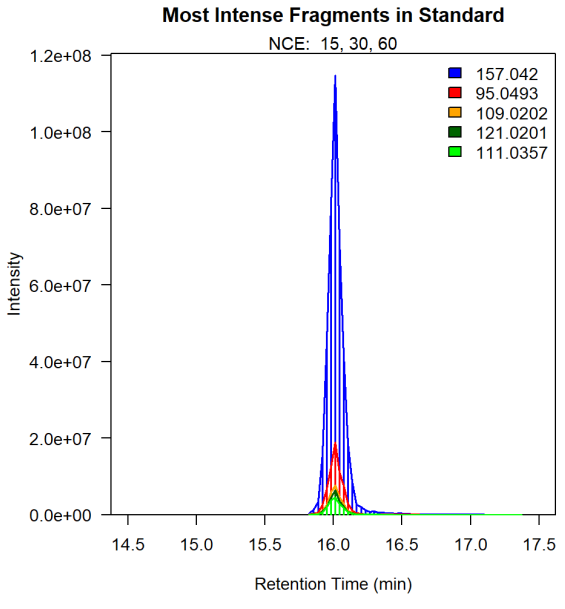

Sample and standard were injected in different sequences. Sample was not spiked.

Edetic acid (EDTA)
SHG05, Level 1
[M+H]+ 293.09794
(STD 100 ng/L)

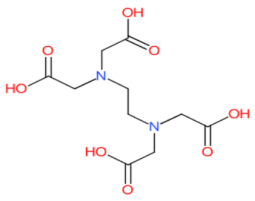

Normalized Extracted Ion Chromatogram (MS1)

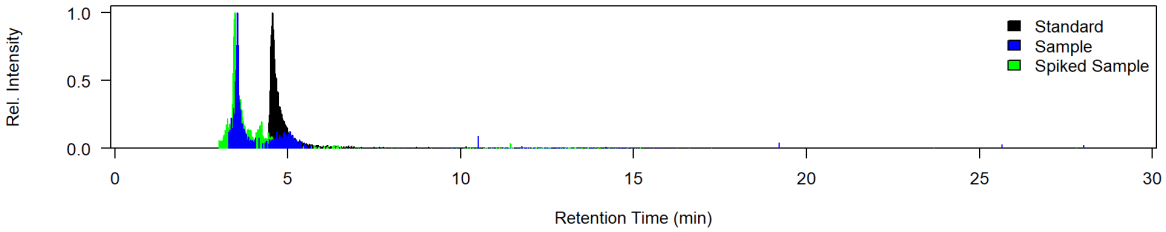

Extracted Ion Chromatogram (MS1)

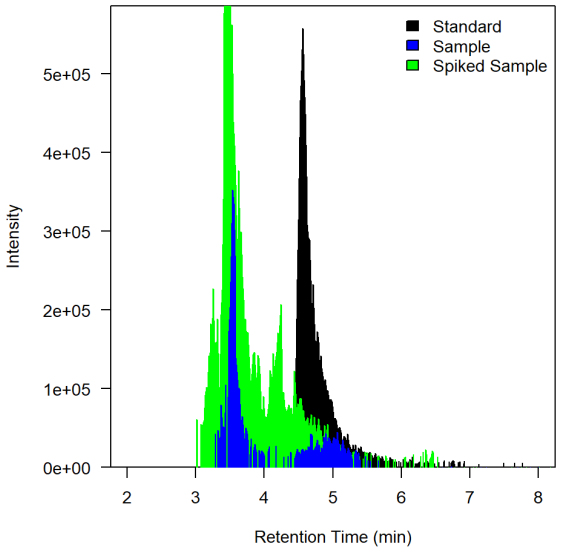

Most Intense Fragments in Sample

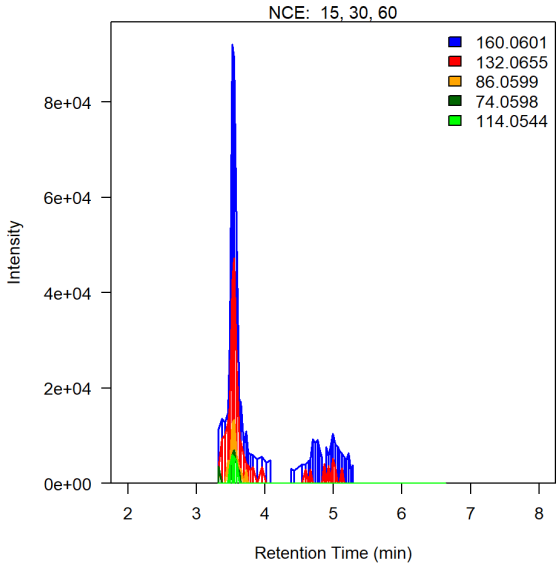

Most Intense MS2 Scan

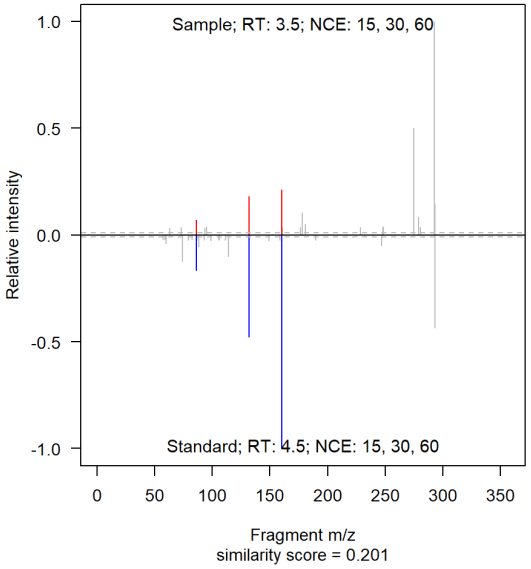

Most Intense Fragments in Standard

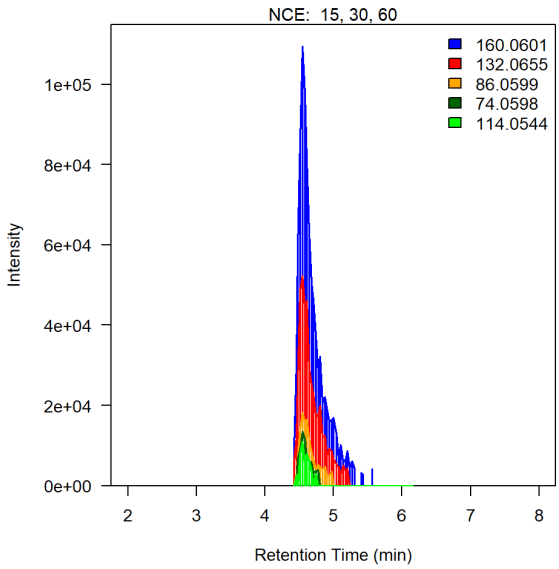

·Acrylamido-2-methyl-1-propanesulfonic acid (AMPS)
BSG05, Level 1
[M-H]- 206.04925
(STD 100 ng/L)

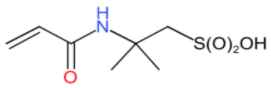

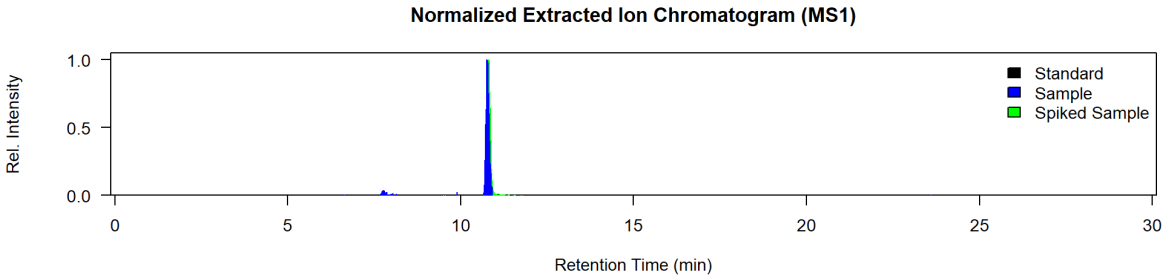

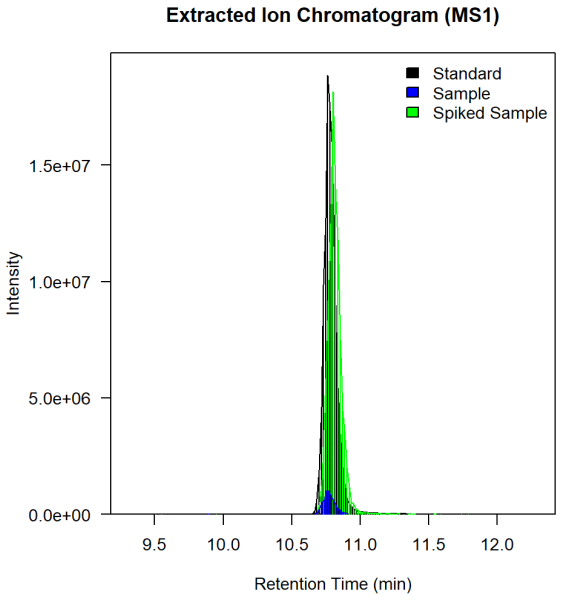

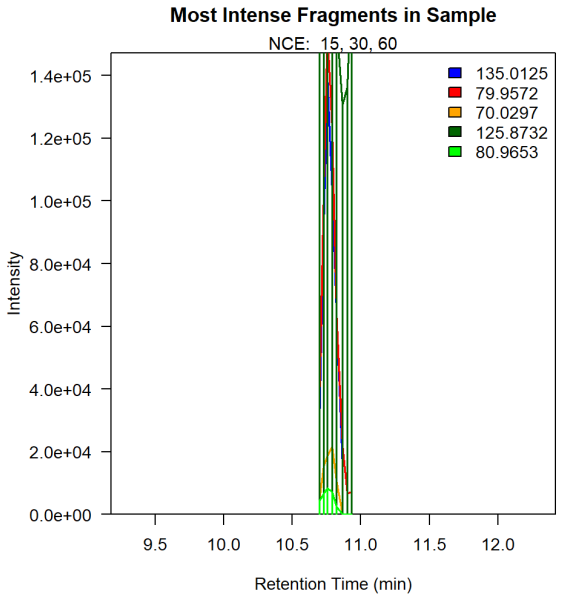

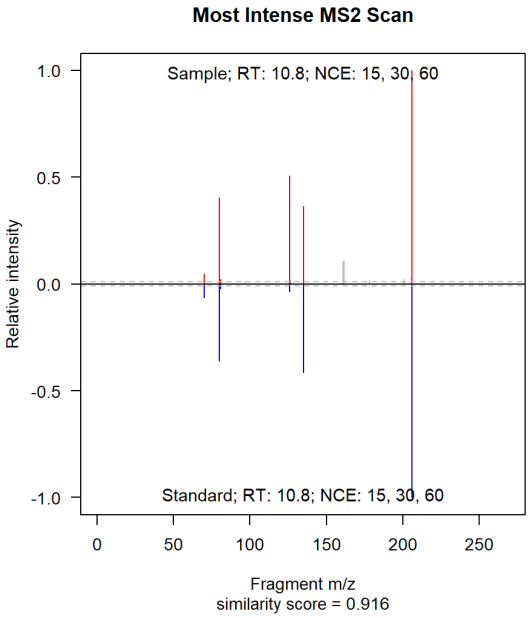

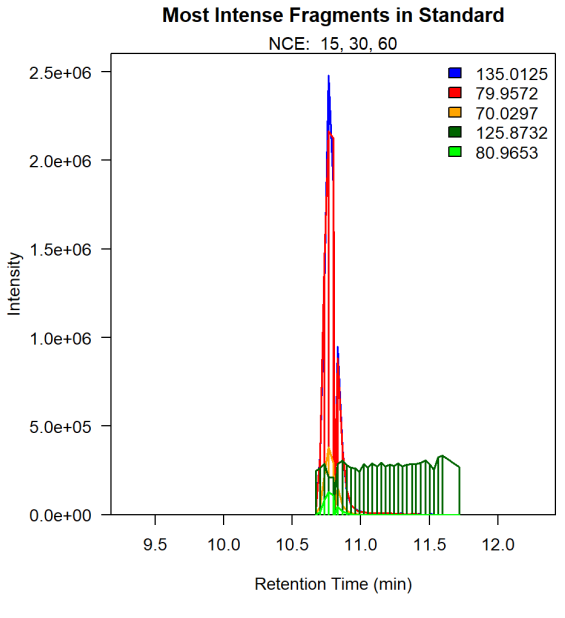

Perfluorobutylsulphonamide
Pooled Sample, Level 1
[M-H]- 297.95898
(STD 10 ng/L)

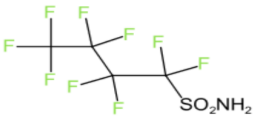

Normalized Extracted Ion Chromatogram (MS1)

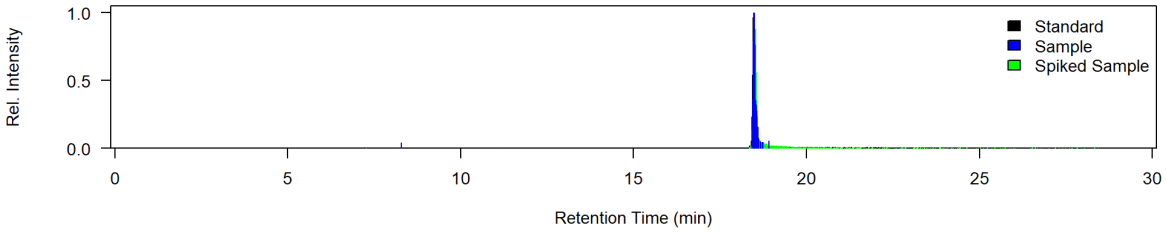

Extracted Ion Chromatogram (MS1)

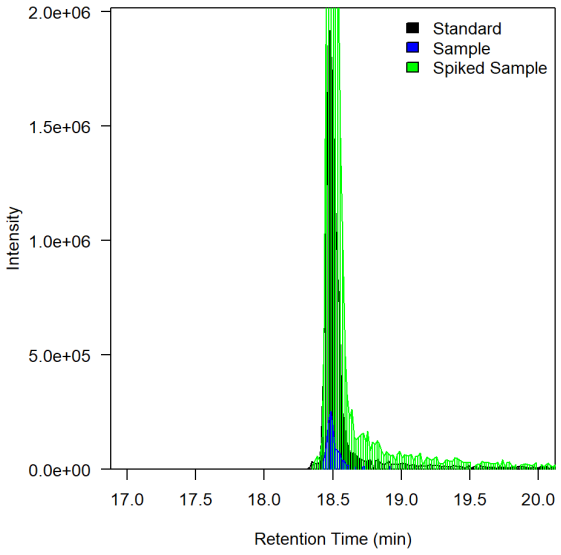

Most Intense Fragments in Sample

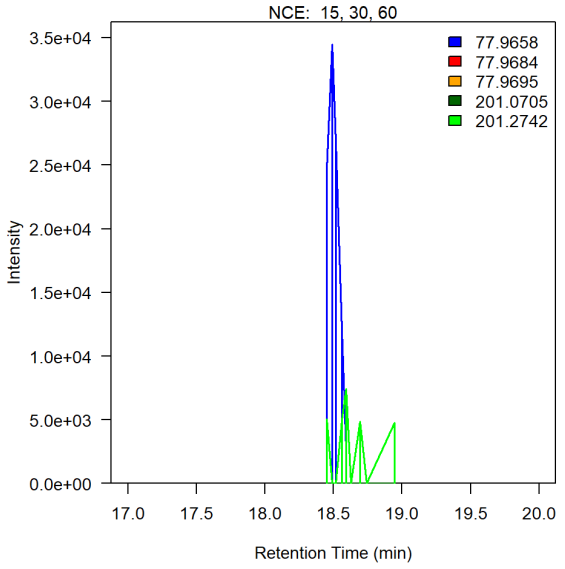

Most Intense MS2 Scan

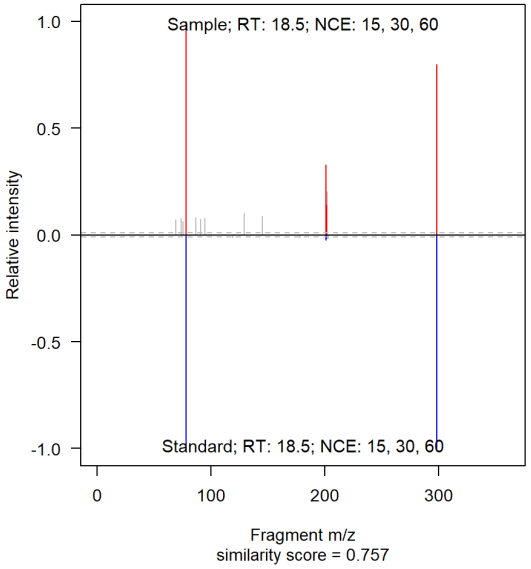

Most Intense Fragments in Standard

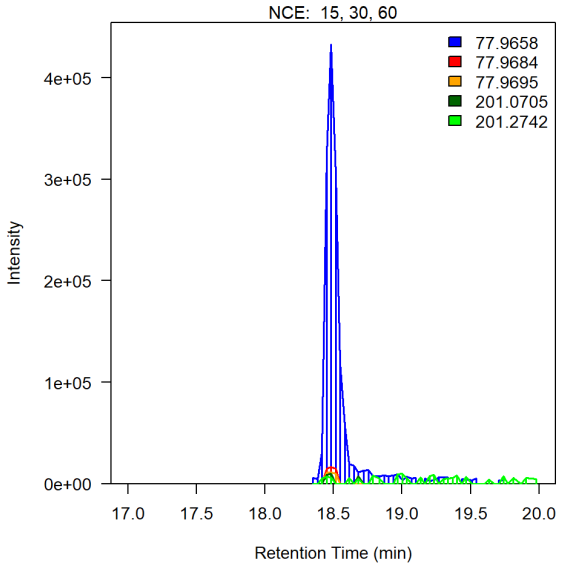

Methenamine
SHG05, Level 1
[M+H]+ 141.11347
(STD 100 ng/L)

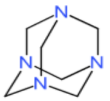

Normalized Extracted Ion Chromatogram (MS1)

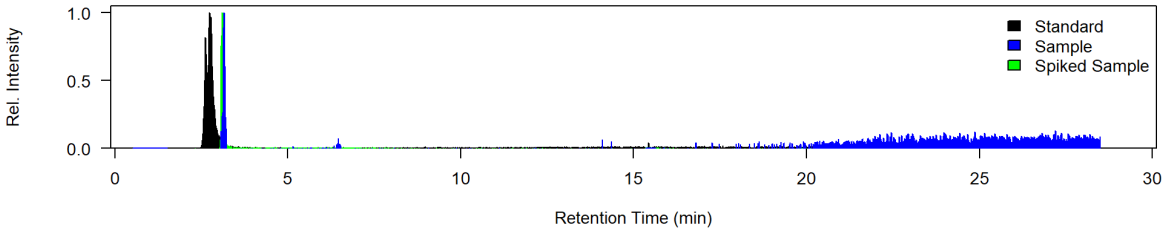

Extracted Ion Chromatogram (MS1)

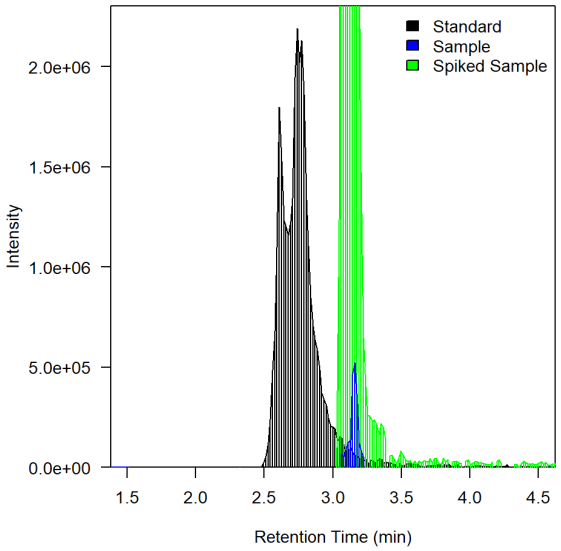

Most Intense Fragments in Sample

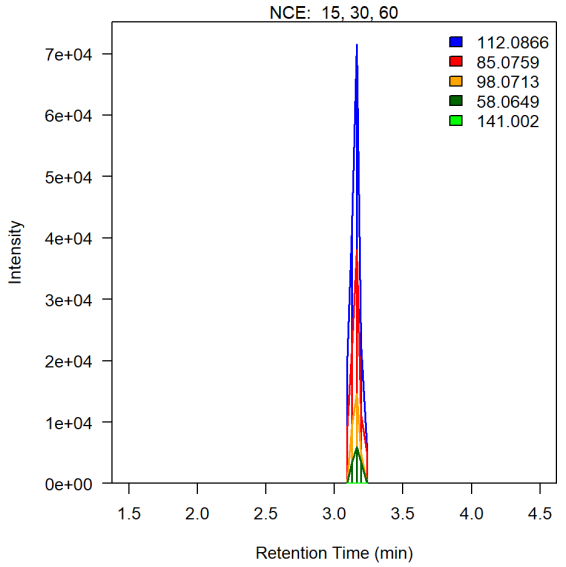

Most Intense MS2 Scan

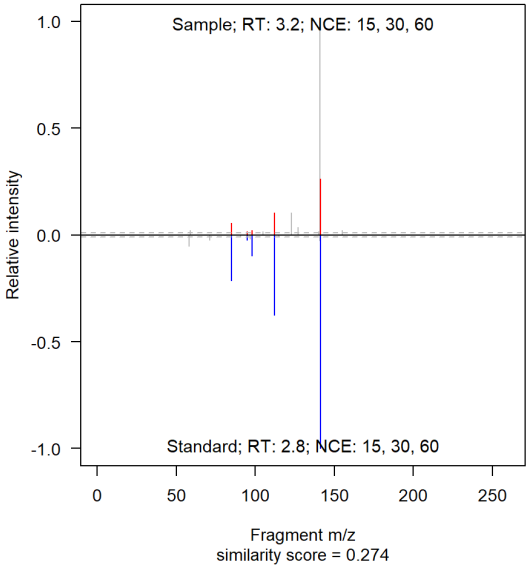

Most Intense Fragments in Standard

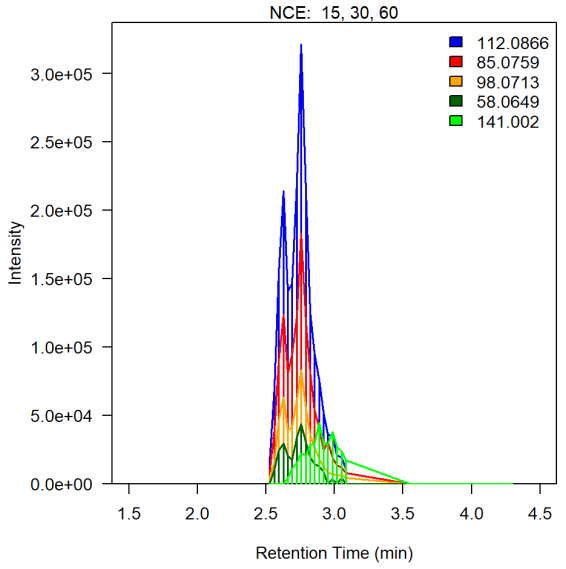

Dimethylbenzenesulfonic acid (isomers)
GEQ01, Level 1
[M-H]- 185.02779
(STD 100 ng/L)

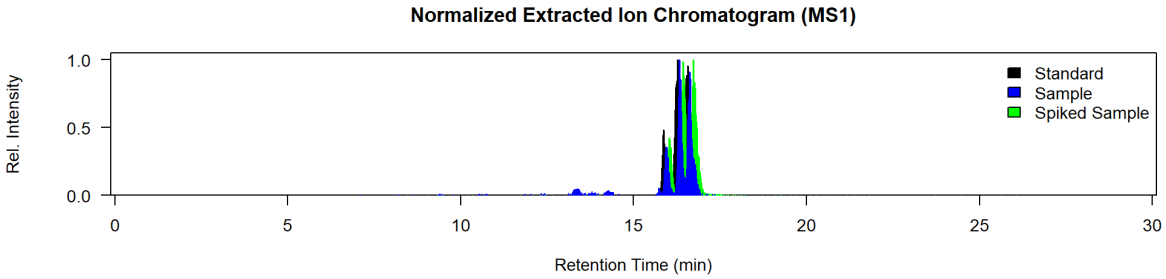

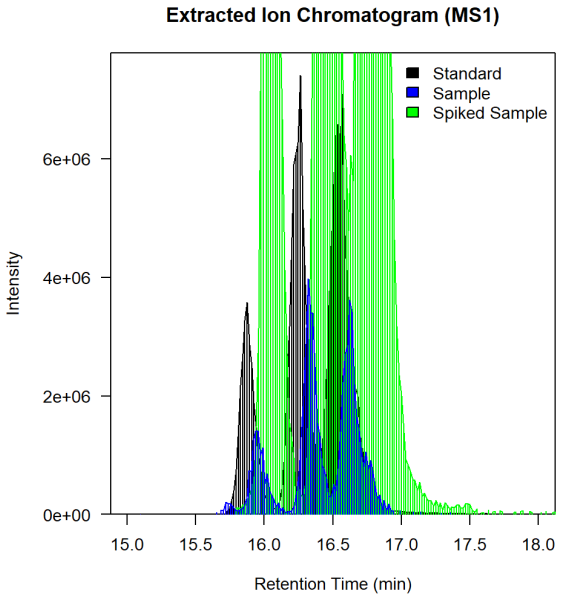

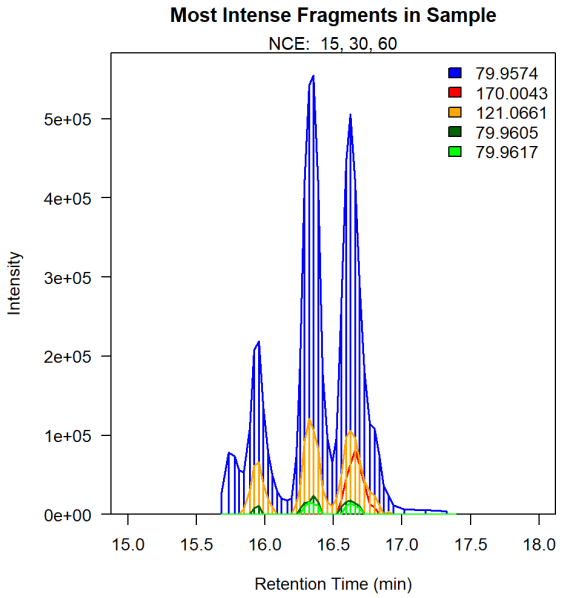

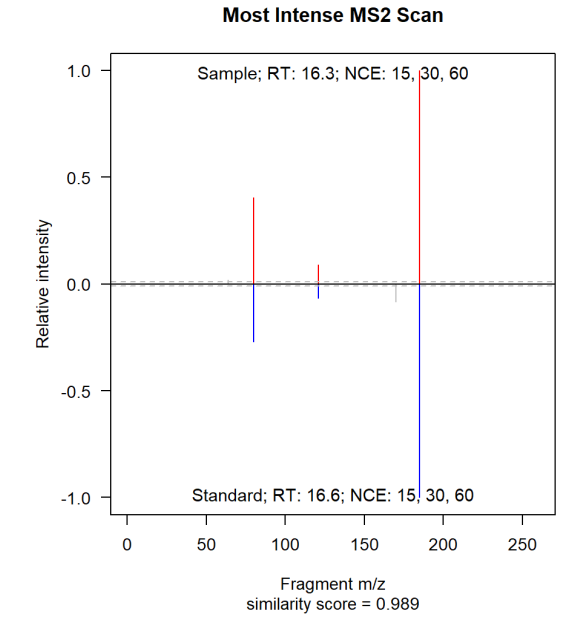

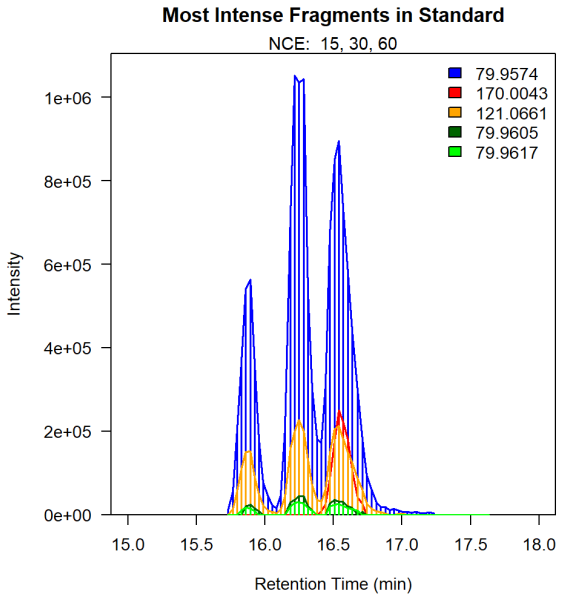

p-Toluenesulfonic acid
GEQ01, Level 1
[M-H]- 171.01214
(STD 1000 ng/L)

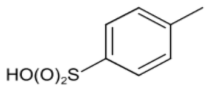

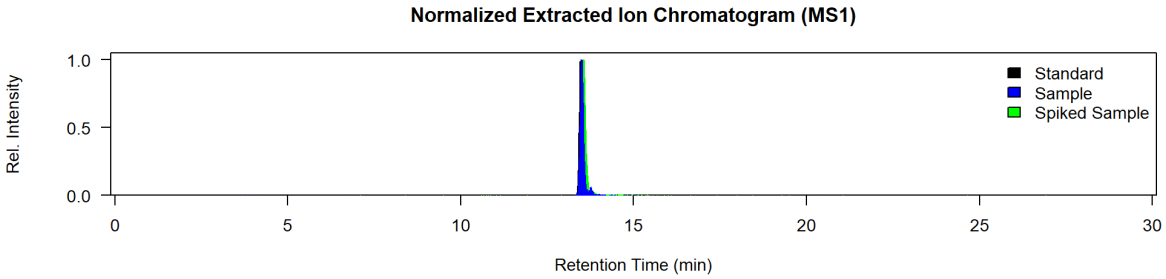

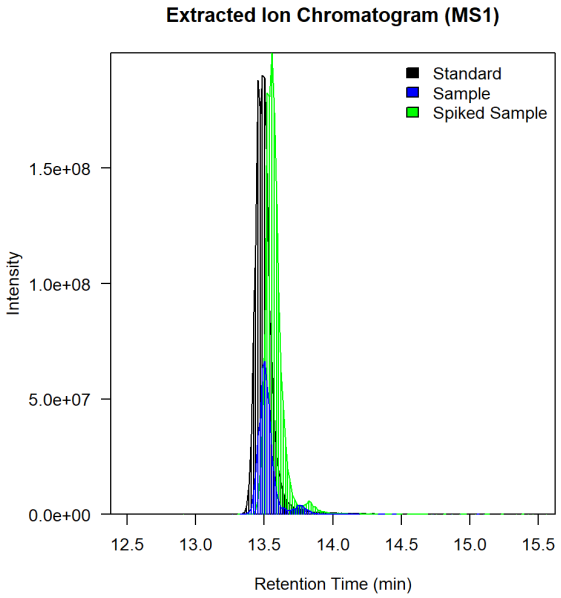

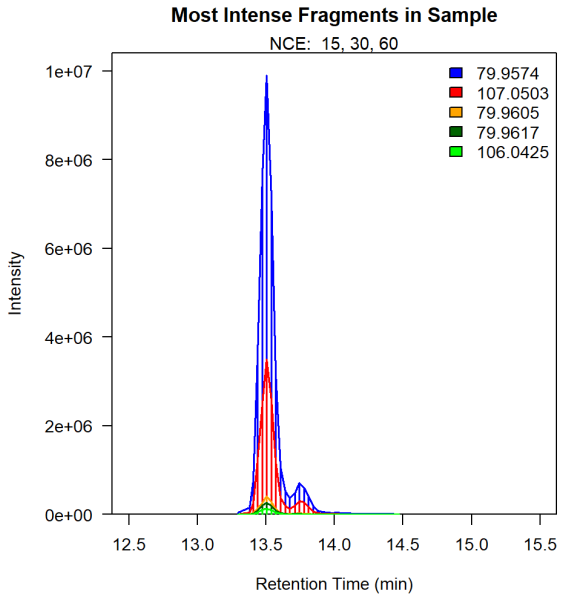

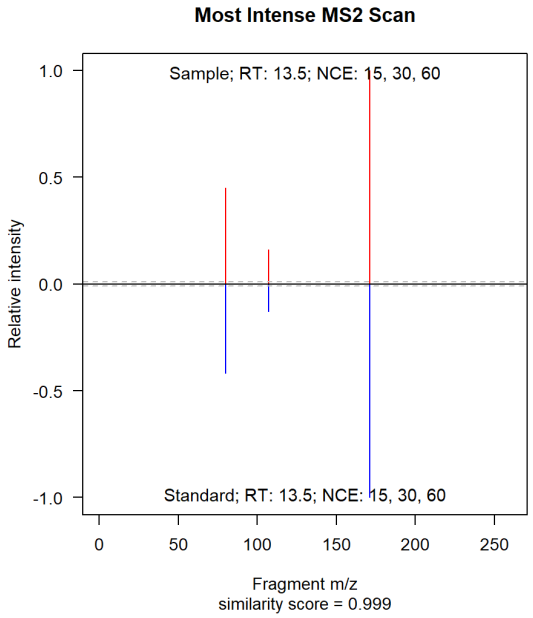

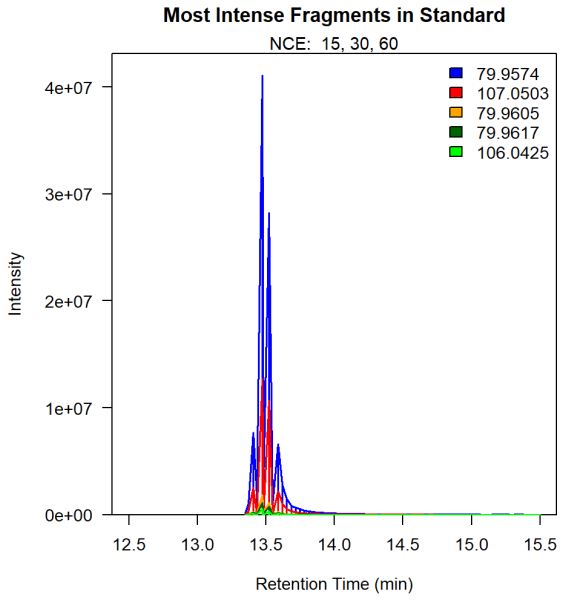

5-Methoxy-2H-benzotriazole
BLG10, Level 1
[M+H]+ 150.06619
(STD 100 ng/L)

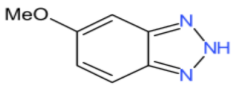

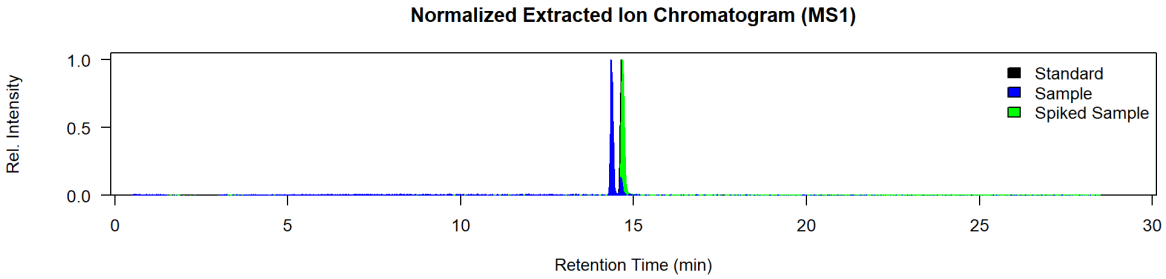

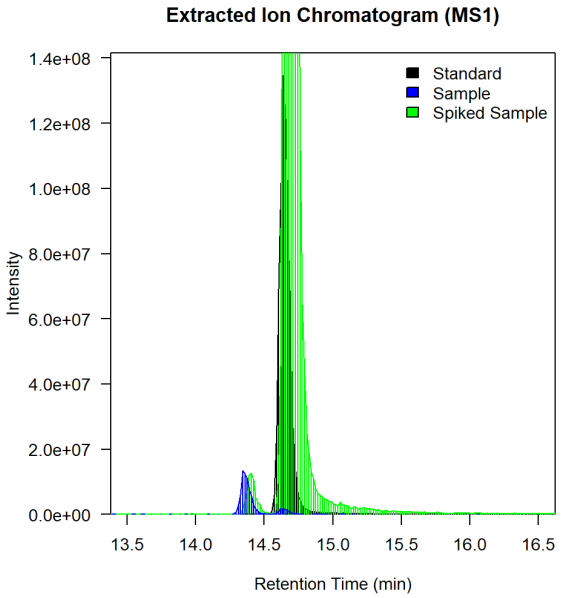

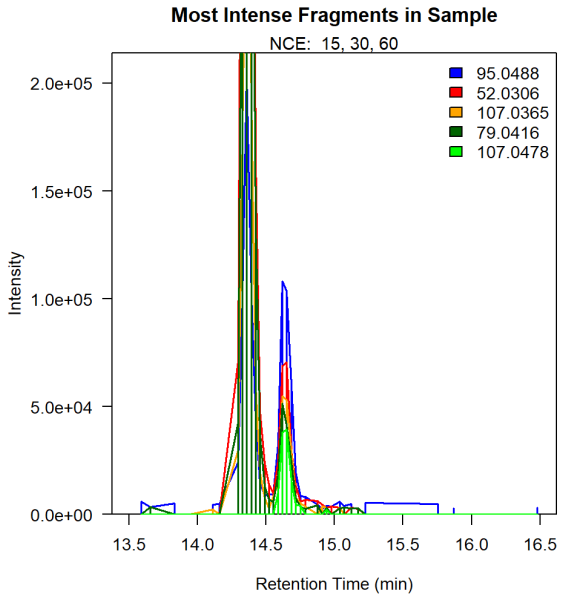

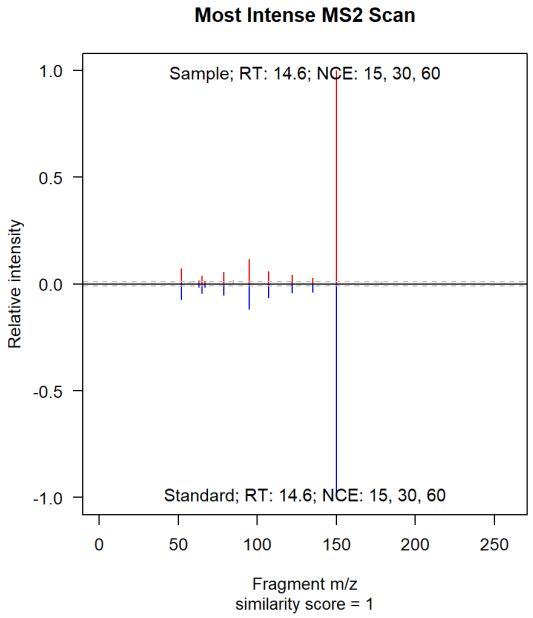

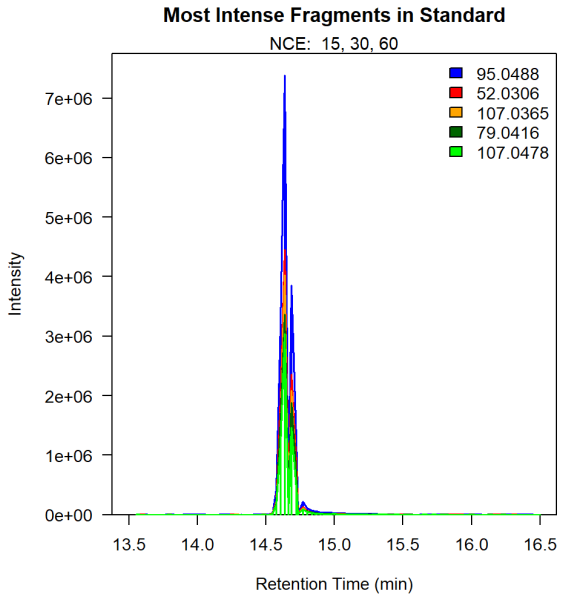

Isomer of 5-Methoxy-2H-benzotriazole
BLG10, Level 3
[M+H]+ 150.06619
(STD 100 ng/L)

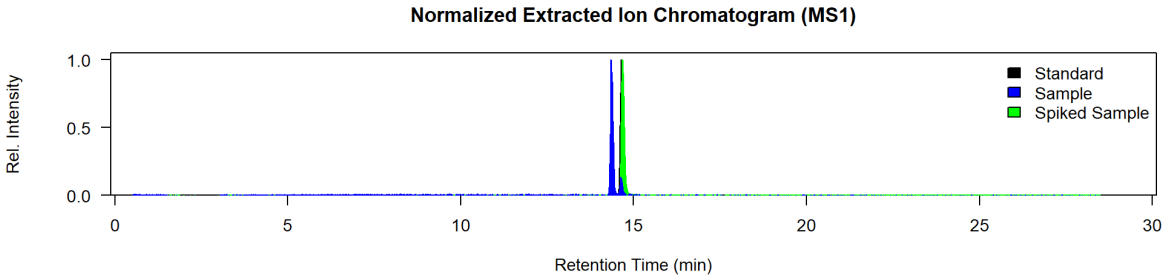

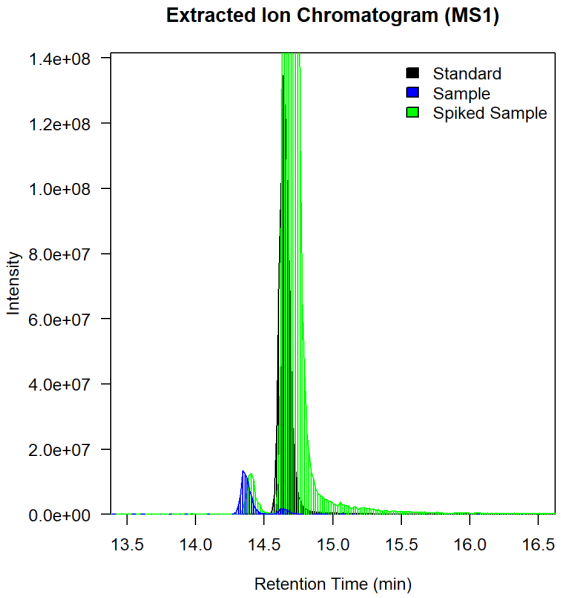

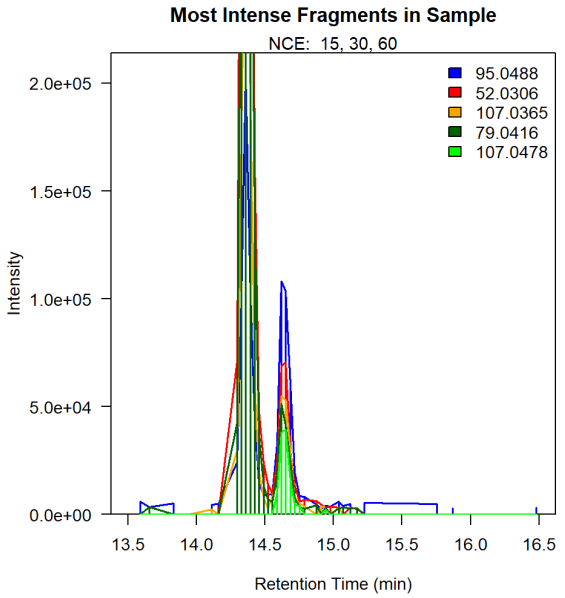

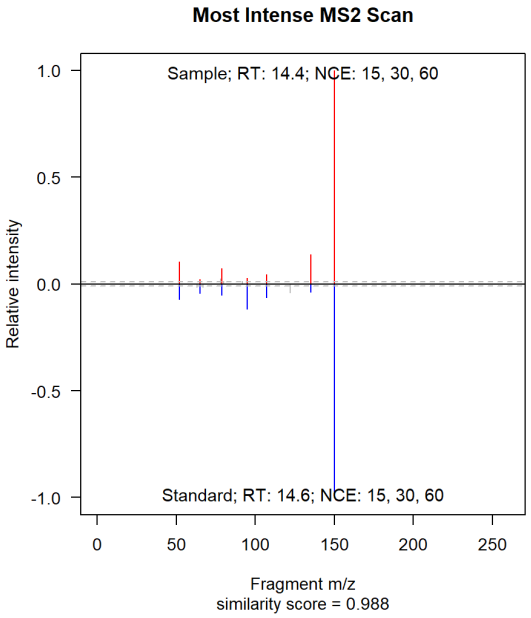

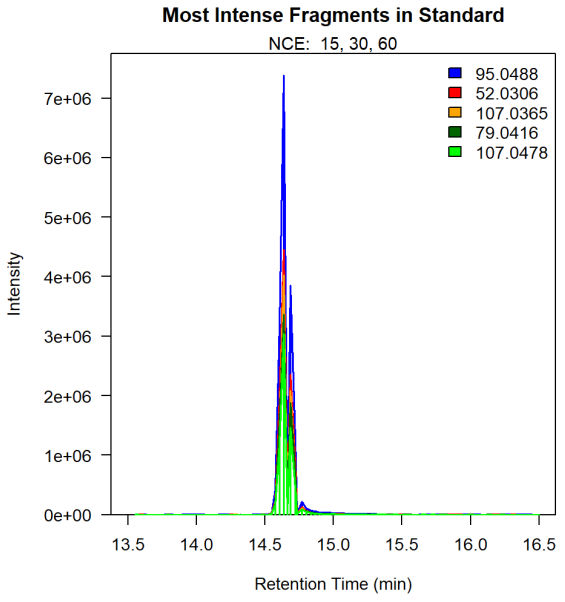

Propyphenazone
GEQ01, Level 1
[M+H]+ 231.14919
(STD 10 ng/L)

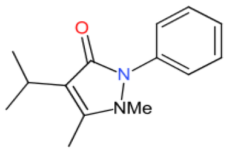

Normalized Extracted Ion Chromatogram (MS1)

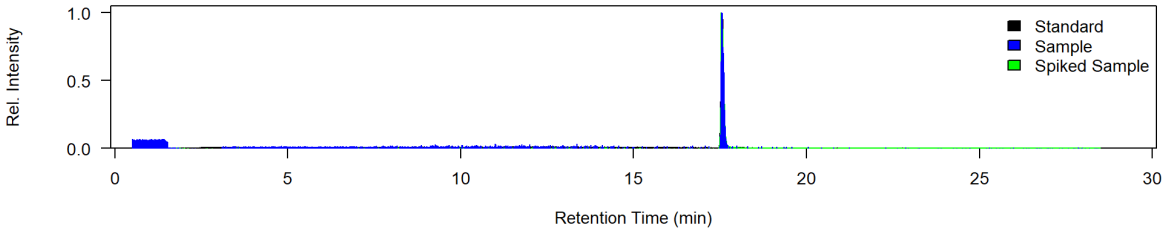

Extracted Ion Chromatogram (MS1)

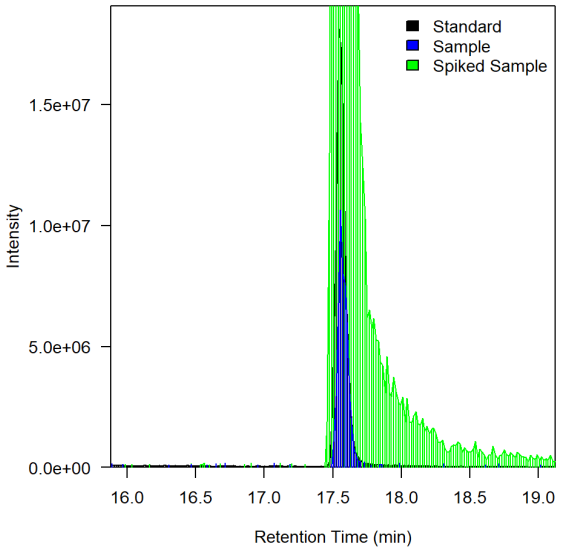

Most Intense Fragments in Sample

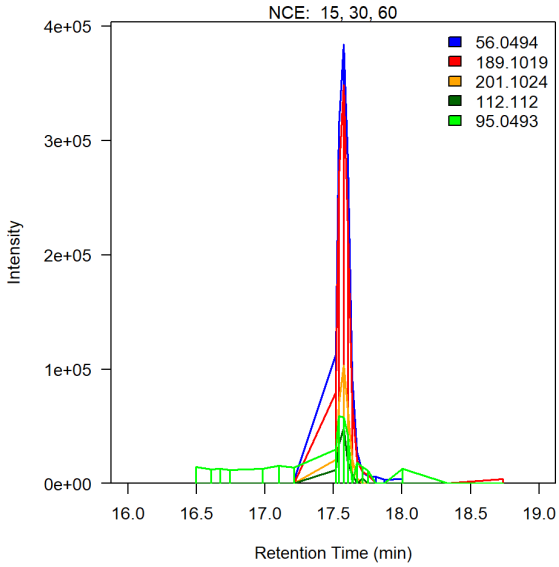

Most Intense MS2 Scan

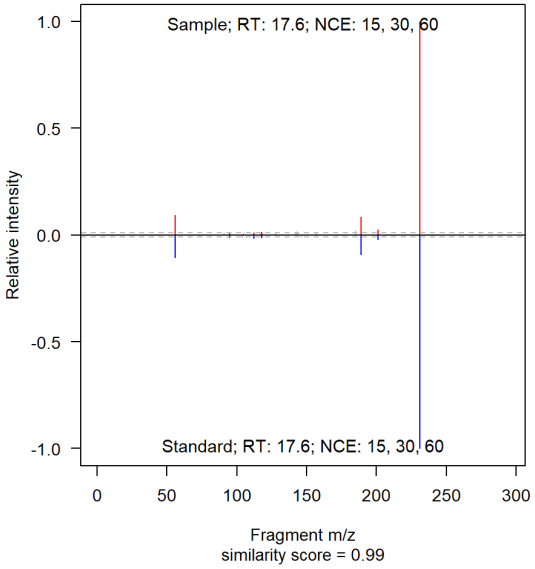

Most Intense Fragments in Standard

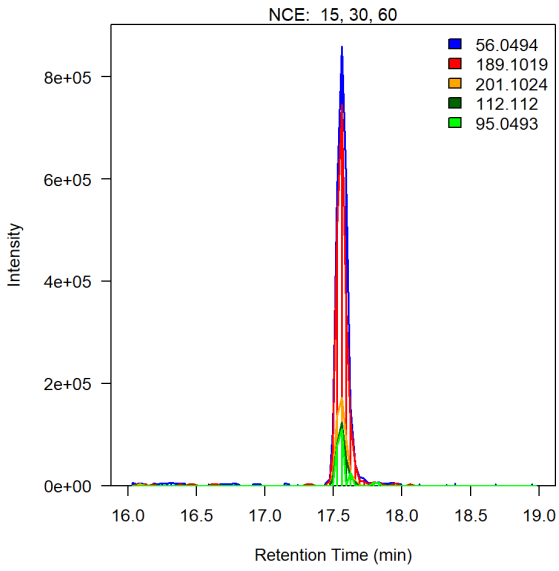

Pyrimidinol (2-Isopropyl-6-methyl-4-pyrimidone)
GEQ01, Level 1
[M+H]+ 153.1022395
(STD 100 ng/L)

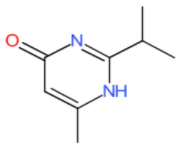

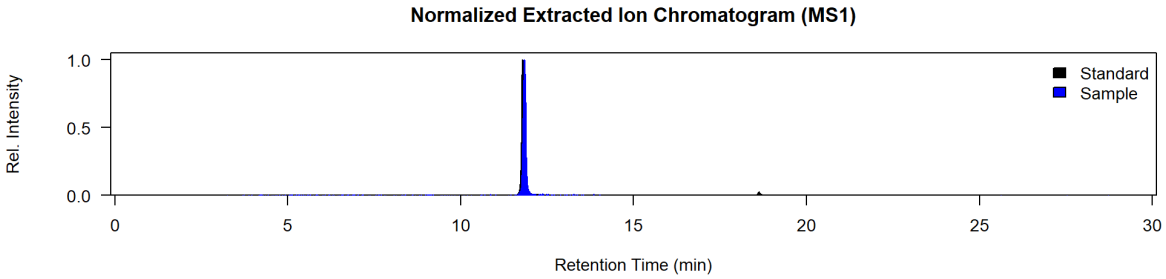

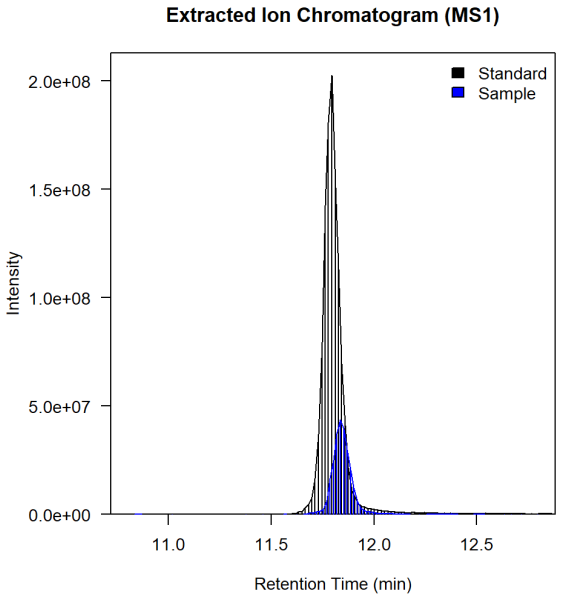

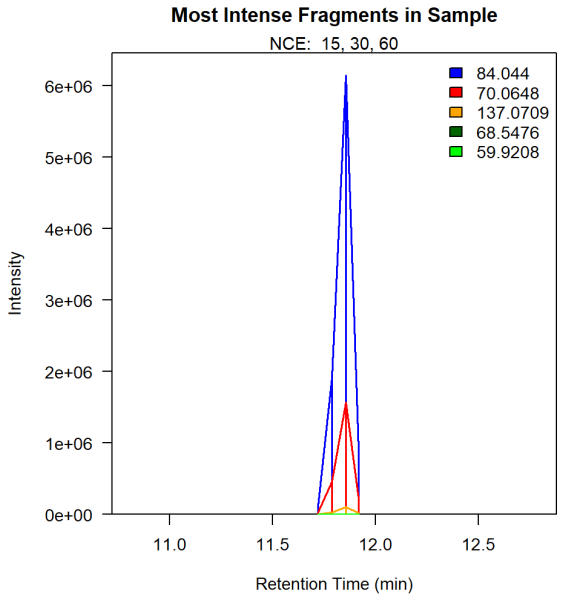

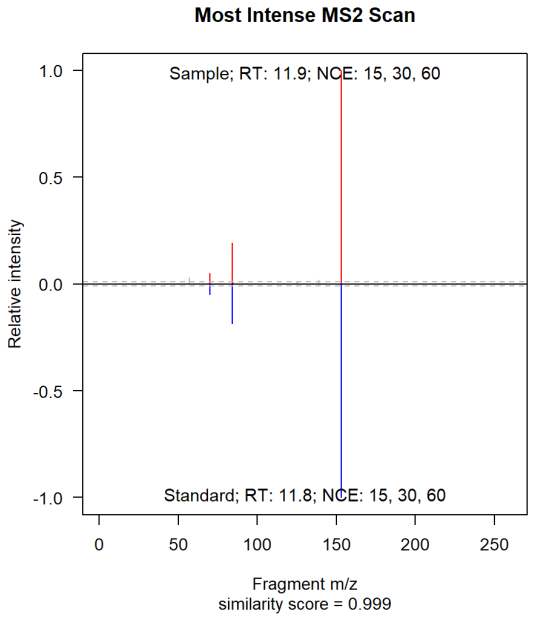

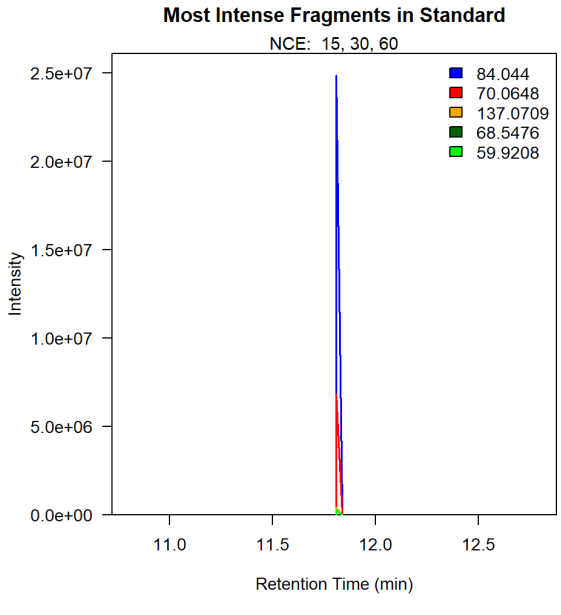

Fluometuron
VDG36, Level 1
[M+H]+ 233.08962
(STD 100 ng/L)

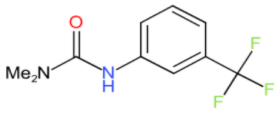

Normalized Extracted Ion Chromatogram (MS1)

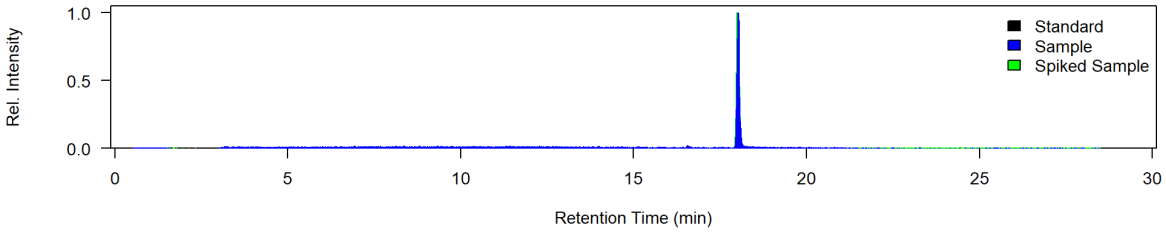

Extracted Ion Chromatogram (MS1)

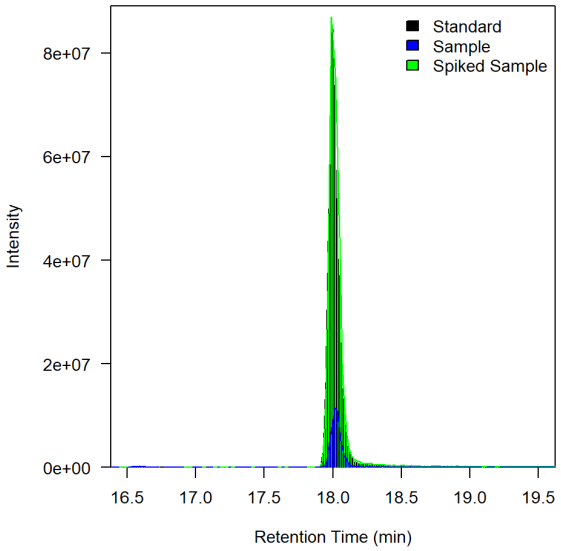

Most Intense Fragments in Sample

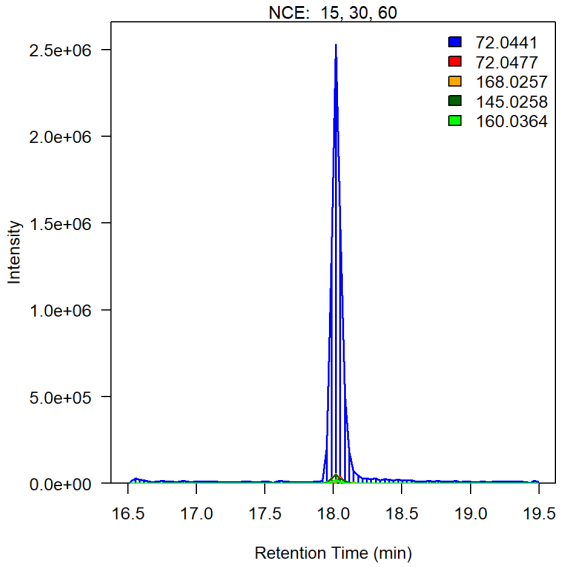

Most Intense MS2 Scan

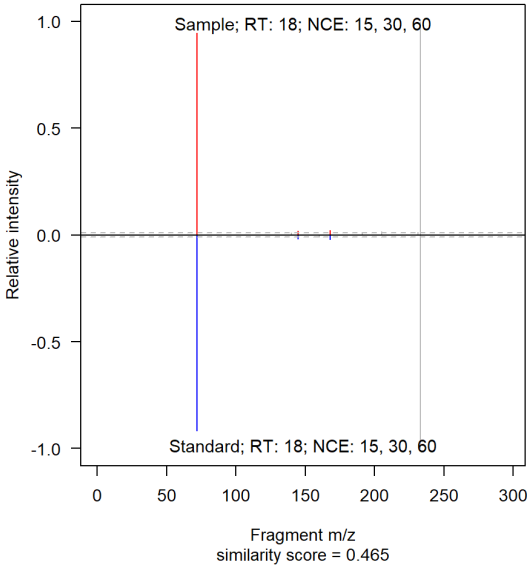

Most Intense Fragments in Standard

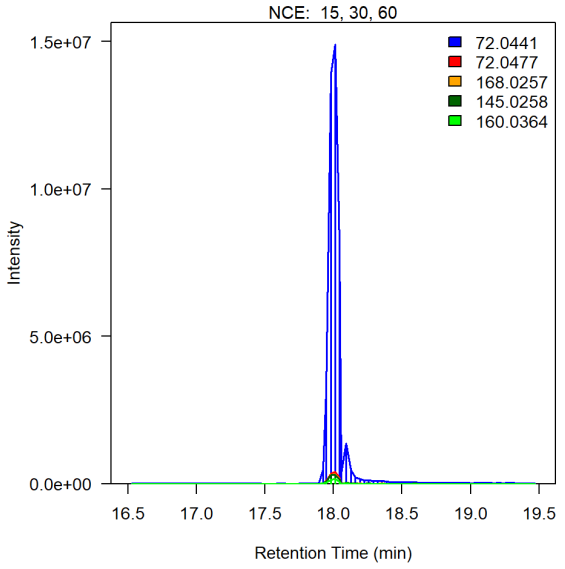

Sulisobenzone
Pooled Sample, Level 1
[M+H]+ 309.04274
(STD 100 ng/L)

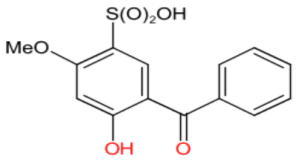

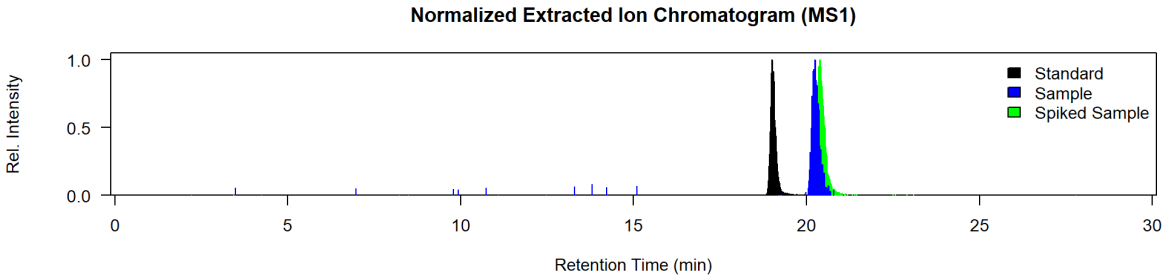

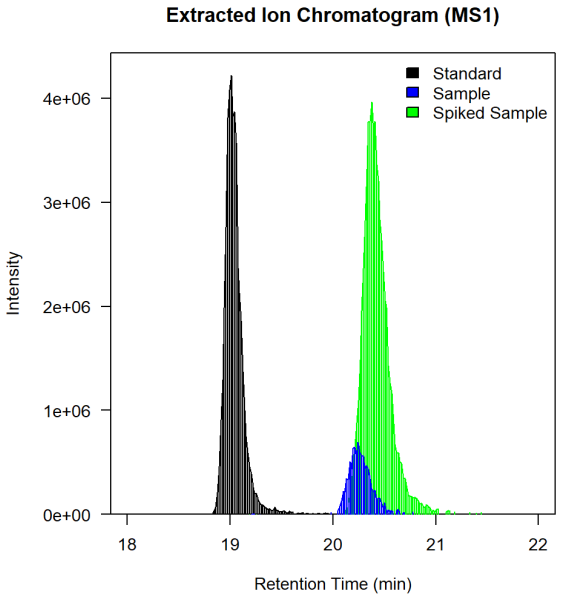

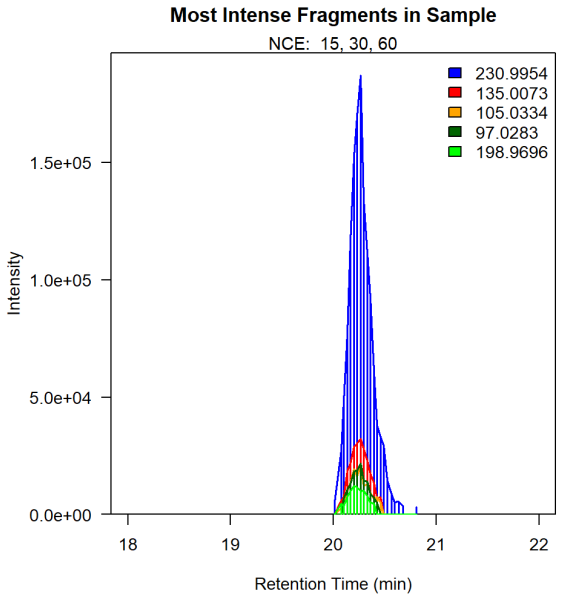

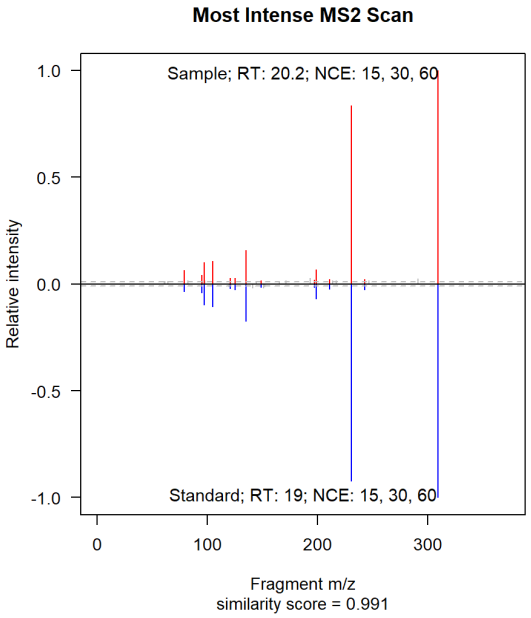

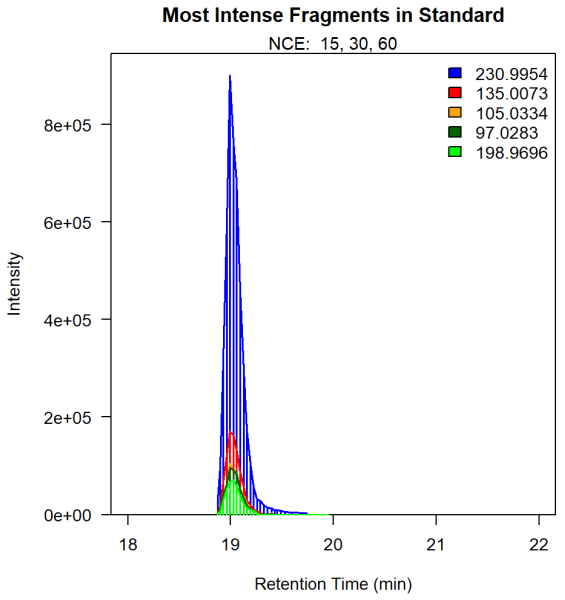

Sulisobenzone
Pooled Sample, Level 1
[M-H]- 307.02818
(STD 100 ng/L)

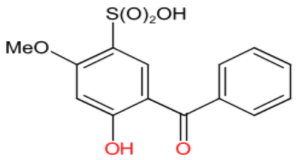

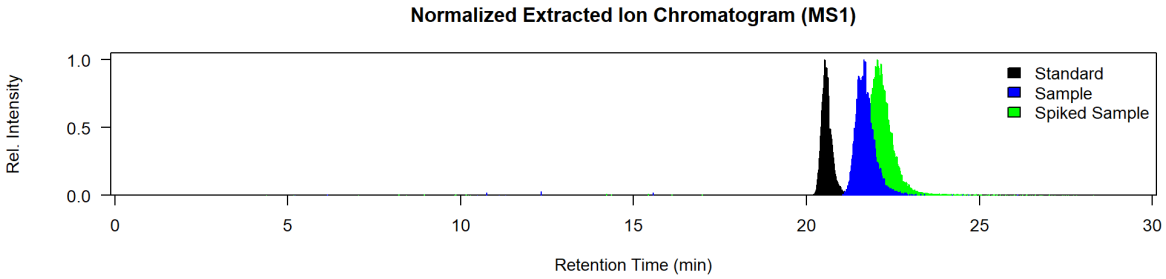

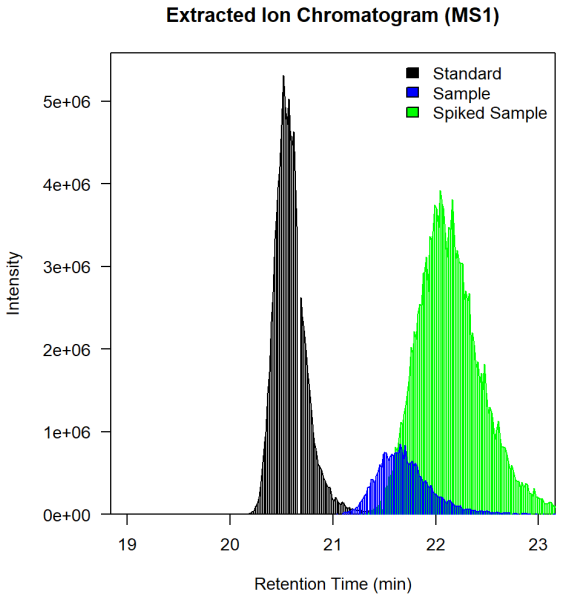

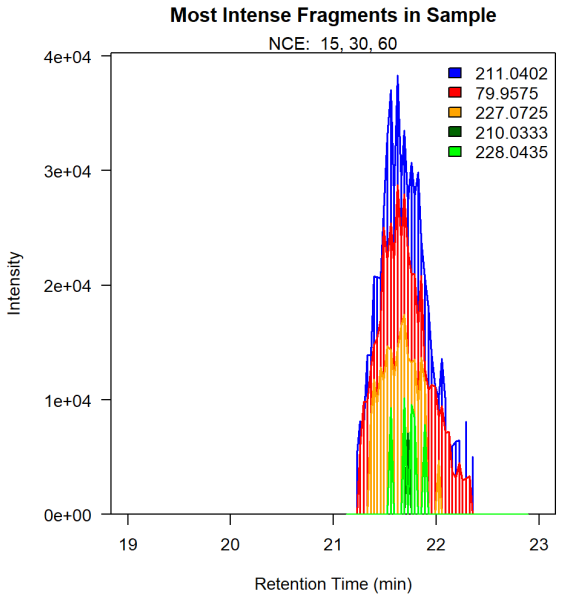

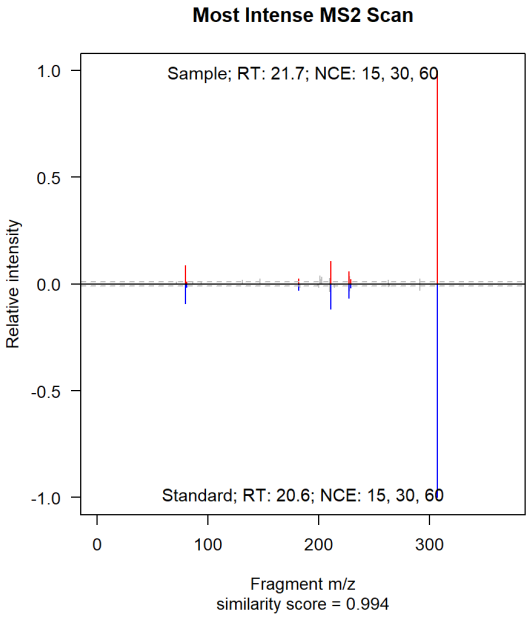

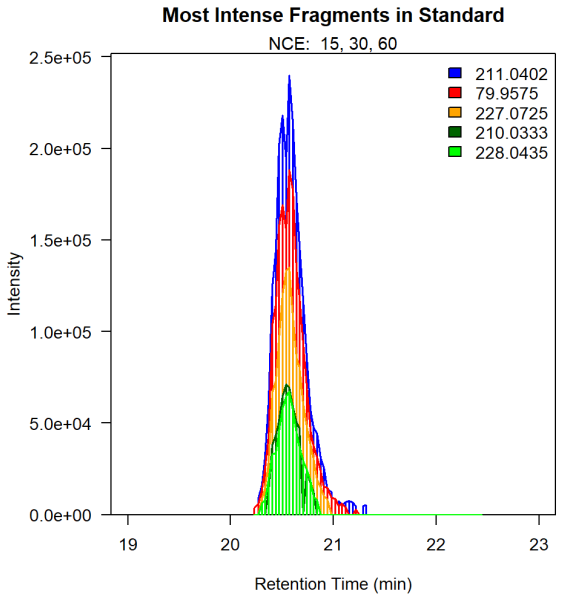

Iopromide TP 643
NTG41, Level 2a
[M+H]+ 643.80354

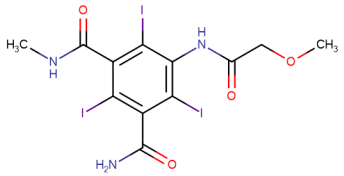

Extracted Ion Chromatogram (MS1)

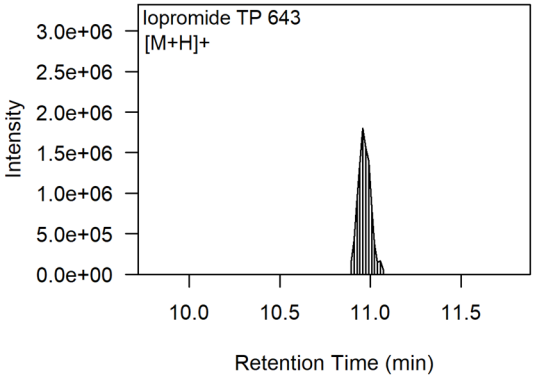

Most Intense Fragments in Sample

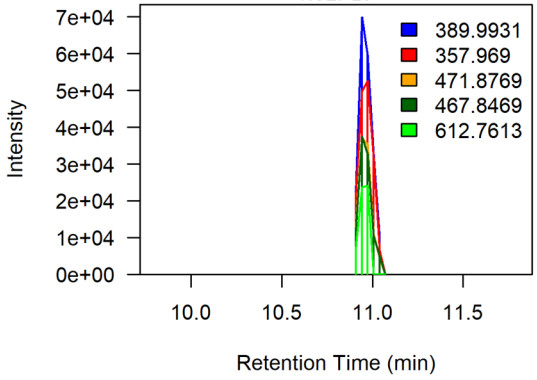

MS/MS Spectrum
Level 2a (Schulz et al. 2008, EST 42 (19))

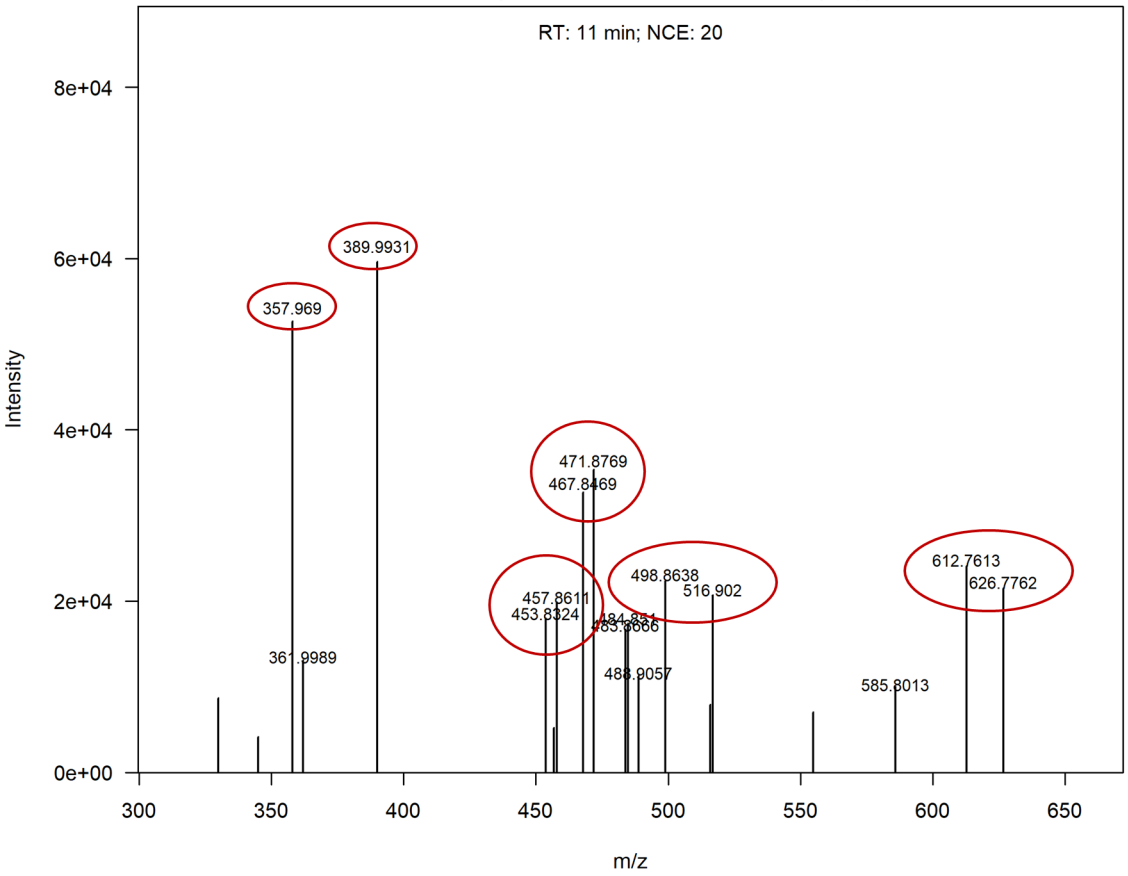

Iopromide TP 701 A
AGG28, Level 2a
[M+H]+ 701.80903

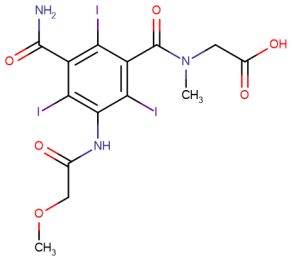

Extracted Ion Chromatogram (MS1)

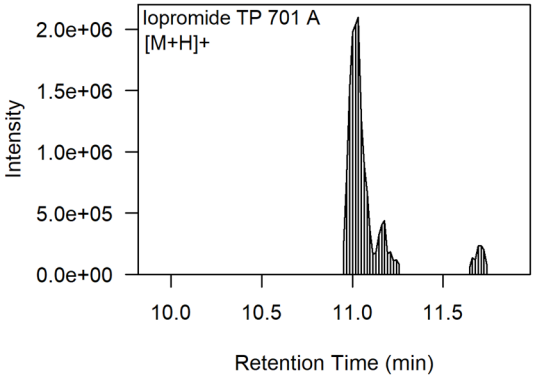

Most Intense Fragments in Sample

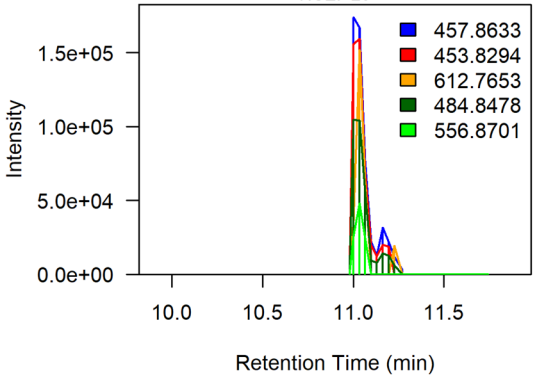

MS/MS Spectrum
Level 2a (Schulz et al. 2008, EST 42 (19))

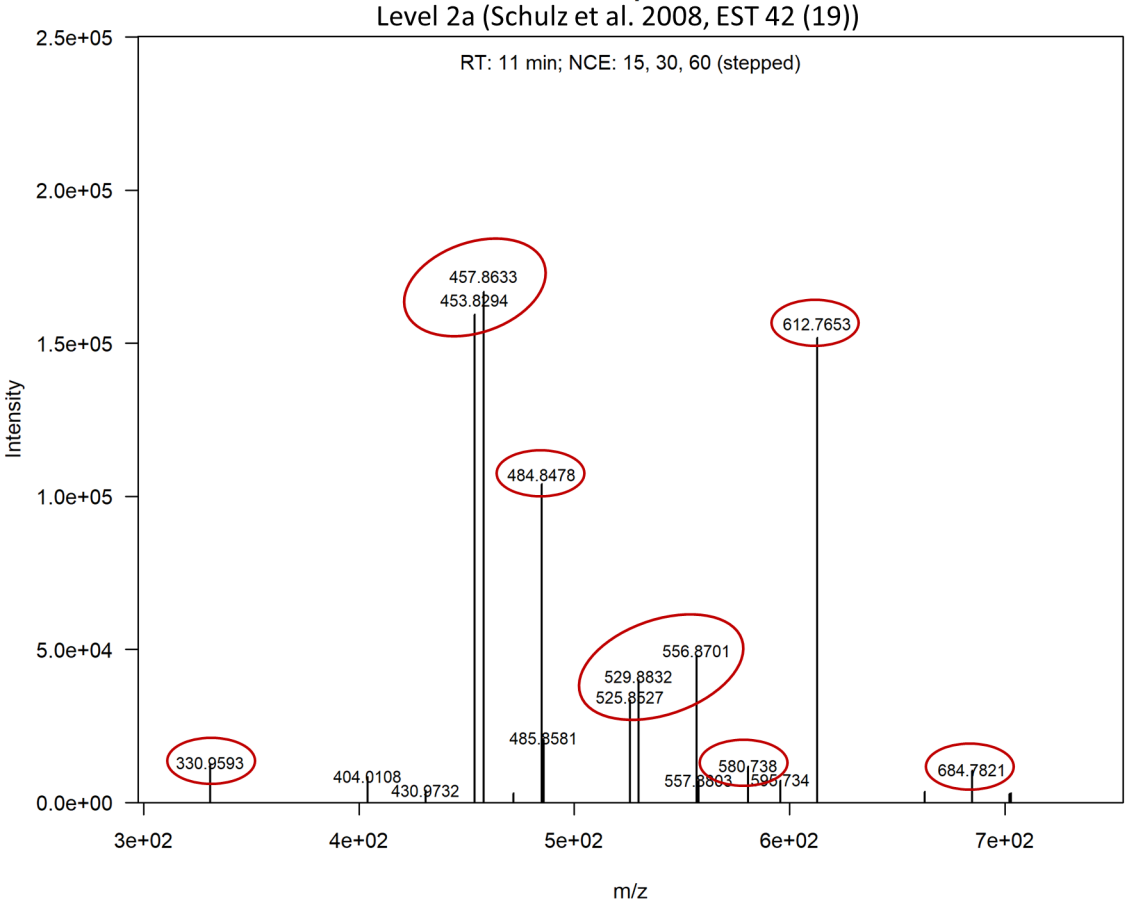

Iomeprol TP 629
SHG05, Level 2a
[M+H]+ 629.78786

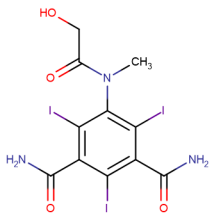

Extracted Ion Chromatogram (MS1)

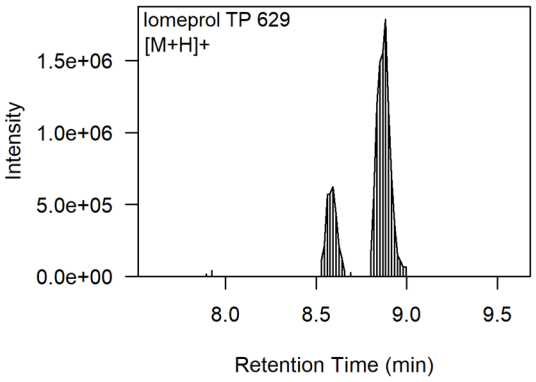

Most Intense Fragments in Sample

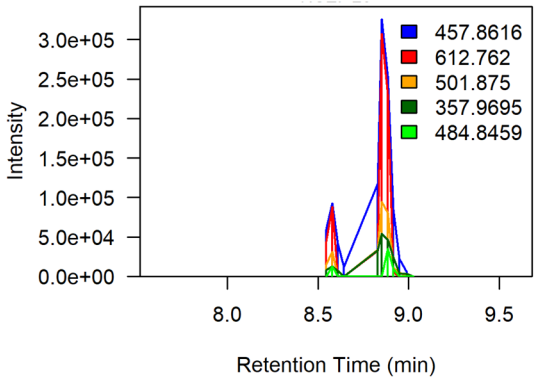

MS/MS Spectrum
Level 2a (Kormos et al. 2009, Anal Chem 81)

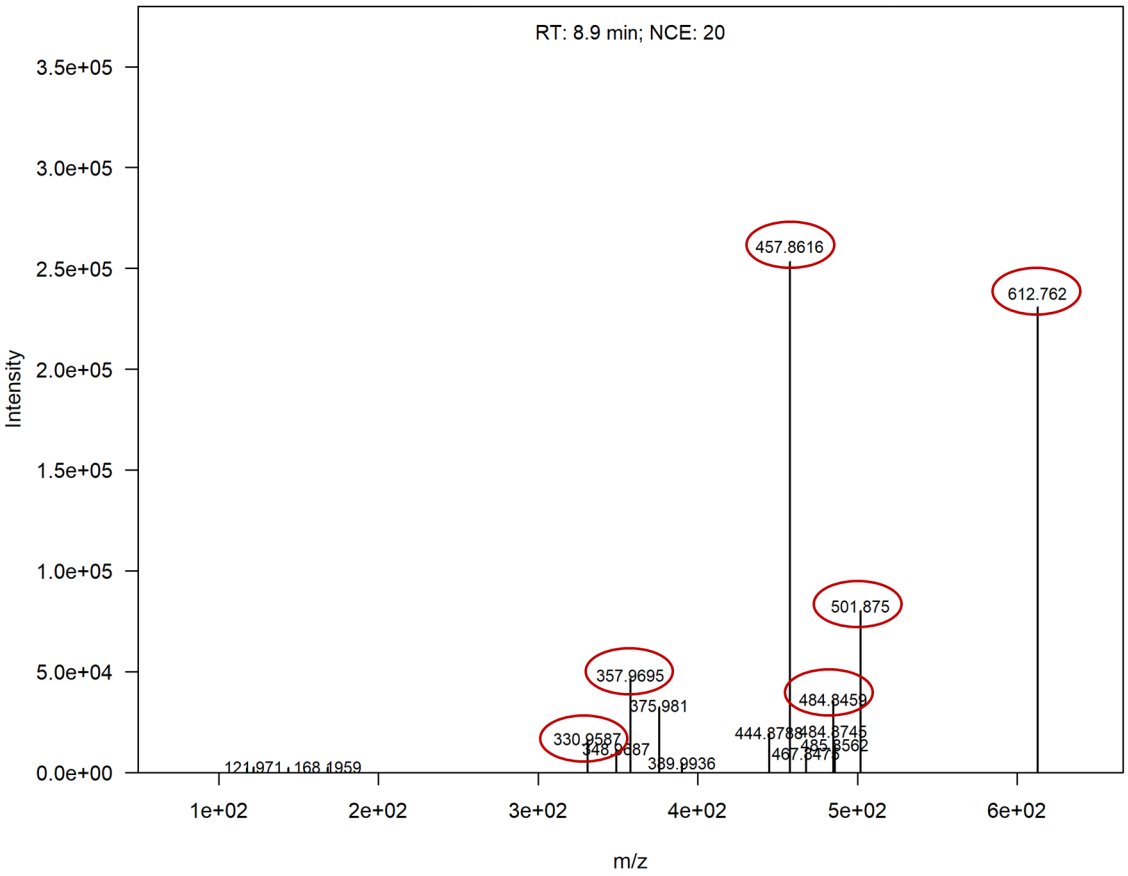

Triphenylphosphine oxide
AGG29, Level 2a
[M+H]+ 279.0933

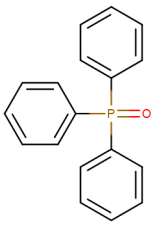

Extracted Ion Chromatogram (MS1)

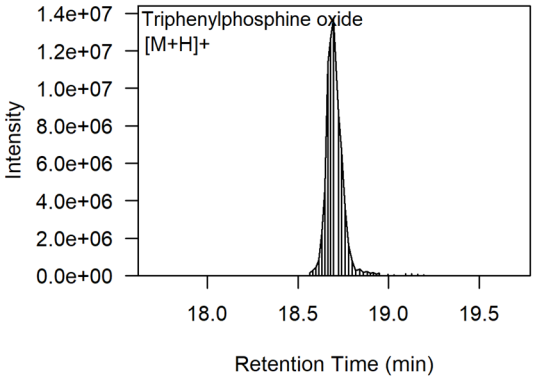

Most Intense Fragments in Sample

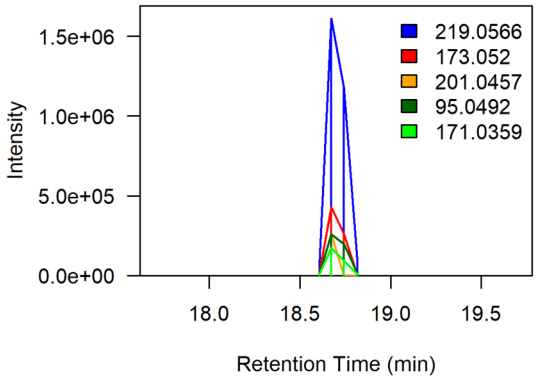

MS/MS Spectrum
Level 2a (library match mzCloud)

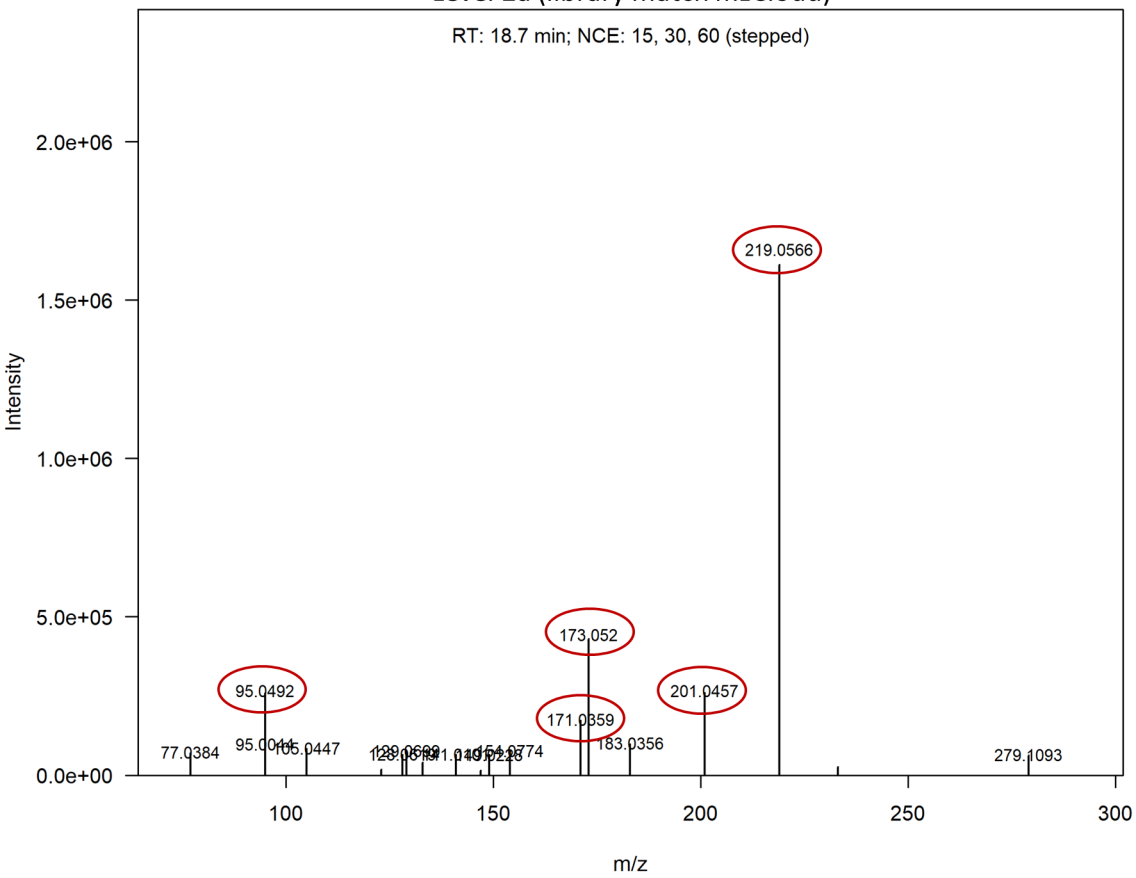

Hexa(methoxymethyl)melamine
VDG27, Level 2a
[M+H]+ 391.22996

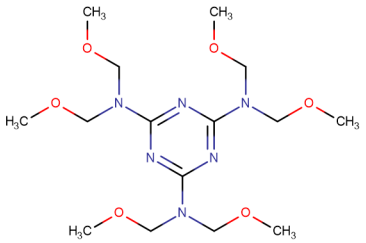

Extracted Ion Chromatogram (MS1)

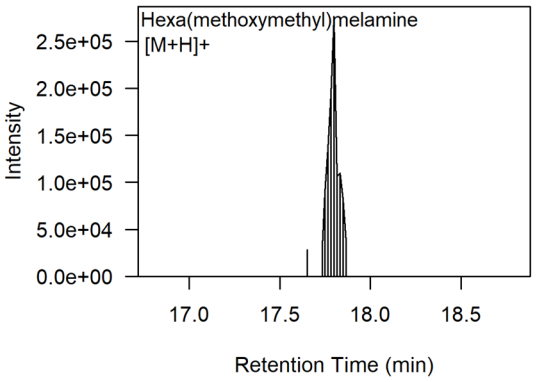

Most Intense Fragments in Sample

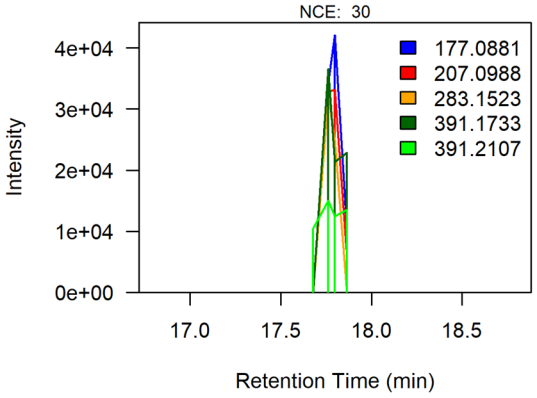

MS/MS Spectrum
Level 2a (library match mzCloud)

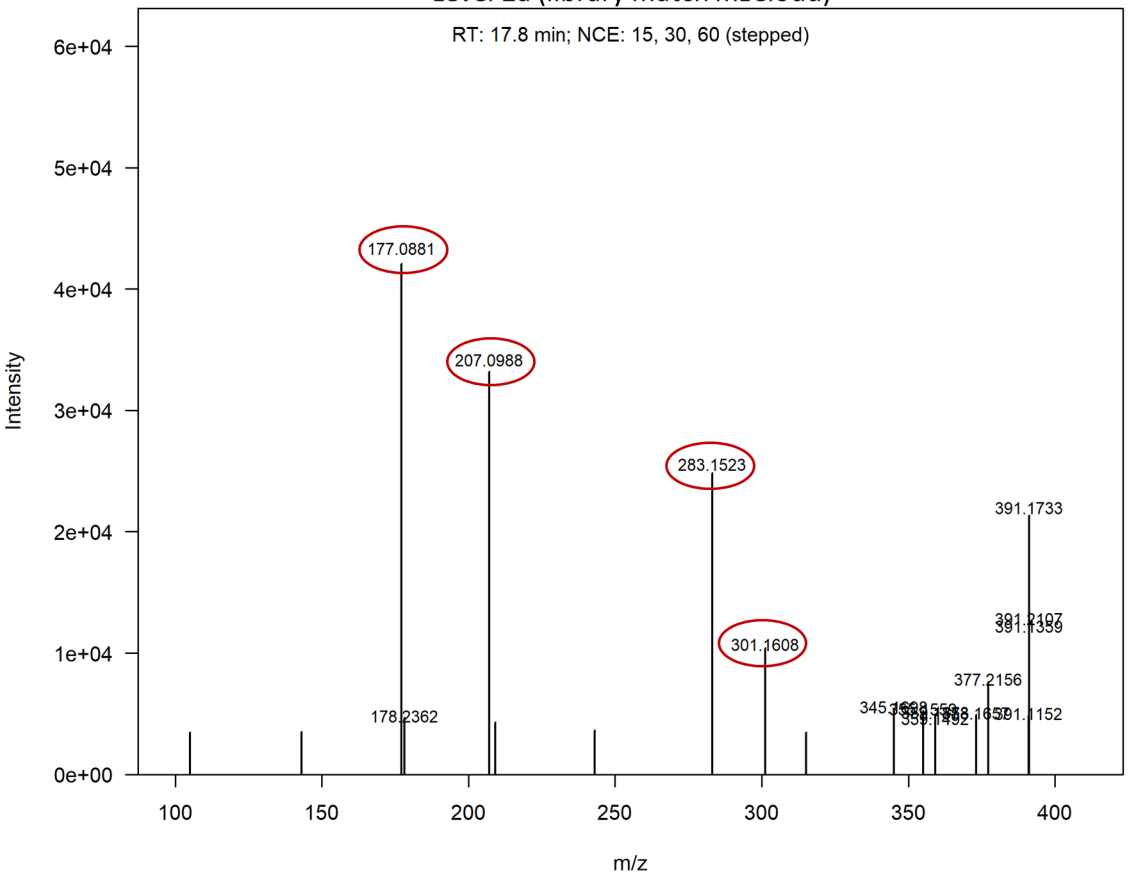

Metolachlor TP CGA357704
NTG41, Level 2a
[M-H]- 278.103396

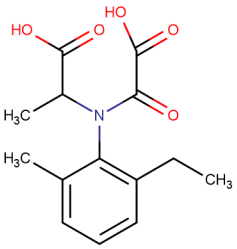

Extracted Ion Chromatogram (MS1)

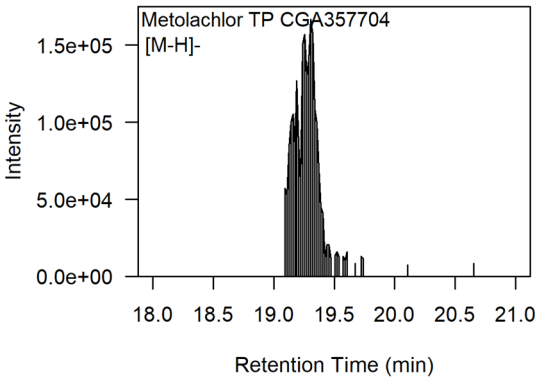

Most Intense Fragments in Sample

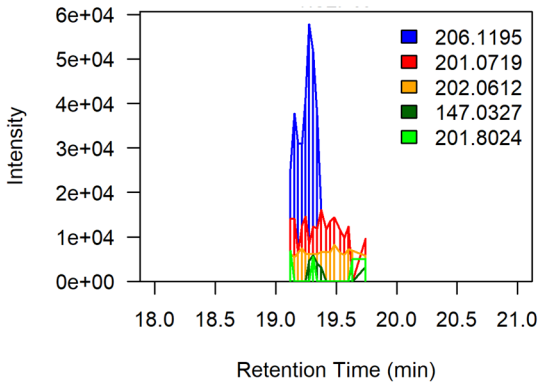

MS/MS Spectrum

Level 2a (Reemtsma et al. 2013, J. Chrom. A 1271 (1))

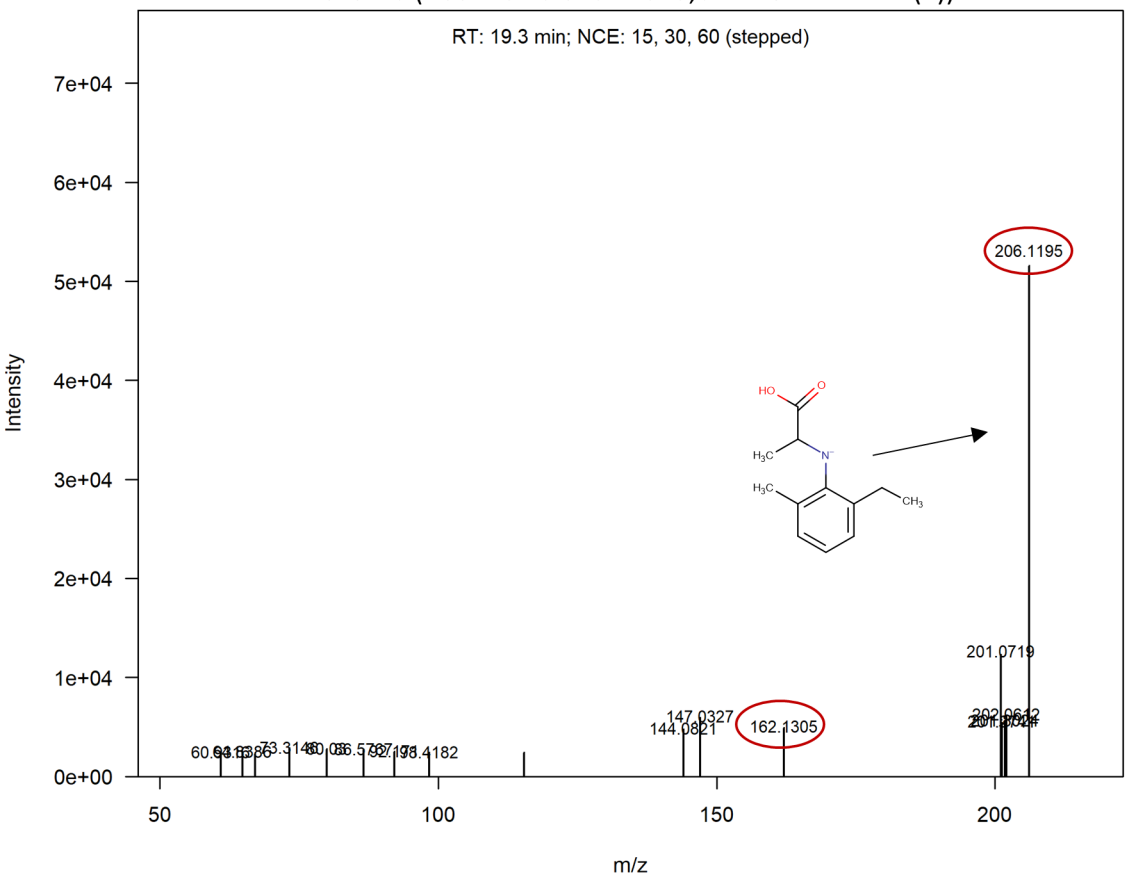

Chlorendic Acid
GEQ01, Level 2a
[M-H]- 384.8169

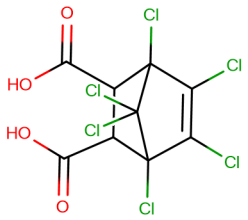

Extracted Ion Chromatogram (MS1)

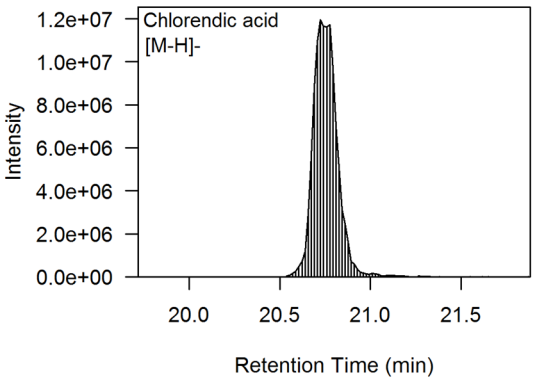

Most Intense Fragments in Sample

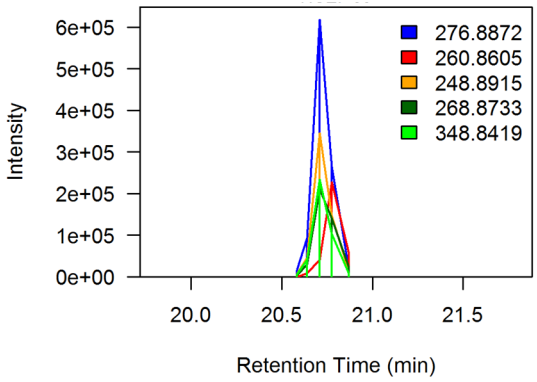

MS/MS Spectrum
Level 2a (library match mzCloud)

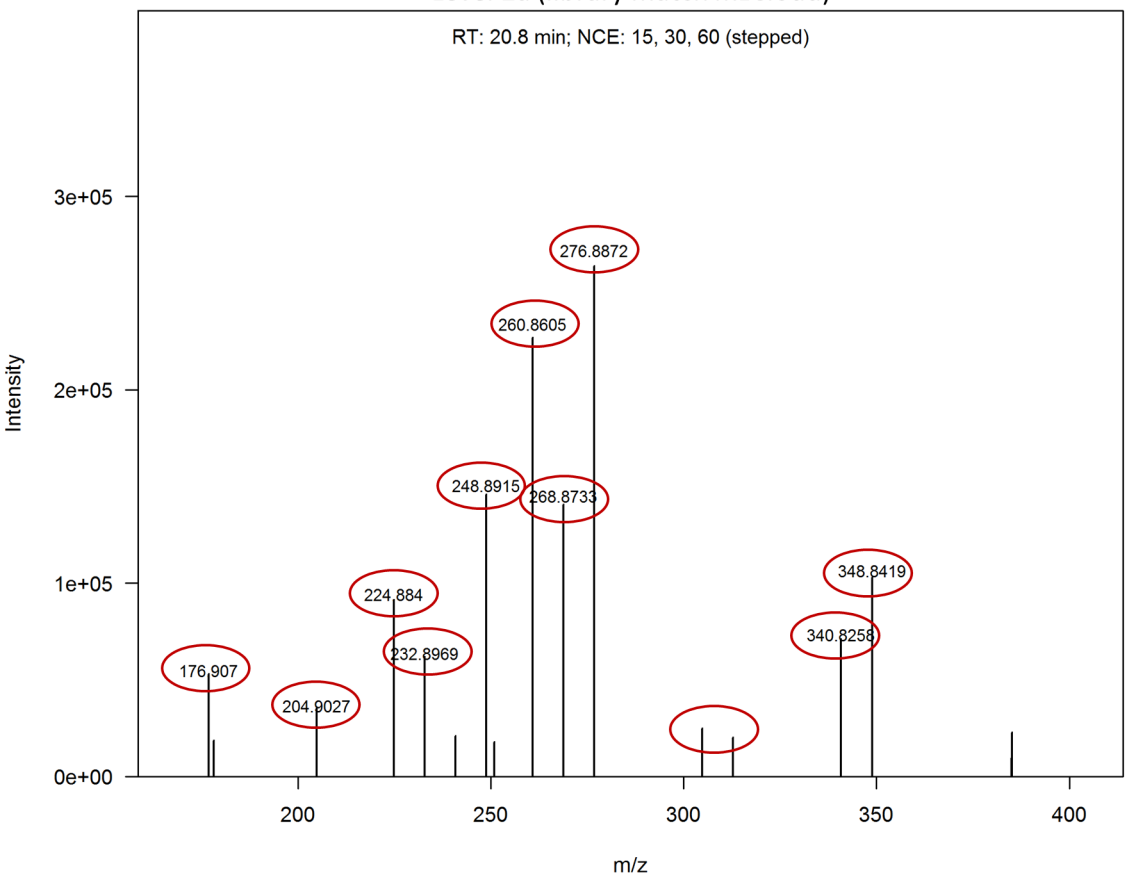

Isomer of 5,6-Dimethyl-2H-benzotriazole
BLG10, Level 3
[M+H]+ 148.08692
(STD 100 ng/L)

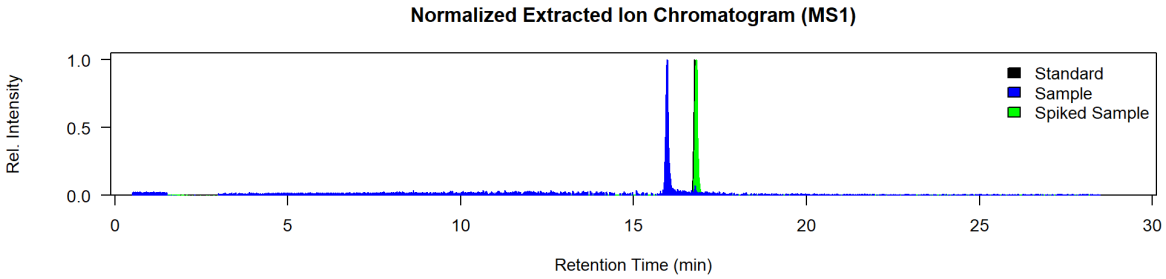

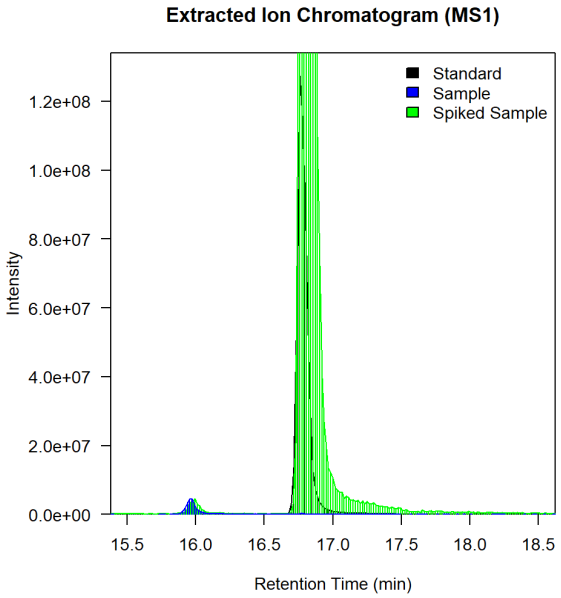

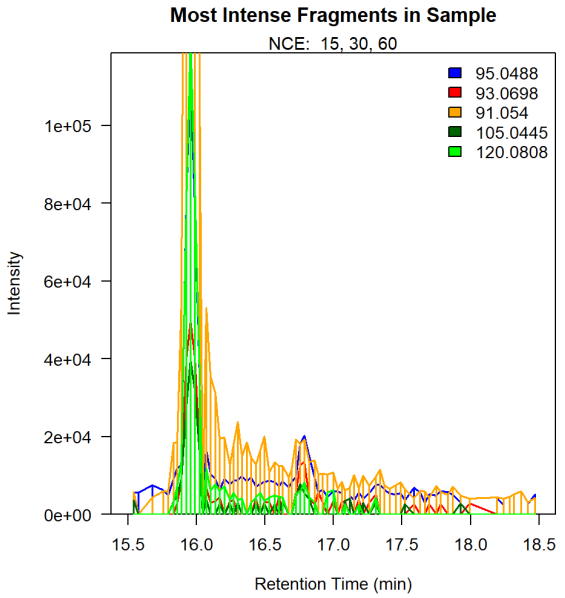

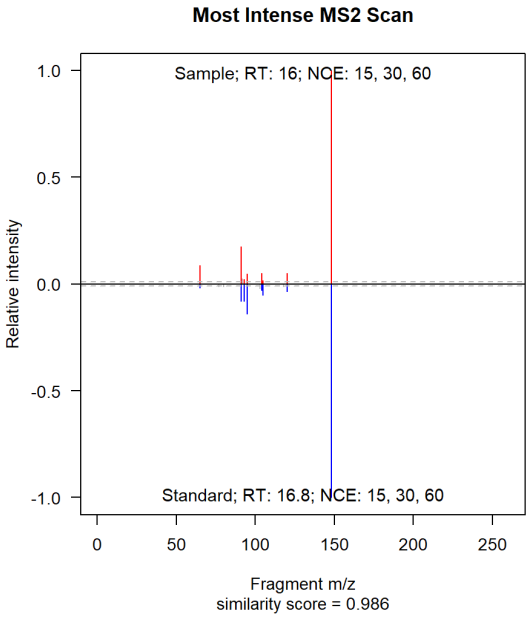

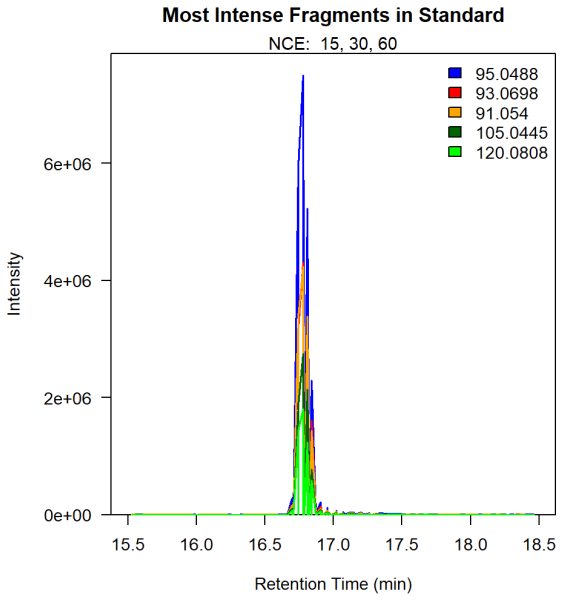

Naphthalenedisulfonic acid (isomers)
GEQ01, Level 3
[M-H]- 286.96895
(STD for 2 isomers: 1000 ng/L)

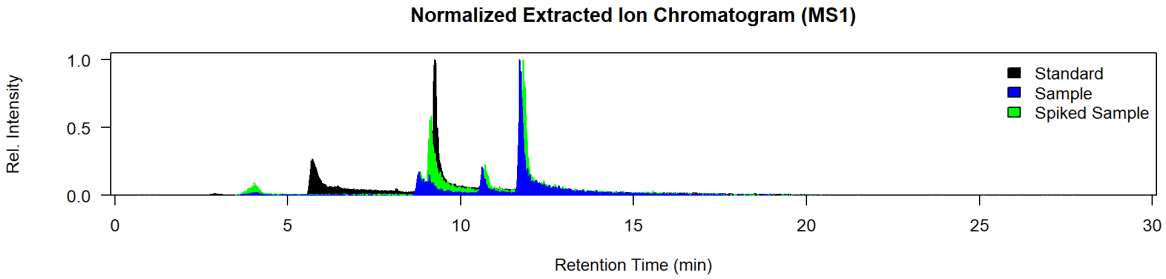

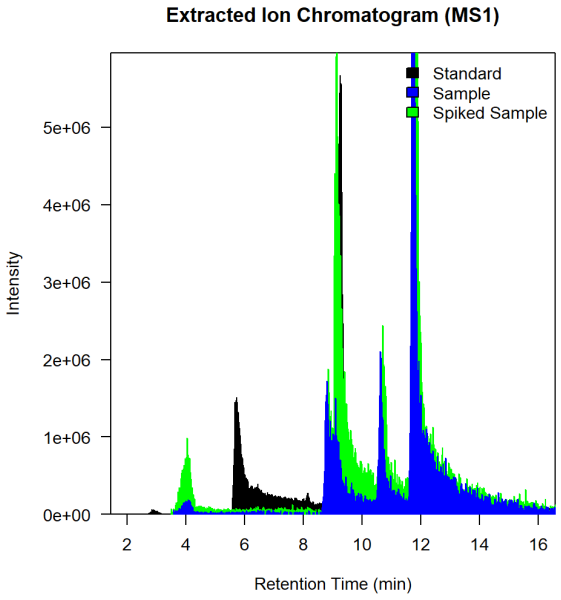

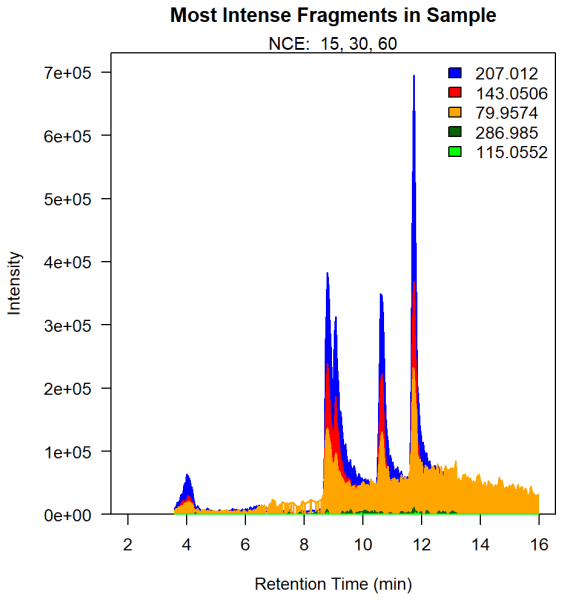

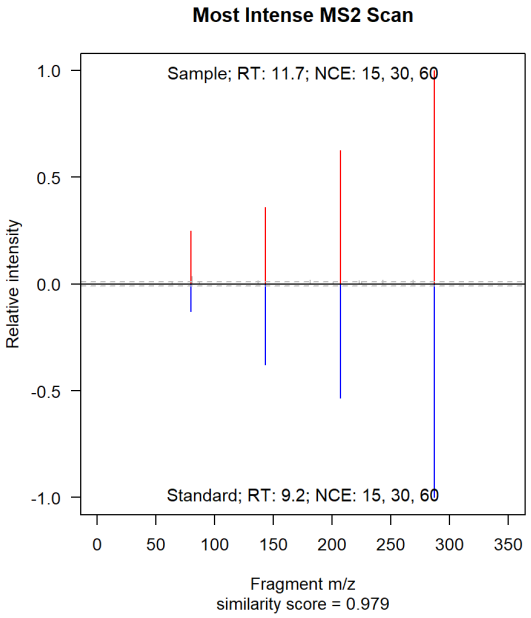

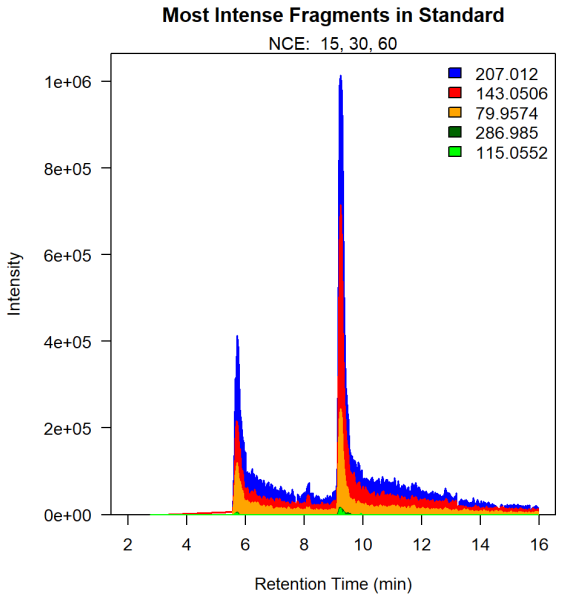

References

Arp, H.P. and Hale, S.E., 2020. S36 | UBAPMT | Potential Persistent, Mobile and Toxic (PMT) substances (Version NORMAN-SLE-S36.0.2.0) [Data set], Zenodo. http://doi.org/10.5281/zenodo.3637611.

Bolton, E. and Schymanski, E.L., 2020. PubChemLite tier0 and tier1 (Version PubChemLite.0.2.0) [Data set], Zenodo. http://doi.org/10.5281/zenodo.3611238.

Dührkop, K., Shen, H., Meusel, M., Rousu, J. and Bocker, S., 2015. Searching molecular structure databases with tandem mass spectra using CSI:FingerID. Proc Natl Acad Sci U S A 112(41), 12580-12585.

Dührkop, K., Fleischauer, M., Ludwig, M., Aksenov, A.A., Melnik, A.V., Meusel, M., Dorrestein, P.C., Rousu, J. and Bocker, S., 2019. SIRIUS 4: a rapid tool for turning tandem mass spectra into metabolite structure information. Nat Methods 16(4), 299-302.

Fischer, S., 2017. S17 | KEMIMARKET | KEMI Market List MS-ready (12/05/2017) (Version NORMAN-SLE-S17.0.1.3) [Data set], Zenodo. http://doi.org/10.5281/zenodo.3653175.

Gatto, L. and Lilley, K.S., 2012. MSnbase - an R/Bioconductor package for isobaric tagged mass spectrometry data visualization, processing and quantitation. Bioinformatics (28), 288-289.

Gerlich, M. and Neumann, S., 2013. MetFusion: integration of compound identification strategies. J Mass Spectrom 48(3), 291-298.

Kiefer, K., Müller, A., Singer, H. and Hollender, J., 2019. New Relevant Pesticide Transformation Products in Groundwater Detected Using Target and Suspect Screening for Agricultural and Urban Micropollutants with LC-HRMS. Water research 165.

Kiefer, K., Müller, A., Singer, H. and Hollender, J., 2020. S60 | SWISSPEST19 | Swiss Pesticides and Metabolites from Kiefer et al 2019 (Version S60.0.1.1) [Data set], Zenodo. http://doi.org/10.5281/zenodo.3766352.

Kormos, J.L., Schulz, M., Wagner, M. and Ternes, T.A., 2009. Multistep Approach for the Structural Identification of Biotransformation Products of Iodinated X-ray Contrast Media by Liquid Chromatography/Hybrid Triple Quadrupole Linear Ion Trap Mass Spectrometry and 1H and 13C Nuclear Magnetic Resonance. Analytical chemistry 81(22), 9216-9224.

Letzel, T., Grosse, S. and Sengel, M., 2017. S2 | STOFFIDENT | HSWT/LfU STOFF-IDENT Database of Water-Relevant Substances (Version NORMAN-SLE-S2.0.1.0) [Data set], Zenodo. http://doi.org/10.5281/zenodo.2621452.

Norman Network, Aalizadeh, R., Alygizakis, N.A., Schymanski, E.L., Slobodnik, J. and Fischer, S., 2020. S0 | SUSDAT | Merged NORMAN Suspect List: SusDat (Version NORMAN-SLE-S0.0.2.2) [Data set], Zenodo. http://doi.org/10.5281/zenodo.3695732.

Reemtsma, T., Alder, L. and Banasiak, U., 2013. A multimethod for the determination of 150 pesticide metabolites in surface water and groundwater using direct injection liquid chromatography-mass spectrometry. Journal of chromatography A 1271(1), 95-104.

Ruttkies, C., Schymanski, E.L., Wolf, S., Hollender, J. and Neumann, S., 2016. MetFrag relaunched: incorporating strategies beyond in silico fragmentation. Journal of Cheminformatics 8(3).

Ruttkies, C., Neumann, S. and Posch, S., 2019. Improving MetFrag with statistical learning of fragment annotations. BMC Bioinformatics 20(1), 376.

Schollée, J.E., 2018. TFAnalyzeR, version 1.0.1, Analysis of TraceFinder Target Screening, Zenodo, DOI: 10.5281/zenodo.3234748.

Schulz, M., Loffler, D., Wagner, M. and Ternes, T.A., 2008. Transformation of the X-ray contrast medium iopromide in soil and biological wastewater treatment. Environ Sci Technol 42(19), 7207-7217.

Schulze, S., Zahn, D., Montes, R., Rodil, R., Quintana, J.B., Knepper, T.P., Reemtsma, T. and Berger, U., 2019. Occurrence of emerging persistent and mobile organic contaminants in European water samples. Water Res 153, 80-90.

Schymanski, E.L., 2019. MetFrag Local CSV: CompTox (7 March 2019 release) Wastewater MetaData File (Version WWMetaData_4Oct2019) [Data set], Zenodo. http://doi.org/10.5281/zenodo.3472781.

Schymanski, E.L., 2020. ReSOLUTION: SOLUTIONS for High ReSOLUTION Mass Spectrometry. R package. https://rdrr.io/github/schymane/ReSOLUTION/.

Stravs, M.A., Schymanski, E.L., Singer, H.P. and Hollender, J., 2013. Automatic recalibration and processing of tandem mass spectra using formula annotation. J Mass Spectrom 48(1), 89-99.